



FUNDAÇÃO UNIVERSIDADE FEDERAL DO ABC  
Centro de Ciências Naturais e Humanas (CCNH)

---

PÓS-GRADUAÇÃO EM FÍSICA

ABORDAGENS PRÁTICAS PARA TEORIAS DE  
CALIBRE: FUNÇÕES DO GRUPO DE  
RENORMALIZAÇÃO EM DOIS LAÇOS DENTRO  
DA REGULARIZAÇÃO IMPLÍCITA 4D

Dafne Carolina Arias Perdomo

---

Santo André

2022

Dafne Carolina Arias Perdomo

# Abordagens práticas para teorias de calibre: funções do grupo de renormalização em dois laços dentro da Regularização Implícita 4D



Tese de doutorado apresentada ao Programa de  
Pós-Graduação em Física da Universidade Federal do  
ABC (UFABC), como requisito parcial para à  
obtenção do título de Doutor em Física.

Orientador: Prof. Dr. MARCOS SAMPAIO

Co-orientador: Prof. Dr. ADRIANO CHERCHIGLIA

Santo André - SP

Setembro de 2022

---

Sistema de Bibliotecas da Universidade Federal do ABC  
Elaborada pelo Sistema de Geração de Ficha Catalográfica da UFABC  
com os dados fornecidos pelo(a) autor(a).

Arias Perdomo, Dafne Carolina

Abordagens práticas para teorias de calibre : funções do grupo de renormalização em dois laços dentro da Regularização Implícita 4D / Dafne Carolina Arias Perdomo. — 2022.

140 fls. : il.

Orientador: Marcos Donizeti Rodrigues Sampaio

Coorientador: Adriano Cherchiglia

Tese (Doutorado) — Universidade Federal do ABC, Programa de Pós-Graduação em Física, Santo André, 2022.

1. Implicit Regularization. 2. Regularization schemes. 3. Gauges theories. 4. Anomalous dimension. 5. Renormalization. I. Rodrigues Sampaio, Marcos Donizeti. II. Cherchiglia, Adriano. III. Programa de Pós-Graduação em Física, 2022. IV. Título.

---

## **Declaração de Atendimento às Observações da Banca**

Este exemplar foi revisado e alterado em relação à versão original, de acordo com as observações levantadas pela banca examinadora no dia da defesa, sob responsabilidade única da autora e com a anuência dos orientadores.



**MINISTÉRIO DA EDUCAÇÃO**  
**Fundação Universidade Federal do ABC**

Avenida dos Estados, 5001 – Bairro Santa Terezinha – Santo André – SP  
CEP 09210-580 · Fone: (11) 4996-0017

**FOLHA DE ASSINATURAS**

Assinaturas dos membros da Banca Examinadora que avaliou e aprovou a Defesa de Tese de Doutorado do candidato, DAFNE CAROLINA ARIAS PERDOMO realizada em 21 de Setembro de 2022:

Documento assinado digitalmente



**ALEX GOMES DIAS**  
Data: 27/09/2022 11:43:24-0300  
Verifique em <https://verificador.iti.br>

**Prof.(a) ALEX GOMES DIAS**  
UNIVERSIDADE FEDERAL DO AB

**Prof.(a) BRIGITTE HILLER**  
UNIVERSIDADE DE COIMBRA



Assinado por: Brigitte  
Anabelle Vaz de Abreu Hiller  
Identificação: 811204135  
Data: 2022-09-27 às 21:17:43

**Prof.(a) FERNANDO FEBRES CORDERO**

DocuSigned by:  
*Fernando Febres Cordero*  
10F5DC1976394ED

Documento assinado digitalmente



**MARCELO AUGUSTO LEIGUI DE OLIVEIRA**  
Data: 21/09/2022 19:14:06-0300  
Verifique em <https://verificador.iti.br>

**Prof.(a) MARCELO AUGUSTO LEIGUI DE OLIVEIRA**  
UNIVERSIDADE FEDERAL DO ABC

**Prof.(a) ALEX HEINZ LADISLAUS BLIN**  
UNIVERSIDADE DE COIMBRA

Assinado por: **ALEX HEINZ LADISLAUS BLIN**

Num. de Identificação: CR-PT-06  
Data: 2022.09.28 11:09:30+01'00'

**Prof.(a) CELSO CHIKAHIRO NISHI**  
UNIVERSIDADE FEDERAL DO ABC

**Prof.(a) ORLANDO LUIS GOULART PERES**  
UNIVERSIDADE ESTADUAL DE CAMPINAS

**Prof.(a) PEDRO GALLI MERCADANTE**  
UNIVERSIDADE FEDERAL DO ABC

Documento assinado digitalmente



**MARCOS DONIZETI RODRIGUES SAMPAIO**  
Data: 21/09/2022 16:44:44-0300  
Verifique em <https://verificador.iti.br>

**Prof.(a) MARCOS DONIZETI RODRIGUES SAMPAIO**  
UNIVERSIDADE FEDERAL DO ABC - Presidente

\* Por ausência do membro titular, foi substituído pelo membro suplente descrito acima: nome completo, instituição e assinatura



Universidade Federal do ABC

---

## **Folha de Citação de Apoio à CAPES**

This study was financed in part by the Coordenação de Aperfeiçoamento de Pessoal de Nível Superior - Brasil (CAPES) - Finance Code 001

---

ARIAS PERDOMO, Dafne Carolina

ABORDAGENS PRÁTICAS PARA TEORIAS DE CALIBRE:  
FUNÇÕES DO GRUPO DE RENORMALIZAÇÃO EM DOIS LAÇOS  
DENTRO DA REGULARIZAÇÃO IMPLÍCITA 4D / Dafne Carolina  
Arias Perdomo - Santo André, Universidade Federal do ABC, 2022.

140 fls. XX cm

Orientador: MARCOS SAMPAIO

Tese (doutorado) - Universidade Federal do ABC, Programa de Pós-  
Graduação em Física, 2022

1. Implicit Regularization. 2. Regularization schemes. 3. Gauge  
theories. 4. Anomalous dimension. 5. Renormalization. I. ARIAS PER-  
DOMO, Dafne Carolina. II. Programa de Pós-Graduação em Física, 2022.  
III. Abordagens práticas para teorias de calibre: funções do grupo de renor-  
malização em dois laços dentro da Regularização Implícita 4D





---

Niels Abel, 1828 (Mathematician):

“Divergent series are the devil’s invention...”

---



---

## Resumo

Os dados coletados no LHC não indicam desvios significativos das previsões do Modelo Padrão (SM). Considerando que observáveis de precisão podem ser previstos já em dois e três laços, é evidente a necessidade de desenvolver testes rigorosos do SM. Calculamos a função  $\beta$  de 2 laços de Yang-Mills puro (YM), Eletrodinâmica Quântica (QED) e Cromodinâmica Quântica (QCD) usando o método do campo do fundo (BFM) usando Regularização Implícita (IREG). Também calculamos a função  $\gamma$  (a dimensão anômala do campo) de 2 laços da QED. Uma comparação completa com abordagens dimensionais, como regularização dimensional convencional (CDR) e redução dimensional (DRED), é apresentada. Sutilezas relacionadas à álgebra de Dirac em integrais divergentes na presença de laços gluônicos ou fermiônicos, bem como esquemas de renormalização são cuidadosamente discutidas dentro na IREG. Finalmente, dois algoritmos para o cálculo automatizado da função  $\beta$  e da função  $\gamma$  foram desenvolvidos no Mathematica. Algumas das estratégias computacionais aplicadas são apresentadas.

**Palavras chave:** Regularização Implícita, esquemas de regularização, teorias de calibre, dimensão anômala, renormalização.

## Abstract

The data collected at the LHC do not indicate significant deviations from the predictions of the Standard Model (SM). Taking into account that precision observables can be predicted already at two and three loops, it is evident the necessity to develop stringent tests of the SM. We compute the 2-loop  $\beta$ -function of pure Yang-Mills (YM), Quantum Electrodynamics (QED), and Quantum Chromodynamics (QCD) using the background field method (BFM) in a full setup using Implicit Regularization (IREG). We also calculate the 2-loop  $\gamma$ -function (field anomalous dimension) of QED. A thorough comparison with dimensional approaches such as conventional dimensional regularization (CDR) and dimensional reduction (DRED) is presented. Subtleties related to Dirac algebra inside divergent integrals in the presence of gluonic or fermionic loops as well as renormalization schemes are carefully discussed within IREG. Finally, two algorithms for the automated calculation of the  $\beta$ -function and the  $\gamma$ -function were developed in Mathematica. Some of the computational strategies applied are presented.

**Keywords:** Implicit Regularization, regularization schemes, gauges theories, anomalous dimension, renormalization.



---

## Acknowledgments

I thank my father, Dr. Pio José Arias González, who has been my guide and my personal superhero throughout this process of studying and doing physics. Not all people are blessed with a father who is also a theoretical physicist (let alone a father working in the same area of Quantum Field Theory). I have always admired my father's passion and good will in science. He is a man of extreme ethics, always willing to help his colleagues, regardless of their political positions or personal problems. I thank him for all the useful discussions regarding QFT and research methodology, which have obviously been a great influence on the writing of this thesis. Furthermore, I am grateful for his strength, which is an example for me to follow. Doing science and getting along in academic life is a task that requires resilience and a great will to move forward even in the face of adversity. Many have abandoned their position as professors in Venezuela due to the crisis, but my dad is still there working and doing science.

I thank my advisor, Dr. Adriano Cherchiglia, for all his help in the most critical moments of this research work. Adriano is an excellent young researcher with a great intuition for particle physics. He has a genius that never fails to impress me. After each meeting, all his advises and opinions were more than important for the development of this work. I also thank him for his friendship and patience, being willing to help whenever possible.

I also thank my advisor Dr. Marcos Sampaio for the trust placed in me to carry out this work. At a very critical moment for me, during what was August 2017, I chose to leave Venezuela (again) to pursue a Ph.D. I'm still not sure what Marcos saw in me, but thanks to him agreeing to work with me, I had the opportunity not only to leave my country again to work but also to have a better training in physics. These 4 years in Brazil have changed my life for the better, and I owe it to Marcos for giving me the opportunity.

I thank my co-advisor for the sandwich program, Dr. Brigitte Hiller, for receiving me at the Universidade de Coimbra to participate in the CAPES-PrInt program. During my time in Coimbra I was able to do the 1-loop calculations that appear in this work as well as learn to use computational tools to carry out the 2-loop computations. Finding not only strong but also kind women who do science is always a blessing and a great motivation. I am happy and grateful to have met Brigitte.

I thank my family: my mother Zulay, my brother Pio, and my cousin Yaritza which I have missed them deeply in these 4 years and I would give everything for a hug from my mom. Furthermore, I also thank my uncles and aunts: Pedro, Xiomara, Mariela, Asdrubal, Ana, Gustavo, Irene, Adriana, Juan and my cousins Luis, Wesley, Javier and Jennifer. All have supported me to get to where I am.

---

I thank my colleagues from the Laboratory L213 in the UFABC's Block L: Dr. Giovane, Dr. William, Dr. Diego, and Dr. Julio. Having good co-workers makes the learning process more bearable. The lab felt massive and lonely after they graduated.

I thank the students of the implicit regularization group: Yuri, Ana, and, Ricardo. As well as the professors who are members of the Journal Club of Particles and Fields of the UFABC. Each discussion and each meeting helped me to be a better researcher.

In this very difficult process of doing a Ph.D. I thank all the friends made along the way, especially Kariny and Ana. Brilliant young women in their careers as experimental physicists. Every laugh, every hug, every conversation was a great support in this thesis.

I thank my Hispanic friends: Gaby, Pamela, Yubiry, María Abreu, William Njoku (honorary Hispanic), and Sofia. And I also thank my eternal friends Angel, Mota, Oswaldo Daniel, and Yusneida. Friends with whom you can speak your native language and who love and care about you, it is always necessary. I thank Fátima and Kuzma for having received me in their República in which I lived during the first 2 and a half years of the Ph.D. They were both friends and parents who cared for me throughout this period.

During the Ph.D. I not only learned and received classes, I also learned to teach and share knowledge. I would like to thank Natália for having motivated me to start this process, being my first student. Each class and each conversation made me discover how much I love this process of teaching.

Finally, I thank Mélissa, the big dodo. I thank her first: the love and the company. Having been away from your family for more than 4 years, it is precious to know that you have such a kind person by your side who becomes your family, who does not make you feel alone. I also thank her for having taught me to forgive, from my master's degree in France until now it was very difficult for me to forgive myself for everything that happened in the past, and she taught me to see that I was a person who had grown a lot since that stage. Finally: I thank her for her patience. That strength and the ability to be so present, even in the distance, is something that I appreciate every day.

To the jury that read this thesis: thank you very much for your patience. All your comments and criticisms are welcome.

These studies were financed in part by the Coordenação de Aperfeiçoamento de Pessoal de Nível Superior - Brasil (CAPES) - Finance Code 001. Thus, I acknowledge CAPES for the given financial support in the form of a Ph.D. scholarship.



---

List of Publications:

- Cherchiglia, A., Arias-Perdomo, D.C., Vieira, A.R. et al. Two-loop renormalisation of non-Abelian gauge theories in 4D Implicit Regularisation. PoS(EPS-HEP2021)725. <https://doi.org/10.22323/1.398.0725>
  - Arias-Perdomo, D.C.; Cherchiglia, A.; Hiller, B.; Sampaio, M. A Brief Review of Implicit Regularization and Its Connection with the BPHZ Theorem. Symmetry 2021, 13, 956. <https://doi.org/10.3390/sym13060956>
  - Cherchiglia, A., Arias-Perdomo, D.C., Vieira, A.R. et al. Two-loop renormalisation of gauge theories in 4D implicit regularisation and connections to dimensional methods. Eur. Phys. J. C 81, 468 (2021). <https://doi.org/10.1140/epjc/s10052-021-09259-6>
-



<b>1</b>	<b>Introduction and motivation</b>	<b>27</b>
1.1	Thesis review and main contributions . . . . .	32
<b>2</b>	<b>Renormalization of gauge theories</b>	<b>36</b>
2.1	Introduction: About regularization and renormalization . . . . .	36
2.2	Gauge theories at 2-loop . . . . .	38
2.2.1	The electron self-energy at 2-loop . . . . .	39
2.2.2	The quark self-energy at 2-loop . . . . .	40
2.3	The Renormalization Group Functions . . . . .	41
2.3.1	The $\beta$ -function . . . . .	43
2.3.2	The anomalous dimensions . . . . .	44
2.4	The background field method . . . . .	44
<b>3</b>	<b>Regularization methods and Implicit Regularization</b>	<b>50</b>
3.1	Implicit regularization . . . . .	50
3.1.1	IREG procedure . . . . .	50
3.1.2	Practical example: the electron propagator at 1-loop within IREG . .	53
3.1.3	The finite terms in IREG . . . . .	57
3.2	Dimensional schemes . . . . .	59
3.2.1	The electron propagator with DS . . . . .	61
3.3	$I_{log}$ in CDR: correspondence at 1-loop. . . . .	63
3.3.1	About correspondence to higher orders . . . . .	64
<b>4</b>	<b>Practical approaches to 2-loop calculations</b>	<b>69</b>
4.1	Methodology . . . . .	69

4.1.1	Algorithm: $\beta$ -function . . . . .	69
4.1.2	Algorithm: anomalous dimensions . . . . .	71
4.2	Quadratically divergent terms . . . . .	72
4.3	Gauge theories with IREG at 2-loop: examples . . . . .	74
4.3.1	Example 1: 2-loop approach in pure Yang-Mills . . . . .	74
4.3.2	Example 2: Quadratic terms in 2-loop QED . . . . .	77
4.4	The $\beta$ -function in IREG and DS . . . . .	78
4.5	The anomalous dimensions in gauge theories . . . . .	80
4.6	The gauge-fixing parameter in IREG . . . . .	80
<b>5</b>	<b>The two-loop gauge <math>\beta</math>-function for Abelian and non-Abelian theories</b>	<b>83</b>
5.1	Pure Yang-Mills . . . . .	83
5.1.1	Summary of results for pure YM . . . . .	87
5.2	QED . . . . .	90
5.2.1	Summary of results for QED . . . . .	92
5.3	QCD . . . . .	93
5.3.1	Summary of results for QCD . . . . .	93
<b>6</b>	<b>The anomalous dimensions at 2-loop within IREG</b>	<b>97</b>
6.1	Electron-propagator structure and renormalization in QED . . . . .	97
6.2	The amplitudes for the massless case . . . . .	99
6.3	Non-local terms and counterterms . . . . .	100
6.3.1	$Z_\Psi$ at 1-loop order . . . . .	100
6.3.2	$Z_\Psi$ at 2-loop order . . . . .	101
6.4	The renormalization constant of the electron field . . . . .	102
6.5	The anomalous dimension at 2-loop . . . . .	103
6.6	The gauge parameter dependence for $\gamma$ -function . . . . .	104
6.7	Results of $\gamma$ -function for the massless case . . . . .	105
6.8	Perspectives and discussion: the anomalous mass dimension for QED and non-Abelian theories . . . . .	105
6.8.1	The renormalization constant of the mass in QED . . . . .	106
6.8.2	Mass insertion and helicity flip . . . . .	107
6.8.3	Amplitudes and counterterms for massive QED . . . . .	108
6.8.4	Quark mass anomalous dimension in QCD . . . . .	109
<b>7</b>	<b>Conclusions</b>	<b>112</b>

<b>Appendices</b>	<b>115</b>
<b>A Appendix A: Notations, Feynman rules, and list of acronyms</b>	<b>116</b>
<b>B Appendix B: Another application example of IREG at 1-loop</b>	<b>118</b>
<b>C Appendix C: The Background Field Method for Yang-Mills at 1-loop order</b>	<b>121</b>
<b>D Appendix D: Electron propagator of QED at 1-loop with CDR and DRED</b>	<b>127</b>
D.1 Electron-propagator in CDR at 1-loop . . . . .	128
D.1.1 Finite terms with CDR . . . . .	130
D.2 Electron-propagator in DRED at 1-loop . . . . .	130
<b>E Appendix E: Explicit results of integrals</b>	<b>132</b>
E.1 General IREG integrals . . . . .	132
E.1.1 1-loop: two point functions . . . . .	132
E.1.2 1-loop: three point functions . . . . .	132
E.1.3 2-loop: explicit results involving logarithms . . . . .	133
E.1.3.1 One point functions . . . . .	133
E.1.3.2 Two point functions . . . . .	133
E.1.3.3 Three point functions . . . . .	133
E.1.4 2-loop: overlapped integrals . . . . .	133
E.2 Integrals for QED . . . . .	134
E.2.1 Massless case . . . . .	134
<b>Bibliography</b>	<b>137</b>

## LIST OF FIGURES

1.1	Standard Model of particle physics. . . . .	28
1.2	Dinosaur plot. . . . .	29
1.3	Higgs productions via gluon fusion. . . . .	29
1.4	Quark propagator correction. . . . .	30
2.1	The vertices with three and with four bosons's interactions in a YM theory. .	39
2.2	1-loop electron self-energy contributions. . . . .	40
2.3	2-loop electron self-energy contributions. . . . .	40
2.4	The correction of the quark propagator at 1-loop level. . . . .	42
2.5	The correction of the quark propagator at 2-loop level. . . . .	42
2.6	Evolution of the coupling with energy scale. . . . .	44
2.7	Gauge-fixed renormalization diagrams. . . . .	47
2.8	Determination of the renormalization factor $\delta_\alpha$ . . . . .	48
3.1	Graphic representation of the framework in dimensional methods. . . . .	60
3.2	Internal and external gluons. . . . .	62
3.3	Electron self-energy corrections withing DRED. . . . .	62
4.1	Topologies at 2-loop for the 2-point function. . . . .	70
4.2	Algorithm used in our automatic calculation. . . . .	71
4.3	Algorithm used for the automatic calculation. . . . .	72
4.4	Process at 2-loop in pure Yang-Mills. . . . .	74
4.5	Feynman rules for the BFM. . . . .	75
5.1	Diagrams for the calculation of the pure YM $\beta$ -function at 1-loop. . . . .	83
5.2	2-loop correction to the 2-point function of the BF A for pure Yang-Mills. . .	84

5.3	Counterterms diagrams. . . . .	86
5.4	Diagram for the calculation of QED's $\beta$ -function at one-loop. . . . .	91
5.5	Two-loop correction to the two-point function of the background field - fermionic contribution of QCD . . . . .	93
6.1	Mass insertion example. . . . .	107
C.1	Diagrams for the calculation of the pure YM $\beta$ -function at one-loop. . . . .	121
C.2	Tadpole diagrams for the calculation of the pure YM $\beta$ -function at one-loop. . . . .	124

## LIST OF TABLES

3.1	Treatment of internal and external gluons in dimensional methods. . . . .	61
5.1	Results for pure Yang-Mills using IREG where $\rho_{IREG} = I_{log}(\lambda^2) \ln \left[ -\frac{p^2}{\lambda^2} \right]$ . . .	85
5.2	Counterterms results for pure Yang-Mills using IREG where $\rho_{IREG} = I_{log}(\lambda^2) \ln \left[ -\frac{p^2}{\lambda^2} \right]$ . . .	86
5.3	Results for pure Yang-Mills using CDR and DRED, where $\rho = \gamma_E - \ln 4\pi + \ln(p^2/\mu_{DR}^2)$ . . . . .	88
5.4	Counterterms results for pure Yang-Mills using CDR and DRED, where $\rho = \gamma_E - \ln 4\pi + \ln(p^2/\mu_{DR}^2)$ . . . . .	88
5.5	Results for QED using IREG where $\rho_{IREG} = I_{log}(\lambda^2) \ln \left[ -\frac{p^2}{\lambda^2} \right]$ . . . . .	91
5.6	Results QED using CDR and DRED, where $\rho = \gamma_E - \ln 4\pi + \ln(p^2/\mu_{DR}^2)$ . . .	91
5.7	Counterterm results for QED using IREG where $\rho_{IREG} = I_{log}(\lambda^2) \ln \left[ -\frac{p^2}{\lambda^2} \right]$ . . .	92
5.8	Counterterm results for QED using CDR and DRED, where $\rho = \gamma_E - \ln 4\pi + \ln(p^2/\mu_{DR}^2)$ . . . . .	92
5.9	Results for fermionic part of QCD using IREG where $\rho_{IREG} = I_{log}(\lambda^2) \ln \left[ -\frac{p^2}{\lambda^2} \right]$ . . .	94
5.10	Results for fermionic part of QCD using CDR and DRED. . . . .	94
5.11	Results for fermionic part of QCD using IREG where $\rho_{IREG} = I_{log}(\lambda^2) \ln \left[ -\frac{p^2}{\lambda^2} \right]$ . . .	94
5.12	Results for fermionic part of QCD using CDR and DRED. . . . .	95

---

## DEDICATORY

In fond memory of my grandmother, Bayú. Thank you for waiting for me even  
though I couldn't make it.

---





---

**Part 1:**

Theory

---



## CHAPTER 1

## INTRODUCTION AND MOTIVATION

Inside Quantum Field Theory (QFT), perturbation theory is tailored to calculate and study the behavior of particles at high energies. To achieve this, QFT incorporates concepts of quantum mechanics and special relativity. Moreover, QFT is, until now, one of the most successful paradigms from the experimental and theoretical perspective, being the Standard Model of particles (SM) one of the most representative examples of it. The SM is the theory that describes the fundamental building blocks of matter and their interactions. Thus, using QFT, we have the necessary tools to calculate observables in particle physics and compare them with the corresponding experimental measurements.

The SM describes the universe as composed of six quarks, six leptons, their corresponding anti-particles, the Higgs boson, and four known interactions, each mediated by a fundamental particle<sup>1</sup>. Many decades ago, Murray Gell-Mann proposed the quarks to explain the behavior of particles discovered through high-energy atomic collisions. The quarks postulated by Gell-Mann were a mathematical device, and not something physical. At that time, the model of partons also appears submitted by Feynman in an article of the year 1969 (1), where such partons were proposed to study the collisions of particles with the presence of hadrons in the initial state. Sometime later, it was concluded that the partons of Feynman were the same quarks (and gluons) that Gell-Mann conceived.

Currently, the SM is a successful theory with an impressive agreement between theory and experiment Fig. 1.2 (2). Nevertheless, experiments in the Large Hadron Collider (LHC), for example, have not identified physical evidence beyond the standard model (BSM). Unraveling physics BSM has entreated theoretical predictions for observables beyond the next-to-leading-order (NLO). Their precise calculations are as important as finding new particles because

---

<sup>1</sup>The Standard Model describes three fundamental forces, but does not include gravity.

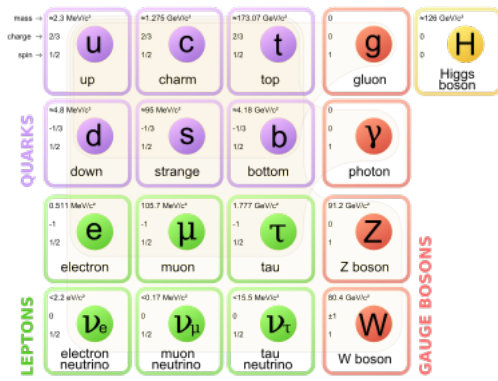


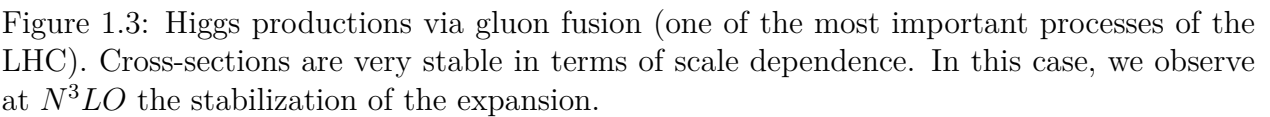
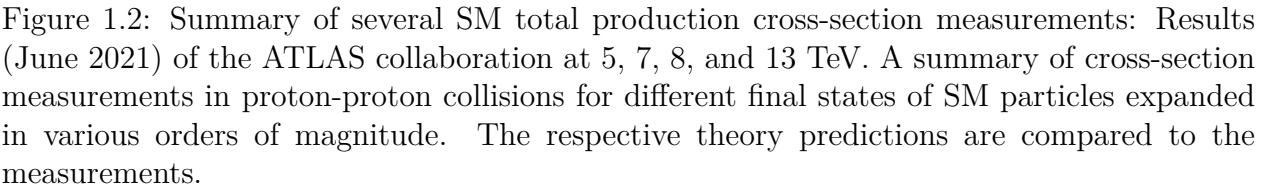
Figure 1.1: Standard Model of particle physics: the assembly of physical laws that governs the behavior of elementary particles. This theory is based on 3 fundamental concepts: the theory of special relativity, quantum mechanics and the principle of invariance by symmetries. The Yukawa interaction is also used in the SM to describe the coupling between the Higgs field and the massless quark and lepton fields.

they help to confirm, redress, or refute new models. An example of the need for computations in  $N^3LO$  is the QCD corrections to gluon-fusion Higgs boson production at 13 TeV (3). The stability of the perturbation expansion, measured by the total cross section, is observed in the third-order  $N^3LO$  approximation Fig. 1.3. Because experimental uncertainties are expected to drop below the accuracy of theoretical predictions, QCD theoretical uncertainties ought to be reduced at many levels so BSM physics can be ascertained.

As shown in Fig. 1.2, one of the observables that theoretical physicists calculate and experimental physicists measure is the cross-section which describes the probability that two particles will collide and interact in a certain way. It is a measurement of the probability that an event occurs. For a collision process, the cross-section is obtained from the square of scattering amplitudes. For that reason, the calculation of amplitudes is at the core of QFT. These amplitudes contain all the dynamical information required to understand the interaction processes between particles. For example, when analyzing collisions in hadron colliders, the cross-section  $\sigma$  is given by:

$$\sigma(p_1 p_2 \rightarrow X) = \underbrace{\sum_{ij} \int dx_1 \int dx_2 f_i^{p_1}(x_1) f_j^{p_2}(x_2)}_{\text{Non-perturbative parton distributions}} \times \underbrace{\hat{\sigma}(ij \rightarrow X)}_{\text{Perturbative parton cross-section}}, \quad (1.1)$$

where the  $f_i^{p_j}(x_j)$  are the so-called partonic distribution functions, that reflect the probability of finding the parton  $i$  in the hadron  $j$  with a total fraction of momentum  $x_j$ . The cross-section  $\hat{\sigma}(ij \rightarrow X)$  is known as the partonic hard cross-section, in which only point particles (the partons) intervene. Equation (1.1) was proposed heuristically in 1969 by Feynman (1).



As mentioned, we can write:

$$\hat{\sigma} \propto |A|^2, \quad (1.2)$$

where  $A$  is the scattering amplitude. From the theoretical physics standpoint, for the high-precision calculation of  $A$ , we need an expansion in perturbation theory (whenever it is possible to apply it). In the context of QCD, for example, this amplitude is expanded as a power series in the strong coupling,  $\alpha_s$ , according to:

$$A = \alpha_s \left( A^{\text{tree}} + \frac{\alpha_s}{2\pi} A^{1\text{-loop}} + \left( \frac{\alpha_s}{2\pi} \right)^2 A^{2\text{-loop}} + \dots \right), \quad (1.3)$$

where the first coefficient  $A^{\text{tree}}$  is known as the tree amplitude, the second  $A^{1\text{-loop}}$  is the 1-loop amplitude and continues. The names come because these coefficients are related to Feynman diagrams, as in Fig. 1.4. Such predictions rely on Feynman diagram calculations to evaluate scattering amplitudes. Therefore, making theoretical predictions involves adding more and more terms to the series to get the same precision as an experimental measurement.

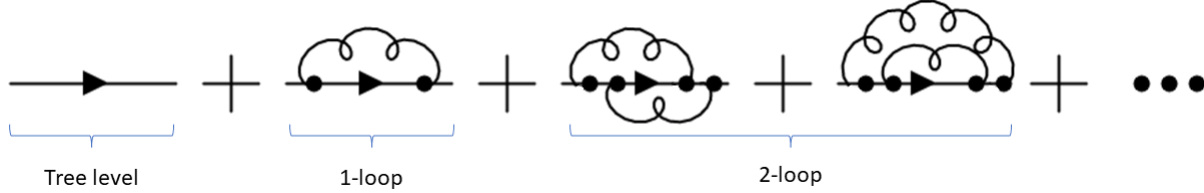


Figure 1.4: Quark propagator radiative corrections: At the tree level, we have the quark propagator represented by a line that contains no loops. All such processes receive higher-order contributions, known as radiative corrections, from diagrams that do contain loops. At 1-loop, we have the first correction and so on. This process and its corrections are represented by Feynman diagrams. These diagrams constitute pictorial representations of the mathematical expressions that govern the behavior of particles.

However, despite the success of QFT, this does not mean that the theory does not have relevant drawbacks when it comes to perturbation theory. From the Lagrangian of a theory, we can build the necessary rules to draw diagrams like the ones in Fig. 1.4. For example, for  $\phi^4$ :

$$\mathcal{L}_{\phi^4} = \frac{1}{2}(\partial_\mu \phi)^2 - \frac{1}{2}m^2\phi^2 - \underbrace{\frac{g}{4!}\phi^4}_{\text{interaction term}}, \quad (1.4)$$

we have:

$$\text{---} \overset{p}{\text{---}} = \frac{i}{p^2 - m^2}; \quad (1.5)$$

$$\begin{array}{c} \diagup \\ \diagdown \end{array} \begin{array}{c} \diagdown \\ \diagup \end{array} = -ig, \quad (1.6)$$

where propagators are represented in the diagrams as internal lines, while the vertices represent the interactions, they are “contact” terms between the fields. Additionally, we must impose momentum conservation at each vertex, and integrate over the undetermined momenta on each loop. In the end, it means that for every diagram with one or more loops, we really have a momentum space integral. These integrals will appear in any calculation, even at first order in perturbation theory. In general, these integrals produce a divergent result. Returning to our example, if we apply the Feynman algorithm to the next perturbative diagram in  $\phi^4$ , we get the amplitude:

$$\begin{array}{c} \begin{array}{c} \text{---} \overset{p_1}{\text{---}} \quad \text{---} \overset{p_4}{\text{---}} \\ \text{---} \overset{p_2}{\text{---}} \quad \text{---} \overset{p_3}{\text{---}} \end{array} \end{array} = (-ig)^2 \frac{1}{2} \int_k \frac{i^2}{(k^2 - m^2)[(k - p)^2 - m^2]}, \quad (1.7)$$

where  $p = p_1 + p_2$ . The integral in Eq. (1.7) is divergent. Consequently, when performing higher-order calculations in QFT, we would like to understand the nature of divergent integrals.

As we saw, doing higher order calculations in QFT, divergences are present beyond leading order calculations. One of these types of divergences is the so-called ultraviolet divergences (**UV-div**) which arises explicitly when the momentum of the loop integral goes to infinity. They must be removed before numerical evaluation of Feynman amplitudes in *NLO*, and higher others. The process to remove the divergences is one of the key toolkits for perturbative precision calculations in collider physics (and others). For the implementation of an efficient computational code, we seek for practical regularization schemes. These regularization schemes help to separate the divergences in QFT. Recently, novel schemes have been proposed aiming at improving the conventional dimensional regularization (CDR) (4). For

---

example, in dimensional-specific quantum field theories, such as supersymmetric ones (5; 6), CDR needs modifications such as dimensional reduction (DRED) (7), which leads to additional terms at the Lagrangian level. For that reason, the problem of **UV-div** in  $N^2LO$  and  $N^3LO$  would be greatly simplified in a purely 4-dimensional scheme. *Implicit regularization* (IREG) is one of these non-dimensional methods (4). The IREG technique looks promising for numerical implementations and extraction of **UV-div** in  $NLO$  and higher orders.

Thus, we can see that **UV-div** are all-over beyond leading order in cross-section calculations and must be judiciously removed in automated computation codes for the evaluation of scattering amplitudes. One of our objectives is to understand these difficulties when they arise in 2-loop order for gauge theories and tackle them with IREG. In this thesis, we implement second order ( $N^2LO$ ) techniques. The approach we used to handle the **UV-div** is through the regularization scheme IREG. We discussed how the IREG technique works in 2-loop order. We applied it to gauge theories to compute the coefficients of the renormalization group functions (RG). One of the objectives of the RG functions analysis is to discover how certain parameters (the coupling constant, the mass, the field strength) change with the scale of interest. If you have more knowledge regarding the coefficients of the RG functions, you have control over the evolution of your parameters. Therefore, these coefficients are good for evaluating and testing conjectures. We calculate the  $\beta$ -function in a minimal subtraction scheme ( $\overline{IREG}$ ) for pure Yang-Mills (YM), quantum electrodynamics (QED), and quantum chromodynamics (QCD). Furthermore, we compute the  $\gamma$ -function of QED at 2-loop order, being the main original result not yet submitted for publication. These calculations constitute a consistency test for the IREG method. Thanks to this, we developed tools with FeynArts based on IREG for efficient computational code to evaluate these beyond LO amplitudes.

## 1.1 Thesis review and main contributions

This thesis is divided into seven chapters and four appendices in which the theoretical aspects of this research are described. We show in particular our results for gauge theories:

- **Chapter 1:** the chapter presents the current status of precision calculations, an introduction to the origin of divergences in QFT, and a little discussion about regularization schemes. This chapter expresses the motivation behind theoretical precision computations in particle physics. The chapter mentions the regularization schemes which are covered in the next chapters: CDR, DRED, and IREG.
- **Chapter 2:** we make a discussion of the terminology used in this work: regularization, regularization schemes, renormalization, and renormalization schemes. We also present



the functions of the renormalization group for gauge theories. In the end, we discuss the Background Field Method (BFM).

- **Chapter 3:** in this chapter, we provide a brief panorama of regularization schemes with a focus on IREG rules that will be used throughout the thesis. We use as an example to present the IREG rules the calculation of the amplitude of the electron propagator at 1-loop order. We also discuss some subtleties related to Dirac Algebra inside divergent integrals between IREG and dimensional methods.
- **Chapter 4:** we discuss the algorithm that we are implementing in our work for calculating the  $\beta$ -function at 2-loop for gauge theories. We present also the algorithm used for the  $\gamma$ -function. We study an example at 2-loop order for Yang-Mills and QED. We present the  $\beta$ -function and the procedure to calculate its first two coefficients in the different regularization schemes. We also discuss the anomalous dimension in gauge theories as well as the gauge-fixing parameter in IREG. Finally, in Chapter. 4, the use of these algorithms seems to indicate that with IREG for gluonic loops we have to apply Feynman's rules to the entire 2-loop diagram before using IREG. Meanwhile, for fermionic loops, we have to apply the rules to the sub-diagram first, and then contract with the fermion lines of the other loop before applying IREG.
- **Chapter 5:** in this chapter, we present the corresponding results for the  $\beta$ -function at 2-loop for YM, QED, and QCD with IREG at 2-loop order. We define the expansion of the  $\beta$ -function in the adimensional coupling constant as:

$$\beta = -g_R \left[ \beta_0 \left( \frac{\tilde{g}_R}{4\pi} \right)^2 + \beta_1 \left( \frac{\tilde{g}_R}{4\pi} \right)^4 \right]; \quad (1.8)$$

The 2-loop contributions for the gauge  $\beta$  coupling in YM were found to be:

$$\beta_0|_{\text{IREG}} = \frac{11C_A}{3}; \quad (1.9)$$

$$\beta_1|_{\text{IREG}} = \frac{34C_A^2}{3}; \quad (1.10)$$

QED:

$$\beta_0|_{\text{IREG}} = -\frac{4}{3}; \quad (1.11)$$

$$\beta_1|_{\text{IREG}} = -4; \quad (1.12)$$

---

and QCD:

$$\beta_0|_{\text{IREG}} = 11 - \frac{2}{3}n_f; \quad (1.13)$$

$$\beta_1|_{\text{IREG}} = 102 - \frac{38}{3}n_f; \quad (1.14)$$

which were compared with the results from dimensional schemes. The  $\beta$ -function IREG results match the results of the dimensional methods. For the YM and QCD calculations, we implemented the Background Field Method (BFM) with IREG.

- **Chapter 6:** in this chapter, we present the corresponding results for the  $\gamma$ -function (the anomalous dimension of the field) at 2-loop for QED with IREG at 2-loop order. We calculate the 2-loop contribution of the  $\gamma$ -function for QED:

$$\begin{aligned} \gamma_1 e^2 &= \frac{e^2}{16\pi^2}, \\ \gamma_2 e^4 &= -\frac{1}{3} \frac{e^4}{2(4\pi)^4}. \end{aligned} \quad (1.15)$$

For this result, it was crucial to consider the gauge parameter dependency. Finally, we present the perspectives of future works that are in development for massive gauge theories.



## CHAPTER 2

## RENORMALIZATION OF GAUGE THEORIES

## 2.1 Introduction: About regularization and renormalization

As discussed in the introduction, perturbation theory in QFT leads to the appearance of divergent integrals; to work with these divergences, we introduce two new principles: regularization and renormalization.

Regularization is a mathematical procedure that systematically applies various mathematical operations to separate and isolate the divergences. The different types of regularization techniques to deal with the divergences are known as regularization schemes. Among them, we can find implicit regularization (IREG), dimensional regularization (CDR), dimensional reduction (DRED), and others.

After selecting a regularization scheme to isolate the divergences occurring in the integrals of our theory, we could think that our computation is finished. However, the expression is still dependent on energy scales. We need a method that not only allows us to isolate the divergences but also to isolate them without modifying the physical predictions of our theory. This is why we require renormalization.

Renormalization is the technique to understand the nature of the divergence and absorb them into the parameters of the theory. To absorb the divergences, we use the counterterms. They are, in principle, arbitrary terms. If we take  $\phi^4$  theory as an example, we saw for the diagram in Eq. (1.7) that at the first order of perturbation theory, we have divergences. If we define the field, the mass, and the coupling constant in Eq. (1.4), we can cancel the divergence for the 2 and 4-point functions. Thus, let us see how we can introduce the counterterms in  $\phi^4$ . First, we redefine a new set of variables:

$$\begin{aligned}
 \phi_0 &= Z_\phi^{1/2} \phi_R, \\
 m_0^2 &= Z_m m_R^2, \\
 g_0 &= Z_g g_R,
 \end{aligned} \tag{2.1}$$

where  $Z_\phi^{1/2}$ ,  $Z_m$  and  $Z_g$  will be chosen to cancel the infinities, they are the *renormalization constants*. Therefore, Eq. (1.4) changes to:

$$\mathcal{L}_{\phi_R^4} = \frac{1}{2}(\partial_\mu Z_\phi^{1/2} \phi_R)^2 - \frac{1}{2}Z_m m_R^2 (Z_\phi^{1/2} \phi_R)^2 - \frac{Z_g g_R}{4!} (Z_\phi^{1/2} \phi_R)^4. \tag{2.2}$$

Now, redefining again:

$$\begin{aligned}
 Z_\phi &= 1 + A, \\
 Z_\phi Z_m &= 1 + B, \\
 Z_\phi^2 Z_g &= 1 + C,
 \end{aligned} \tag{2.3}$$

we can write not only a new part of the Lagrangian but also new rules for it. The counterterms A, B, and C are the counterterms we mentioned before, they will contribute to the absorption of the divergence order by order. Thus:

$$\mathcal{L}_{\phi_R^4} = \frac{1}{2}(1 + A)(\partial_\mu \phi_R)^2 - \frac{1}{2}m_R^2(1 + B)\phi_R^2 - \frac{(1 + C)g_R \phi_R^4}{4!} \tag{2.4}$$

which can be rewritten as:

$$\mathcal{L}_{\phi_R^4} = \underbrace{\frac{1}{2}(\partial_\mu \phi_R)^2 - \frac{1}{2}m_R^2 \phi_R^2}_{\text{free Lagrangian}} - \underbrace{\frac{g_R}{4!} \phi_R^4}_{\text{interaction term}} + \underbrace{\frac{1}{2}A(\partial_\mu \phi_R)^2 - \frac{1}{2}Bm_R^2 \phi_R^2 - \frac{g_R}{4!}C\phi_R^4}_{\text{counterterms Lagrangian}}. \tag{2.5}$$

As we mentioned, we can deduce:

$$\text{----} \otimes \text{----} = i(Ap^2 - Bm_R^2), \tag{2.6}$$

---



$$= -ig_R C \quad (2.7)$$

Note again that by introducing these counterterms, new Feynman rules and diagrams were added to the theory. Different renormalization schemes can be applied to guarantee that the parameters are canceled. Unlike regularization schemes, renormalization schemes are the way regularized infinities will be removed by the counterterms. The word renormalization comes from the fact that we will modify the normalization of the variables of the theory to obtain the counterterms. Different physical or non-physical schemes can be adopted to decide how we cancel those infinities.

In this chapter, we will concentrate only on renormalization. In particular: We will discuss briefly the renormalization of the main theories used in this research, specifically, quantum electrodynamics (QED) and quantum chromodynamics (QCD). Also, we will introduce the Background Field Method (BFM) and the Renormalization Group (RG) functions.

## 2.2 Gauge theories at 2-loop

We will briefly introduce in this section gauge theories. When we talk about gauge invariance in a gauge field theory, the idea is that we could admit different field configurations which yield identical observables (8). There is no unique description for these systems. In other words, there is some inherent “ambiguity” in our physical descriptions. Therefore we can choose from which particular formulation to adopt in a given situation. However, regardless of that gauge’s choice and the freedom our theory gives us, the physical observables must be the same.

A transformation from one physical description to another is a gauge transformation, and the underlying invariance is known as gauge invariance, Ref. (8). These transformations form a mathematical group, and depending on the algebra of the group we can have: Abelian theories or non-Abelian theories <sup>1</sup> (9). Quantum Electrodynamics (QED) <sup>2</sup> is an Abelian theory that describes the interaction between all electrically charged particles. In QED, the only massless spin-1 particle is the photon. Theories like QED are constrained by abelian gauge invariance. By contrast, Yang-Mills (YM) theories are generalizations of QED with

---

<sup>1</sup>An example of non-Abelian theories are based on the  $SU(N)$  group, which is the group of traceless  $N \times N$  matrix fields with determinant 1.

<sup>2</sup>QED is an Abelian theory based on the  $U(1)$  group, the group of  $1 \times 1$  unitary matrices.

massless spin-1 particles that can interact among themselves. These theories are constrained by non-Abelian gauge invariance. QCD is a special case of a Yang-Mills theory <sup>3</sup>.



Figure 2.1: The vertices with three and with four bosons's interactions in a YM theory.

### 2.2.1 The electron self-energy at 2-loop

The QED Lagrangian is:

$$\mathcal{L}_0^{QED} = \bar{\psi}_0(i\not{D} - m)\psi_0 - \frac{1}{4}F_{0\mu\nu}F_0^{\mu\nu}, \quad (2.8)$$

where  $\psi_0$  is the electron field. Moreover:

$$D_\mu\psi_0 = (\partial_\mu + ie_0Q_\mu(x))\psi_0, \quad (2.9)$$

is its gauge covariant derivative,  $Q$  is the gauge field, and:

$$F_{0\mu\nu} = \partial_\mu Q_{0\nu} - \partial_\nu Q_{0\mu} \quad (2.10)$$

is the local invariant electromagnetic tensor.

As stated in (10), to have a photon propagator, we need to add also the term:

$$\Delta\mathcal{L} = -\frac{1}{2a_0}(\partial_\mu Q_0^\mu)^2. \quad (2.11)$$

The last equation Eq. (2.11) is know as the gauge-fixing equation term. The choosing of “ $a_0$ ”, the gauge-fixing parameter, correspond to the choice of the gauge. Some options are:

- $a_0 = 1$ , the Feynman 't Hooft gauge
- $a_0 = 0$ , Landau gauge.

---

<sup>3</sup>QCD is the  $SU(3)$  realization of a YM theory.  $SU(3)$  is the special (determinant equal to 1) unitary group. Its generators are traceless 3x3 unitary matrices.

---

Again, the physics described from QED cannot depend on the value of “ $a_0$ ”. In this work, we chose the Feynman ’t Hooft gauge.

The Lagrangian Eq. (2.8), (2.11) contains the mass  $m$ , the bare fields  $\psi_0$ ,  $Q_0$  and the bare parameters  $e_0$ ,  $a_0$ . The renormalized quantities are:

$$\psi_0 = \sqrt{Z_2}\psi, \quad Q_{0\mu} = \sqrt{Z_3}Q_\mu, \quad e_0 = Z_e e, \quad a_0 = Z_A a, \quad m_0 = Z_m m. \quad (2.12)$$

With this, we can derive the Feynman rules for QED. They can be found in Ref. (10).

The divergent diagrams for QED represent the radiative correction to the photon and electron propagators, as well as the vertex diagram. We will study in this chapter, and the next, the electron propagator, since it is the main correction of this research. For more reference on the other corrections, see Ref. (11).

At 1-loop level, in Fig. 2.2 we can find the corrections to the electron propagator. We will discuss the calculation of the Green’s functions for this diagram in Chapter. 3 and Appendix. D.

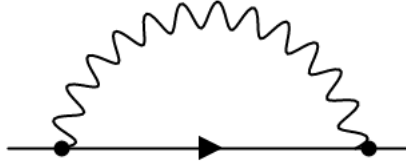


Figure 2.2: 1-loop electron self-energy contributions.

At 2-loop, in Fig. 2.3 we can find the corrections to the electron propagator:

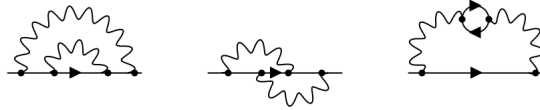


Figure 2.3: 2-loop electron self-energy contributions.

These diagrams in Fig. 2.3, were first calculated in (11) within Implicit Regularization (IREG). In contrast to (11), we adopt a different method for the 2-loop calculation that we will explain in the Chapter. 4.

### 2.2.2 The quark self-energy at 2-loop

The QCD Lagrangian reads



$$\mathcal{L}_0^{QCD} = -\frac{1}{4}F_{0\mu\nu}^a F_0^{a\mu\nu} - \frac{1}{2\xi}\partial^\mu Q_{0\mu}^a \partial^\nu Q_{0\nu}^a + \bar{\Psi}_0^i (i\not{D}_\mu^{ij} - m_0\delta^{ij})\Psi_0^j - \partial^\mu \bar{c}_0^a D_\mu^{ab} c_0^b \quad (2.13)$$

(for simplicity, we write down only one flavor according to the notation in Ref. (12); (13)) with  $D_\mu^{ab}$  and  $D_\mu^{ij}$  being the adjoint and fundamental representation of the color group  $SU(3)$ . Furthermore:

$$\begin{aligned} F_{0\mu\nu}^a &= \partial_\mu Q_{0\nu}^a - \partial_\nu Q_{0\mu}^a + g_0 f^{abc} Q_{0\mu}^b Q_{0\nu}^c, \\ D_\mu &= (\partial_\mu - ig_0 Q_{0\mu}^a t_r^a), \end{aligned} \quad (2.14)$$

$\xi$  is the gauge-fixing parameter,  $f^{abc}$  are real antisymmetric constants (under the exchange of any pair of indices),  $t^a$  are the generators of  $SU(N)$ , where  $SU(N)$  is the group of  $N \times N$  unitary matrices with determinant 1;  $Q_{0\mu}^a$  are the gauge fields coupled to Dirac fermions  $\Psi_0$  and to the ghost fields  $c_0$ . Index 0 stands for bare quantities.

The Lagrangian in Eq. (2.13), contains the bare fields  $\Psi_0$ ,  $Q_{0\mu}^a$ ,  $c_0^a$  and the bare parameters  $m_0$ ,  $\xi$  and  $g_0$ . For Eq. (2.13), the divergence are renormalized by absorbing them into the counterterms. The usual definitions are:

$$\begin{aligned} Q_{0\mu}^a &= Z_3^{1/2} Q_\mu^a, \\ c_0^a &= \tilde{Z}_3^{1/2} c^a, \\ \Psi_0 &= Z_2^{1/2} \Psi, \\ g_0 &= Z_g g, \\ m_0 &= Z_m m. \end{aligned} \quad (2.15)$$

Concerning Eq. (2.15), the only relevant diagram at 1-loop to compute the quark self-energy is Fig. 2.4. Turning to the 2-loop quark correction, in Fig 2.5 we can see the relevant diagrams. Notice that compared to QED in Fig. 2.3, at 2-loop order we have more diagrams in QCD. As we mentioned at the beginning of this section, the bosons in non-Abelian theories can interact with each other.

## 2.3 The Renormalization Group Functions

To explain the functions of the renormalization group, we will use a scalar theory for simplicity. For  $\phi^3$ - theory, using the field definitions (change of variables):

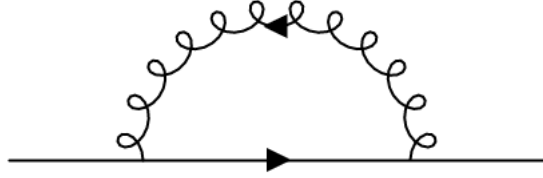


Figure 2.4: The correction of the quark propagator at 1-loop level.

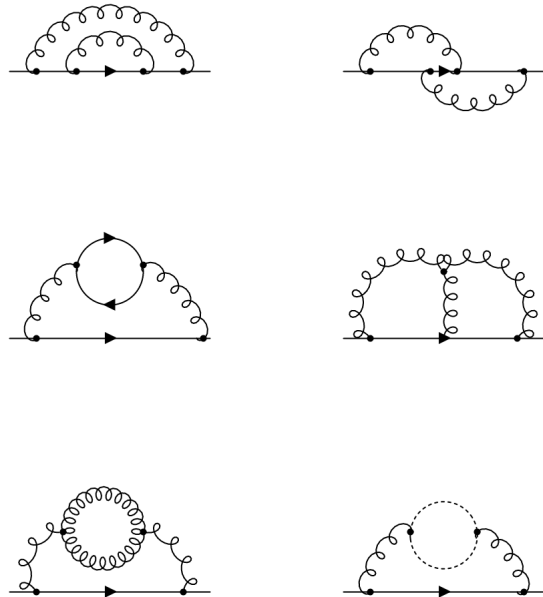


Figure 2.5: The correction of the quark propagator at 2-loop level.

$$\begin{aligned}
 \phi_0 &= Z_\phi^{1/2} \phi_R; \\
 m_0 &= Z_m^{1/2} m_R; \\
 g_0 &= Z_g g_R,
 \end{aligned} \tag{2.16}$$

we can re-write the Lagrangian in 2 parts:

$$\mathcal{L}_{\phi_R^3} = \underbrace{\frac{1}{2}(\partial_\mu \phi_R)^2 - \frac{1}{2}m_R^2 \phi_R^2}_{\text{free lagrangian}} - \underbrace{\frac{g_R}{3!} \phi_R^3}_{\text{interaction term}} + \underbrace{\frac{1}{2}A(\partial_\mu \phi_R)^2 - \frac{1}{2}Bm_R^2 \phi_R^2 - \frac{g_R}{3!}C\phi_R^3}_{\text{counterterms lagrangian}}. \tag{2.17}$$

where the counterterms A, B and, C are:

$$\begin{aligned}
 A &= Z_\phi - 1; \\
 B &= Z_m Z_\phi - 1; \\
 C &= Z_g Z_\phi^{3/2} - 1.
 \end{aligned} \tag{2.18}$$

Thus, we define the renormalization group functions for the general renormalization scale  $\lambda$  as:

$$\begin{aligned}
 \beta &= \lambda \frac{\partial}{\partial \lambda} g; \\
 \gamma &= \frac{\lambda}{2} \frac{\partial \ln Z_\psi}{\partial \lambda}; \\
 \gamma_m &= \lambda \frac{\partial \ln Z_m}{\partial \lambda}.
 \end{aligned} \tag{2.19}$$

This whole group of dimensionless parameters tells us about the energy scale dependence of the parameters in a renormalizable field theory. They are the renormalization group equations (RG). In the following subsections, we will explain each in more detail.

### 2.3.1 The $\beta$ -function

Physical predictions in our theories cannot depend on unphysical mass scales. Physical observables need to be independent. Let us now see what the  $\beta$ -function looks like for the gauges theories. As show in Eq. (2.19), the  $\beta$ -function is defined by:

$$\beta = \lambda \frac{\partial}{\partial \lambda} g_R, \tag{2.20}$$

where  $g_R$  is the (renormalized) gauge coupling of the theory considered, and  $\lambda$  is the renormalization scale. For example, you can see at 1-loop QED and QCD  $\beta$ -function in Fig. 2.6.



Figure 2.6: Evolution of a gauge coupling with energy scale in theories with  $\beta(g) > 0$  (in the case of the QED coupling) and  $\beta(g) < 0$  (in the case of the QCD coupling). As for QED, as the coupling grows, it becomes non-perturbative. Images obtained from Ref. (14).

### 2.3.2 The anomalous dimensions

In the general case of the anomalous dimensions, they describe the deviation of the scaling laws of various operators considered as a function of the running scales. Regarding for example the anomalous dimension, one has:

$$\gamma = \frac{\lambda}{2} \frac{\partial \ln Z_\psi}{\partial \lambda}. \quad (2.21)$$

The precise formula that relates the  $\beta$ -function and the anomalous dimensions to the counterterms will depend on the specific renormalization prescription of the calculation scheme. In Chapter. 4 and 6, we will discuss the prescription adopted in this research depending on the regularization and renormalization scheme adopted.

## 2.4 The background field method

We will be interested in the 2-loop  $\beta$ -function in non-Abelian gauge theories. As it is well-known, in QED we only need the 2-point photon correction since  $Z_g = Z_A^{-1/2}$ . Concerning non-Abelian theories, the situation is different. One may resort to the background field method (BFM) (15), which guarantees the relation  $Z_g = Z_{\hat{A}}^{-1/2}$  where  $\hat{A}$  is now the gluon background field. This simplifies the computation since only 2-point functions will be needed. Thus, in this thesis, we will only deal with 2-point functions.

The BFM is a technique for quantizing gauge field theories without losing explicit gauge invariance (15). The method was introduced by DeWitt (15; 16). The approach consists of doing a field-shifting, where a background field (BF) is added to the quantum field (QF) in

the action. Let us see how we apply the BFM approach for the pure Yang-Mills generating functional:

$$Z(J) = \int \mathcal{D}_Q \det \left( \frac{\delta G^a}{\delta w^b} \right) \exp \left[ i(S^{YM}(Q) - \frac{1}{2\alpha} G \cdot G + J \cdot Q) \right], \quad (2.22)$$

where  $Q$  is the gauge field,  $J$  is the source function, and the function inside the determinant is the gauge-fixing term.  $S^{YM}$  is the Yang-Mills action in terms of the gauge field  $Q$ :

$$S^{YM}(Q) = -1/4 \int d^4x (F_{\mu\nu}^a)^2 \quad (2.23)$$

with:

$$F_{\mu\nu}^a = \partial_\mu Q_\nu^a - \partial_\nu Q_\mu^a + g f^{abc} Q_\mu^b Q_\nu^c. \quad (2.24)$$

Besides:

$$J \cdot Q \equiv \int d^4x J_\mu^a Q_\mu^a \quad (2.25)$$

and:

$$G \cdot G \equiv \int d^4x G^a G^a. \quad (2.26)$$

By applying the BFM, the generating functional will now depend on the BF,  $\hat{A}$ , as below:

$$\tilde{Z}(J, \hat{A}) = \int \mathcal{D}_Q \det \left( \frac{\delta \tilde{G}^a}{\delta w^b} \right) \exp^{i(S^{YM}(Q+\hat{A}) - 1/2\alpha \tilde{G} \cdot \tilde{G} + J \cdot Q)} \quad (2.27)$$

where the derivative  $\delta \tilde{G}^a / \delta w^b$  is invariant under the gauge transformation:

$$\delta Q_\mu^a = \frac{1}{g} \partial_\mu w^a - f^{abc} w^b (Q_\mu^c + \hat{A}_\mu^c). \quad (2.28)$$

The analogous  $\tilde{Z}$  in Eq. (2.27) is also invariant under the transformations:

$$\begin{aligned} \delta \hat{A}_\mu^a &= \frac{1}{g} \partial_\mu w^a - f^{abc} w^b \hat{A}_\mu^c, \\ \delta Q_\mu^a &= -f^{abc} Q_\mu^b w^c, \\ \delta J_\mu^a &= -f^{abc} w^b J_\mu^c. \end{aligned} \quad (2.29)$$

From previous equations in Eq. (2.29) we get that the sum of both fields transforms the same:

$$\delta(Q_\mu^a + \hat{A}_\mu^a) = \frac{1}{g} \partial_\mu w^a - f^{abc} w^b (Q_\mu^c + \hat{A}_\mu^c). \quad (2.30)$$

In QFT, 1PI Greens functions (diagrams which does not fall into two pieces if you cut one internal line) are generated by the effective action. If we shift with the BF the integration variable in the functional integral Eq. (2.27), we can define the background field effective action (modified expression for the classical action):<sup>4</sup>

$$\begin{aligned}\tilde{\Gamma}(\tilde{Q}, \hat{A}) &= \Gamma(\tilde{Q}, \hat{A}) \\ \tilde{\Gamma}(0, \hat{A}) &= \Gamma(\hat{A}).\end{aligned}\tag{2.31}$$

From Eq. (2.31), we see that the BF effective action with the background gauge field and all the external legs is a generating functional for 1PI graphs (one particle irreducible) in a particular gauge. The last line in Eq. (2.31) ensures that the BFM provides the same S-matrix elements as the conventional approach in a conventional gauge, despite yielding different Green functions.

Before proceeding to our explicit results, it is necessary to discuss briefly the renormalization program in the case of the BFM. We first need to redefine a new set of variables in Eq. (2.27):

$$\hat{A}_o = Z_{\hat{A}} \hat{A}_r; \quad g_o = Z_g g_r; \quad \alpha_o = Z_\alpha \alpha_r,\tag{2.32}$$

where  $\hat{A}$ ,  $g$ ,  $\alpha$  stand for the background gluon field, strong coupling, and gauge-fixing parameter respectively.  $Z_{\hat{A}}$ ,  $Z_g$ , and  $Z_\alpha$  will be chosen to cancel the infinities, they are the renormalization constants. However, the Q gauge field (the gluon) does not need to be renormalized. Within the BFM, these fields only appear inside the loops, therefore when one tries to renormalize them they are canceled with the renormalization factors of the vertices (15).

We said that  $\tilde{\Gamma}(0, \hat{A})$  in Eq. (2.31) is a gauge invariant functional of  $\hat{A}$  under the gauge choice  $\tilde{G}^a = \partial_\mu Q_\mu^a + g f^{abc} \hat{A}_\mu^b Q_\mu^c$ . Thanks to this, the BF and charge renormalizations,  $Z_{\hat{A}}$  and  $Z_g$  respectively, are related. To observe the previous statement, let us use the variable change Eq. (2.32) in the  $F_{\mu\nu}^a$ :

$$F_{\mu\nu}^a F^{a\mu\nu} = Z_A^{1/2} [\partial_\mu A_\nu^a - \partial_\nu A_\mu^a + \underbrace{Z_g Z_{\hat{A}}^{1/2}}_{Z_g = Z_{\hat{A}}^{-1/2}} g f^{abc} A_\mu^b A_\nu^c].\tag{2.33}$$

Therefore, for the infinities in the action to take the gauge-invariant form of a divergent constant times the gauge field strength tensor, we need:

---

<sup>4</sup>Tilde notation refers to analogous quantities and definitions shifted by the BF. They are produced by splitting the generating functional and defining it as BF dependent.

$$Z_g = Z_{\hat{A}}^{-1/2}. \quad (2.34)$$

This previous relation assures us that the knowledge of 2-point functions is the only ingredient necessary to compute the  $\beta$ -function, as in QED. The Greens functions will also respect Ward's identities like the ones in QED. Therefore, the BFM simplifies our calculations (with the disadvantage that we will have more Feynman rules, as it is shown in Fig. 4.5).

Additionally, the gauge-fixing parameter could be left unrenormalized if we had considered a general gauge to perform the calculation. Nonetheless, we adopted in our calculations the Feynman gauge  $\alpha = 1$  (as mentioned in Section.2.2). Therefore, it is necessary to include counterterms related to gauge-fixing renormalization (17; 18). The gauge-fixed renormalization insertion diagrams can be seen in Fig. 2.7.

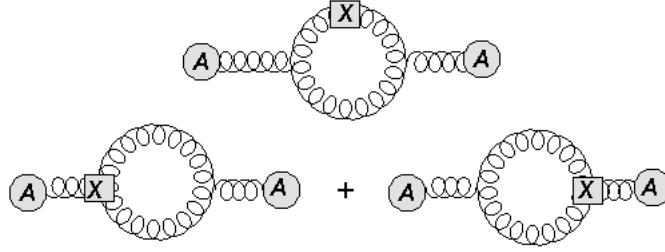


Figure 2.7: Gauge-fixed renormalization diagrams. Boxes with x represent gauge-fixing term insertions resulting from the renormalization of the gauge-fixing parameter. The first diagram is known as the gluon self-energy counterterm, while at the bottom we find the  $AA\hat{A}$  Coupling.

Now, writing again a new redefinition:

$$Z_\alpha = (1 + \delta_\alpha), \quad (2.35)$$

we can write not only a new part of the Lagrangian but also new rules for it.  $\delta_\alpha$  will give the counterterms related to the gauge-fixing renormalization we mentioned before. Thus:

$$\begin{aligned} \mathcal{L}_{\text{GF}} &= -\frac{1}{2\alpha_o} \left[ \partial_\mu Q_a^\mu + g_o f^{abc} (\hat{A}_o)_\mu^b Q_\mu^c \right]^2 \\ &= -\frac{1}{2\alpha_r} \left[ \partial_\mu Q_a^\mu + g_r f^{abc} (\hat{A}_r)_\mu^b Q_\mu^c \right]^2 + \frac{\delta_\alpha}{2\alpha_r} \left[ \partial_\mu Q_a^\mu + g_r f^{abc} (\hat{A}_r)_\mu^b Q_\mu^c \right]^2 \end{aligned} \quad (2.36)$$

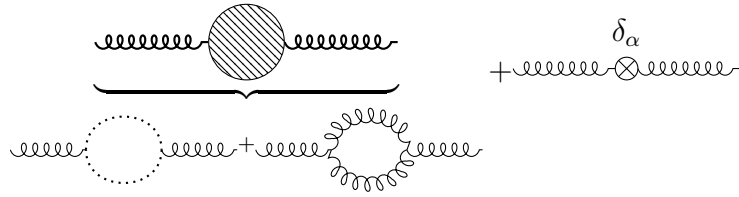


Figure 2.8: Determination of the renormalization factor  $\delta_\alpha$ . It is determined from the quantum corrections to the gluon propagator appearing at 1-loop order.

To obtain an explicit formula to the renormalization factor  $\delta_\alpha$ , it suffices to compute the 1-loop correction to the gluon propagator.





## CHAPTER 3

REGULARIZATION METHODS AND IMPLICIT  
REGULARIZATION

In contrast to the last chapter, we will discuss regularization here. In this direction, we introduce the mathematical method used to sort out the divergences in our 2-loop calculations: Implicit Regularization (IREG). In particular, we present a discussion of the IREG procedure and its rules. Furthermore, we provide an application example at 1-loop order. At the end of the chapter, we analyze the equivalence of final results between other regularization schemes.

### 3.1 Implicit regularization

Implicit regularization (IREG) was proposed as an alternative to traditional dimensional schemes like Dimensional Regularization (CDR) (4). IREG (19; 20; 21) works in momentum space and stays in the physical dimension (4 dimensions). The objective of IREG is to write the **UV-div** in terms of Basic Divergent Integrals (BDI). For example, the **UV-div** part of a general 1-loop Feynman amplitude is

$$I_{log}(\lambda^2) \equiv \int_{-\infty}^{+\infty} \frac{d^4k}{(2\pi)^4} \frac{1}{(k^2 - \lambda^2)^2}, \quad (3.1)$$

where  $\lambda^2$  plays the role of the renormalization group scale in the method.

#### 3.1.1 IREG procedure

In this subsection, we will systematize and generalize the IREG rules for 2-loop amplitudes. To see these rules applied to a 1-loop example, the reader can proceed to the next subsection.

In summary, for a general 2-loop Feynman amplitude  $\mathcal{A}_2$  with  $L$  external legs, let  $k_l$  be the internal (loop) momenta ( $l = 1, 2$ ) and  $p_i$  be the external momenta, the treatment of **UV-div** in IREG can be described as (4; 18):

1. Perform the usual Dirac algebra in the physical dimension.
2. Inside an integral in the internal momentum  $k$  we replace:

$$k^\mu k^\nu \rightarrow \frac{1}{d} k^2 g^{\mu\nu}, \quad (3.2)$$

where  $d$  is the spacetime dimension, and:

$$k^\mu k^\nu k^\rho k^\sigma \rightarrow \frac{1}{d(d+2)} (k^2)^2 (g^{\mu\nu} g^{\rho\sigma} + g^{\mu\rho} g^{\nu\sigma} + g^{\mu\sigma} g^{\nu\rho}). \quad (3.3)$$

This operation is called symmetric integration. In general:

$$\int_k k^{\mu_1} \dots k^{\mu_{2m}} f(k^2) = \frac{1}{(2m)!} \int_k g^{\{\mu_1 \mu_2} \dots g^{\mu_{2m-1} \mu_{2m}\}} f(k^2). \quad (3.4)$$

where  $\int_k = \int_{-\infty}^{+\infty} \frac{d^4 k}{(2\pi)^4}$ . Nevertheless, symmetric integration is **not** allowed in divergent integrals (22) within dimension-specific methods such as IREG. Proceeding otherwise, by rewriting  $k^2 = g^{\mu\nu} k_\mu k_\nu$ , we would obtain different divergent integrals. For example, terms such as

$$\int_k \frac{k^2}{k^2(k-p)^2} = \lim_{\mu^2 \rightarrow 0} I_{\text{quad}}(\mu^2) = 0, \quad (3.5)$$

where  $\mu^2$  is a mass (we will understand the limit in the following sections), and

$$g^{\alpha\beta} \int_k \frac{k_\alpha k_\beta}{k^2(k-p)^2} = -\frac{ip^2}{(4\pi)^2 6} = -\frac{bp^2}{6}. \quad (3.6)$$

are both different. Symmetric integration brings as a consequence the break gauge invariance. In this situation, one way to avoid this problem is to cancel the  $k^2$  terms in the numerator with those in the denominator when possible. We will return to this point in more detail in Section. 4.2.

- 
3. Introduce in the denominator a fictitious mass  $\mu^2$  to avoid spurious infrared divergences <sup>1</sup> in the calculation.

4. Use:

$$\frac{1}{[(p+l)^2 - \mu^2]} = \frac{1}{(l^2 - \mu^2)} - \frac{p^2 + 2p \cdot l}{(l^2 - \mu^2)[(p+l)^2 - \mu^2]}. \quad (3.7)$$

as many times as necessary to isolate the physical parameters (the mass and the external momentum) from the divergent part of the integral.

5. Express the divergent part of the integral in terms of Basic Divergent Integrals (BDI), which may be written as linear combinations of BDI's without Lorentz indices. At 1-loop, basic divergent integrals (BDI's) are:

$$\begin{aligned} I_{log}(\mu^2) &\equiv \int_k \frac{1}{(k^2 - \mu^2)^2}, \\ I_{log}^{\nu_1 \dots \nu_{2r}}(\mu^2) &\equiv \int_k \frac{k^{\nu_1} \dots k^{\nu_{2r}}}{(k^2 - \mu^2)^{r+2}}, \\ I_{quad}(\mu^2) &\equiv \int_k \frac{1}{(k^2 - \mu^2)}, \\ I_{quad}^{\nu_1 \dots \nu_{2r}}(\mu^2) &\equiv \int_k \frac{k^{\nu_1} \dots k^{\nu_{2r}}}{(k^2 - \mu^2)^{r+1}}. \end{aligned} \quad (3.8)$$

6. Remove the  $\mu^2$  dependence by introducing a scale  $\lambda^2$  which plays the role of a renormalization scale.
7. At 2-loop order, the divergent content can be expressed in terms of new BDI at 2-loop. While applying IREG rules to a general massless 2-loop amplitude, one may encounter, for example, an integral of the type:

---

<sup>1</sup>When the field is not massive, we can have divergences due to the lower limit of the integrals. Those are the infrared divergences (**IR-div**). In other words, they are the divergences that arise for small loop momenta.

$$I_{log}^{(2)}(\mu^2) \equiv \int_{k_l} \frac{1}{(k_l^2 - \mu^2)^2} \ln^{2-1} \left( -\frac{k_l^2 - \mu^2}{\lambda^2} \right), \quad (3.9)$$

$$I_{log}^{(2)\nu_1 \cdots \nu_{2r}}(\mu^2) \equiv \int_{k_l} \frac{k_l^{\nu_1} \cdots k_l^{\nu_{2r}}}{(k_l^2 - \mu^2)^{r+1}} \ln^{2-1} \left( -\frac{k_l^2 - \mu^2}{\lambda^2} \right), \quad (3.10)$$

$$I_{quad}^{(2)}(\mu^2) \equiv \int_{k_l} \frac{1}{(k_l^2 - \mu^2)} \ln^{2-1} \left( -\frac{k_l^2 - \mu^2}{\lambda^2} \right). \quad (3.11)$$

$$I_{quad}^{(l)\nu_1 \dots \nu_{r+2}}(\mu^2) \equiv \int_{k_l} \frac{k_l^{\nu_1} \dots k_l^{\nu_{2r}}}{(k_l^2 - \mu^2)^{r+1}} \ln^{l-1} \left( -\frac{k_l^2 - \mu^2}{\lambda^2} \right). \quad (3.12)$$

We will see the application of these rules to a 1-loop example in the next sub-section.

### 3.1.2 Practical example: the electron propagator at 1-loop within IREG

We will develop in this subsection an example with the basic concepts of IREG (4) by considering a familiar example in QED, the 1-loop corrections to the fermion propagator<sup>2</sup>. We write the initial (unregularized) expression using QED's Feynman Rules as:

$$\text{---}\overset{l}{\underbrace{\quad\quad\quad}}\text{---} = -i\Sigma^{(1)}(p,m) = \int_l (-ie\gamma^\beta) \frac{(-ig_{\alpha\beta})}{l^2} (-ie\gamma^\alpha) i \frac{(\not{p} + \not{l}) + m}{(p+l)^2 - m^2} \quad (3.13)$$

where  $p$  is the external momentum, and again  $\int_l = \int_{-\infty}^{+\infty} \frac{d^4 l}{(2\pi)^4}$ . Then, our first step, according to subsection 3.1.1, it is to perform simplifications using Dirac algebra in four dimensions:

$$\begin{aligned}\gamma^\beta \not{p} \gamma_\beta &= -2\not{p}, \\ \gamma^\xi \gamma_\xi &= 4\mathbf{1}.\end{aligned}\tag{3.14}$$

With previous Eq. (3.14), the result is:

$$\Sigma^{(1)}(p, m) = ie^2 2\not{p} \int_l \frac{1}{D} + ie^2 2\gamma^\xi \int_l \frac{l_\xi}{D} - ie^2 4m \int_l \frac{1}{D}, \quad (3.15)$$

<sup>2</sup>In Feynman't Hooft gauge where the gauge parameter is equal to 1.

where  $D = l^2[(p+l)^2 - m^2]$ . Each of the 3 integrals present in this example are **UV-div** divergent. To highlight this, let us look at the superficial degree of divergence,  $\Delta$ , of each integral:

$$\begin{aligned} \int_l \frac{l_\xi}{D} &\rightarrow \Delta = 5 - 4 = 1, \\ \int_l \frac{1}{D} &\rightarrow \Delta = 4 - 4 = 0. \end{aligned} \quad (3.16)$$

When  $\Delta = 1$ , we have a **linear divergence**, and finally, when  $\Delta = 0$  the divergence is **logarithmic**<sup>3</sup>.

The next step in IREG is to introduce a fictitious mass in the propagators, which allows us to control spurious **IR-div** that appear during the evaluation. Therefore, the amplitude can be rewritten as:

$$\begin{aligned} \Sigma^{(1)}(p, m) &= \lim_{\mu^2 \rightarrow 0} ie^2 2\not{p} \int_l \frac{1}{(l^2 - \mu^2)[(p+l)^2 - m^2 - \mu^2]} \\ &+ \lim_{\mu^2 \rightarrow 0} ie^2 2\gamma^\xi \int_l \frac{l_\xi}{(l^2 - \mu^2)[(p+l)^2 - m^2 - \mu^2]} \\ &- \lim_{\mu^2 \rightarrow 0} ie^2 4m \int_l \frac{1}{(l^2 - \mu^2)[(p+l)^2 - m^2 - \mu^2]}, \end{aligned} \quad (3.17)$$

where:

$$\begin{aligned} I_\xi &= \lim_{\mu^2 \rightarrow 0} \int_l \frac{l_\xi}{(l^2 - \mu^2)[(p+l)^2 - m^2 - \mu^2]} = I_\xi \Big|_{div} + I_\xi \Big|_{finite}, \\ I &= \lim_{\mu^2 \rightarrow 0} \int_l \frac{1}{(l^2 - \mu^2)[(p+l)^2 - m^2 - \mu^2]} = I \Big|_{div} + I \Big|_{finite}. \end{aligned} \quad (3.18)$$

At this point, the next step is to use the main observation of IREG that divergent integral should not depend on physical parameters, the external momentum and the mass in this case. To achieve that, the following algebraic identity needs to be used recursively as many times as necessary to isolate the physical parameters in the finite part (20):

$$\frac{1}{[(p+l)^2 - m^2 - \mu^2]} = \frac{1}{(l^2 - \mu^2)} - \frac{p^2 + 2p \cdot l - m^2}{(l^2 - \mu^2)[(p+l)^2 - m^2 - \mu^2]}. \quad (3.19)$$

---

<sup>3</sup>For the logarithmic divergence  $\int_k \frac{1}{D} \propto \frac{1}{(2\pi)^2} \int d\Omega \int_0^{+\infty} \frac{k^3 dk}{k^4} \propto \frac{1}{(2\pi)^2} \int d\Omega \int_0^{+\infty} \frac{dk}{k}$

With the use of Eq. (3.19), the **UV-div** are isolated. Notice also that Eq. (3.19) is similar to Eq. (3.7) with the only difference being the mass since we are working in this example with a massive electron.

For the linear integral in our example, we end up with the following divergent expression<sup>4</sup>

$$I_\xi \Big|_{div} = -2p^\alpha \lim_{\mu^2 \rightarrow 0} \int_l \frac{l_\xi l_\alpha}{(l^2 - \mu^2)^3}, \quad (3.20)$$

and for the logarithmic divergent integral:

$$I \Big|_{div} = \lim_{\mu^2 \rightarrow 0} \int_l \frac{1}{(l^2 - \mu^2)^2}. \quad (3.21)$$

When using Eq. (3.19) to get Eq. (3.20), and Eq. (3.21) we obtain two logarithmic divergent terms. In our example, the logarithmic terms are a particular case of the general expressions, which we define as Basic Divergent Integrals. In the case of this example, the BDI that appear are:

$$I_{log}(\mu^2) \equiv \int_k \frac{1}{(k^2 - \mu^2)^2}, \quad I_{log}^{\nu_1 \nu_2}(\mu^2) \equiv \int_k \frac{k_{\nu_1} k_{\nu_2}}{(k^2 - \mu^2)^3}. \quad (3.22)$$

On the other hand, the finite terms in our linear example Eq. (3.20) after using Eq. (3.19) are:

$$I_\xi \Big|_{finite} = -p^2 \lim_{\mu^2 \rightarrow 0} \int_l \frac{l_\xi}{(l^2 - \mu^2)^3} + m^2 \lim_{\mu^2 \rightarrow 0} \int_l \frac{l_\xi}{(l^2 - \mu^2)^3} \quad (3.23)$$

$$+ \lim_{\mu^2 \rightarrow 0} \int_l \frac{l_\xi (p^2 + 2p \cdot l - m^2)^2}{(l^2 - \mu^2)^3 [(p + l)^2 - m^2 - \mu^2]}, \quad (3.24)$$

and, for the logarithmic divergent integrals:

$$I \Big|_{finite} = - \lim_{\mu^2 \rightarrow 0} \int_l \frac{p^2 + 2p \cdot l - m^2}{(l^2 - \mu^2)^2 [(p + l)^2 - m^2 - \mu^2]}. \quad (3.25)$$

The objective of IREG will be to use Eq. (3.19) as many times as necessary to write the **UV-div** in terms of the Basic Divergent Integrals (BDI) in Eq. (3.22) (19). These BDI could be composed of scalar and tensorial integrals with Lorentz indices  $\nu_1 \cdots \nu_{2r}$ . The last

---

<sup>4</sup>The reader can find the complete deduction in the Appendix B

ones may be expressed as a linear combination of the scalar integrals  $I_{log}(\mu^2)$  or  $I_{quad}(\mu^2)$ , according to the superficial degree of divergence of the original integral plus well-defined surface terms (ST's). Let us demonstrate this with our linear example Eq. (3.20). If:

$$\int_l \frac{\partial}{\partial l^\alpha} \frac{l_\xi}{(l^2 - \mu^2)^2} = \int_l \frac{g_{\xi\alpha}}{(l^2 - \mu^2)^2} - 4 \int_l \frac{l_\xi l_\alpha}{(l^2 - \mu^2)^3} \quad (3.26)$$

$$= g_{\xi\alpha} I_{log}(\mu^2) - 4 I_{log}^{\xi\alpha}(\mu^2) \quad (3.27)$$

$$\equiv \Upsilon_0^{(1)\xi\alpha}, \quad (3.28)$$

therefore, the  $I_{log}^{\xi\alpha}(\mu^2)$  can be written as

$$I_{log}^{\xi\alpha}(\mu^2) = \frac{g_{\xi\alpha}}{4} I_{log}(\mu^2) - \underbrace{\frac{1}{4} \int_l \frac{\partial}{\partial l_\alpha} \frac{l_\xi}{(l^2 - \mu^2)^2}}_{\text{Surface Term}}. \quad (3.29)$$

The  $\Upsilon_0^{(1)\mu\nu}$  is a surface term, arbitrary in principle. STs vanish if and only if momentum routing invariance (MRI)<sup>5</sup> holds in the loops of Feynman diagrams. Moreover, these requirements automatically deliver gauge invariant amplitudes (23) as it was demonstrated for Abelian gauge theories to arbitrary loop order (24) and verified for non-Abelian gauge models (25).

We must not forget that we need to take the limit  $\mu^2 \rightarrow 0$  in the end. Regarding our  $I_\xi$  example, although  $I_{log}(\mu^2)$  parametrizes the **UV-div**, both  $I_{log}(\mu^2)$  and the finite terms, develop an **IR-div** which is spurious since our original integral Eq. (3.15) was **IR** safe. Therefore, as mentioned in Ref. (21), we define a mass-independent scheme in IREG by replacing  $\mu^2$  with an arbitrary mass parameter  $\lambda^2 \neq 0$ . For instance:

$$I_{log}(\mu^2) = I_{log}(\lambda^2) + \frac{i}{(4\pi)^2} \ln \frac{\lambda^2}{\mu^2} \quad (3.30)$$

which enables us to write a basic divergent integral (BDI) as a function of  $\lambda^2$  plus logarithmic functions of  $\mu^2/\lambda^2$ . We will name from now on  $i/(4\pi)^2 = b$ . The Eq. (3.30) is known as the **scale relation** and help us to define pure **UV-div** objects (19). To get Eq. (3.30) consider  $I_{log}(\mu^2)$  in Eq. (3.22). If we derive it to respect with  $\mu^2$ :

$$\frac{d}{d\mu^2} I_{log}(\mu^2) = \int_k \frac{2}{(k^2 - \mu^2)^3}. \quad (3.31)$$

To solve the last integral, we will use the equation below, obtained from Ref. (20):

---

<sup>5</sup>When MRI is required in a Feynman diagram, it means that the physical results will not depend on the way the internal momenta are labeled, as long as energy-momentum conservation at each vertex is respected.



$$\int_k \frac{d^d k}{(2\pi)^d} \frac{1}{(k^2 + 2kQ - M^2)^\alpha} = i \frac{(-1)^\alpha}{(4\pi)^{d/2}} \frac{\Gamma(\alpha - d/2)}{\Gamma(\alpha)} \frac{1}{(Q^2 + M^2)^{\alpha - d/2}}, \quad (3.32)$$

thus

$$\frac{d}{d\mu^2} I_{\log}(\mu^2) = -\frac{b}{\mu^2}. \quad (3.33)$$

Now we integrate:

$$\int_{\lambda^2}^{\mu^2} dI_{\log}(\mu^2) = -b \int_{\lambda^2}^{\mu^2} \frac{d(\mu^2)}{\mu^2} \quad (3.34)$$

$$I_{\log}(\mu^2) = I_{\log}(\lambda^2) + b \ln \left( \frac{\lambda^2}{\mu^2} \right). \quad (3.35)$$

Thus, we can return to the logarithmic integral  $I$  and rewrite it using Eq. (3.30)

$$I = I_{\log}(\lambda^2) + b \ln \left( \frac{\lambda^2}{\mu^2} \right) - \lim_{\mu^2 \rightarrow 0} \int_k \frac{(p^2 + 2p \cdot l - m^2)}{(l^2 - \mu^2)^2 [(p+l)^2 - m^2 - \mu^2]}, \quad (3.36)$$

and for the linear integral part, assuming the surface term to vanish from now on:

$$\begin{aligned} I_\xi &= I_\xi \Big|_{div} + I_\xi \Big|_{finite} \\ &= -2p^\alpha \left[ \frac{g_{\xi\alpha}}{4} I_{\log}(\mu^2) - \frac{1}{4} \Upsilon_0^{(1)\mu\nu} \right] + I_\xi \Big|_{finite} \\ &= -\frac{p_\xi}{2} I_{\log}(\mu^2) + 0 + I_\xi \Big|_{finite} \\ &= -\frac{p_\xi}{2} I_{\log}(\lambda^2) - \frac{p_\xi}{2} b \ln \left( \frac{\lambda^2}{\mu^2} \right) \\ &\quad - p^2 \lim_{\mu^2 \rightarrow 0} \int_l \frac{l_\xi}{(l^2 - \mu^2)^3} + m^2 \lim_{\mu^2 \rightarrow 0} \int_l \frac{l_\xi}{(l^2 - \mu^2)^3} \\ &\quad + \lim_{\mu^2 \rightarrow 0} \int_l \frac{l_\xi (p^2 + 2p \cdot l - m^2)^2}{(l^2 - \mu^2)^3 [(p+l)^2 - m^2 - \mu^2]}. \end{aligned} \quad (3.37)$$

Let us now see what happens with the finite terms.

### 3.1.3 The finite terms in IREG

Collecting the finite parts of the previous example for the electron propagator at 1-loop:

---


$$\begin{aligned}
\tilde{\Sigma}^{(1)}(p, m) = & -ie^2 2\gamma^\xi p^2 \lim_{\mu^2 \rightarrow 0} \int_l \frac{l_\xi}{(l^2 - \mu^2)^3} + ie^2 2\gamma^\xi m^2 \lim_{\mu^2 \rightarrow 0} \int_l \frac{l_\xi}{(l^2 - \mu^2)^3} \\
& + ie^2 2\gamma^\xi \lim_{\mu^2 \rightarrow 0} \int_l \frac{l_\xi (p^2 + 2p \cdot l - m^2)^2}{(l^2 - \mu^2)^3 [(p+l)^2 - m^2 - \mu^2]} \\
& - ie^2 2\not{p} \lim_{\mu^2 \rightarrow 0} \int_l \frac{p^2 + 2p \cdot l - m^2}{(l^2 - \mu^2)^2 [(p+l)^2 - m^2 - \mu^2]} \\
& + ie^2 4m \lim_{\mu^2 \rightarrow 0} \int_l \frac{p^2 + 2p \cdot l - m^2}{(l^2 - \mu^2)^2 [(p+l)^2 - m^2 - \mu^2]},
\end{aligned} \tag{3.38}$$

where we have a part proportional to the momentum  $p$  and the other to  $m$ . The integrals in the first line, render a null result since the integrand are odd and we are integrating over a symmetric interval.

If we resolve the part proportional to  $m$  in Eq. (3.38) using Package-X (26) in Mathematica, we will obtain a result with a logarithm, of which we will also do its expansion<sup>6</sup> :

$$\begin{aligned}
\lim_{\mu^2 \rightarrow 0} \int_l \frac{p^2 + 2p \cdot l - m^2}{(l^2 - \mu^2)^2 [(p+l)^2 - m^2 - \mu^2]} &= -2b - \lim_{\mu^2 \rightarrow 0} \ln \left( \frac{\mu^2}{m^2 + \mu^2} \right) b \\
&= -2b - \lim_{\mu^2 \rightarrow 0} \ln \left( \frac{\mu^2}{m^2} \right) b,
\end{aligned} \tag{3.39}$$

and for the part proportional to  $p$ :

$$\begin{aligned}
& \lim_{\mu^2 \rightarrow 0} \int_l \frac{p^2 + 2p \cdot l - m^2}{(l^2 - \mu^2)^2 [(p+l)^2 - m^2 - \mu^2]} - \lim_{\mu^2 \rightarrow 0} \int_l \frac{[p^2 + 2p \cdot l - m^2]^2}{(l^2 - \mu^2)^3 [(p+l)^2 - m^2 - \mu^2]} \\
&= \lim_{\mu^2 \rightarrow 0} b \left[ \frac{1}{2} \left( -3 - \ln \left( \frac{\mu^2}{m^2 + \mu^2} \right) \right) \right] = -\frac{3}{2}b - \frac{1}{2}b \lim_{\mu^2 \rightarrow 0} \ln \left( \frac{\mu^2}{m^2} \right).
\end{aligned} \tag{3.40}$$

Plugging these finite results, Eq. (3.39) and Eq. (3.40), and adding also the results of the divergent part after using the scale relation Eq. (3.30), we can have the final electron propagator at 1-loop using IREG:

---

<sup>6</sup>In the process of solving the finite integrals, we use on-shell renormalization where  $p^2 = m^2$ .

$$\begin{aligned}
 \Sigma^{(1)}(p, m) &= +ie^2(\not{p} - 4m)I_{\log}(\lambda^2) + ie^2(\not{p} - 4m)b \ln\left(\frac{\lambda^2}{\mu^2}\right) \\
 &\quad - ie^2 4m 2b - ie^2 4m \lim_{\mu^2 \rightarrow 0} \ln\left(\frac{\mu^2}{m^2}\right) b - ie^2 2 \left( -\not{p} \frac{3}{2} b - \not{p} \frac{1}{2} b \lim_{\mu^2 \rightarrow 0} \ln\left(\frac{\mu^2}{m^2}\right) \right) \\
 &= \underbrace{+ie^2(\not{p} - 4m)I_{\log}(\lambda^2)}_{\text{Divergent}} \\
 &\quad - ie^2 \not{p} \left[ -3b - b \ln\left(\frac{\lambda^2}{m^2}\right) \right] - ie^2(-4m) \left[ -2b - b \ln\left(\frac{\lambda^2}{m^2}\right) \right].
 \end{aligned} \tag{3.41}$$

## 3.2 Dimensional schemes

Traditional dimensional schemes (DS) are the most used for calculations in QFT. They are based on analytic continuations of the space from 4 to  $d$  dimensions. We can distinguish two forms of dimensional schemes. The first is conventional dimensional regularization (CDR) which analytically continues the integral into  $d = 4 - 2\epsilon$ . In CDR, all vector bosons are treated as  $d$ -dimensional objects. However, CDR has some disadvantages. Some of them are associated with supersymmetry (SUSY) breaking and others, for example, are related to the presence of  $\gamma_5$  matrices (22).

As is the case for any field theory in general, quantum effects in SUSY lead to divergences, which need to be regularized. However, using CDR, by altering the number of space-time dimensions from 4 to  $d$  dimensions, leads to a mismatch between the fermionic and the bosonic degrees of freedom. This is due to the need to assign different numbers of degrees of freedom to spin-1 and spin-1/2 fields. A direct consequence is the need to introduce symmetry-restoring counterterms since SUSY relations of couplings no longer hold at higher orders using CDR. With this in mind, some variants of CDR such as dimensional reduction (DRED) (27) have been developed. In DS, **UV-div** manifest as poles of form  $1/\epsilon^n$ .

It should be emphasized that there is a general framework in which CDR and DRED can be unified (4; 28; 29). In both cases, the loop momentum integrals are defined in  $d$  dimensions. However, other objects (such as gauge fields and  $\gamma$ -matrices) can remain in 4 dimensions. This distinction may be particularly relevant for non-Abelian theories, where many simplifications can be achieved by considering gluon polarization sums in 4 dimensions (28). The drawback is that a hierarchy of different sub-spaces must be enforced. First, the loop momenta,  $\int d^d f(k)$ , in DS are always  $d$ -dimensional objects. From them, we can get the  $d$ -dim metric  $\hat{g}^{\mu\nu}$ . Second, we can have the metric tensor in 4-dim from the gluon propagators  $g^{\mu\nu}$ . We can decompose the latter 4-dim metric tensor  $g^{\mu\nu}$  into tensor  $\hat{g}^{\mu\nu}$ , a  $d$ -dim subspace component, and  $\tilde{g}^{\mu\nu}$  a

(4- $d$ )-dim subspace (29). With this, we get the following relationships:

$$\begin{aligned}
g^{\mu\nu} &= \hat{g}^{\mu\nu} + \tilde{g}^{\mu\nu}, \\
g^{\mu\nu} g_{\mu\nu} &= 4, \\
\hat{g}^{\mu\nu} \hat{g}_{\mu\nu} &= d, \\
\tilde{g}^{\mu\nu} \tilde{g}_{\mu\nu} &= 4 - d, \\
\hat{g}_{\mu\nu} \tilde{g}^{\nu\rho} &= 0, \\
\tilde{g}_{\mu\nu} \hat{g}^{\nu\sigma} &= 0, \\
g^{\mu\nu} \hat{g}_\nu^\rho &= \hat{g}^{\nu\rho}, \\
g^{\mu\nu} \tilde{g}_\nu^\rho &= \tilde{g}^{\mu\rho};
\end{aligned} \tag{3.42}$$

and with them, we get the following properties in the Dirac algebra (29):

$$\begin{aligned}
\not{p} &= \hat{p}_\mu \gamma^\mu = \hat{p}_\mu (\hat{\gamma}^\mu + \tilde{\gamma}^\mu) = \hat{p}_\mu \hat{\gamma}^\mu + \hat{p}_{\nu\mu} \tilde{g}^{\mu\rho} \hat{p}_\mu \tilde{\gamma}_\rho = \hat{p}_\mu \hat{\gamma}^\mu, \\
\hat{\gamma}^\mu \tilde{\gamma}^\nu &= \hat{g}^{\sigma\mu} \tilde{g}^{\rho\nu} \gamma_\sigma \gamma_\rho = \hat{g}^{\sigma\nu} \tilde{g}^{\rho\mu} (2g_{\sigma\rho} - \gamma_\rho \gamma_\sigma) = 2\hat{g}_\rho^\mu \tilde{g}^{\rho\nu} - \tilde{\gamma}^\nu \hat{\gamma}^\mu = \tilde{\gamma}^\nu \hat{\gamma}^\mu, \\
\tilde{\gamma}^\mu \tilde{\gamma}_\mu &= \frac{1}{2} \tilde{g}_{\mu\nu} \{\tilde{\gamma}^\mu, \tilde{\gamma}^\nu\} = \tilde{g}_{\mu\nu} \tilde{g}^{\mu\nu} = 4 - d, \\
\hat{\gamma}^\mu \tilde{\gamma}_\mu &= \tilde{g}_{\nu\mu} \hat{g}^{\mu\sigma} \gamma_\sigma \gamma^\nu = 0.
\end{aligned} \tag{3.43}$$

Briefly, we can distinguish the next spaces (28) represented in Fig. 3.1:

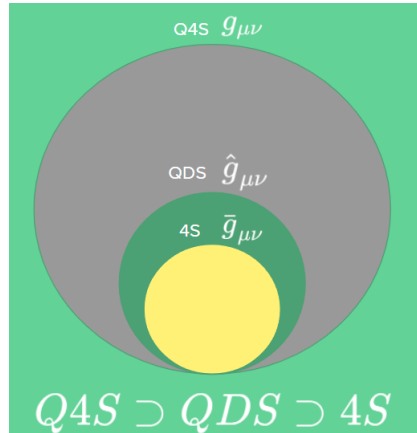


Figure 3.1: Graphic representation of the framework in dimensional methods.

- **4S**: the original 4-dimensional space.

- **Quasi-D-dimensional space (QDS)**: this space is an infinite-dimensional vector space with d-dimensional properties.  $QDS \supset 4S$ .
- **Quasi-4-dimensional space (Q4S)**: this space has to be  $Q4S \supset QDS$  for the dimensionally reduced theory to be gauge invariant. It is not the 4S, but it has certain 4-dimensional properties.

Since  $Q4S \supset QDS$ , we can use an auxiliary space call the “ $\epsilon$ -scalars” space. Therefore, in DRED, we split the boson fields “d” into a boson space “d” plus a boson space  $N = 2\epsilon$ ,

$$Q4S = \underbrace{QDS}_{4-2\epsilon} + \underbrace{Q(2\epsilon)S}_{2\epsilon}, \quad (3.44)$$

which split our lagrangian density:

$$\mathcal{L}^{(4)} = \mathcal{L}^{(d)} + \mathcal{L}^{(2\epsilon)}. \quad (3.45)$$

As we mentioned, the  $\epsilon$ -dimensional boson fields will be called  $\epsilon$ -scalars. They will give origin to new Feynman Rules that could be reviewed in Ref. (7). On the other hand, associated with these Feynman rules we will have new coupling constants associated with the  $\epsilon$ -scalars.

The subtleties regarding the definition of the metric both in the space of d dimensions and in the  $2\epsilon$  can be schematized as seen in the following Table 3.1:

	CDR	DRED
Internal gluon	$\hat{g}_{\mu\nu}$	$g^{\mu\nu}$
External gluon	$\hat{g}_{\mu\nu}$	$g^{\mu\nu}$

Table 3.1: Treatment of internal and external gluons in dimensional methods (28). In CDR, the gluons are regularized in d dimensions with the metric tensor  $\hat{g}_{\mu\nu}$  (QDS). The quasi-4-dimensional space has a metric define as  $g_{\mu\nu}$  (Q4S) and the original quadri-dimensional is represented by  $\bar{g}_{\mu\nu}$  (4S). A complementary metric tensor  $\tilde{g}_{\mu\nu}$  of dimension  $2\epsilon$  is introduced such that  $g_{\mu\nu} = \hat{g}_{\mu\nu} + \tilde{g}_{\mu\nu}$ . Therefore,  $Q4S = QDS \oplus Q2\epsilon S$ . Mathematical consistency and gauge invariance require  $Q4S \supset QDS \supset 4S$  and forbid to identify  $g_{\mu\nu}$  with  $\bar{g}_{\mu\nu}$ .

In this thesis, as we only consider diagrams with **UV-div**, the “internal gluons” are the ones inside a diagram as in Fig. 3.2.

### 3.2.1 The electron propagator with DS

We do not intend in this subsection to make a complete description using DS on how to calculate the propagator of the electron in a 1-loop. For more references, see Appendix D.

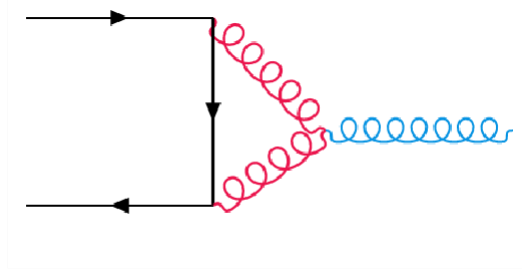


Figure 3.2: Example of **internal** and **external** gluons.

We aim to contrast the main differences regarding the IREG method. The most important aspect is that in dimensional methods, as an analytic continuation of the space to  $d$ -dim is performed, the Dirac algebra is different. For CDR:

$$\begin{aligned}\gamma^\beta \not{p} \gamma_\beta &= (2 - d) \not{p}, \\ \gamma^\xi \gamma_\xi &= d \mathbb{1}.\end{aligned}\tag{3.46}$$

For the DRED, as was mentioned in the previous section, we have new Feynman rules coming from the appearance of new particles called  $\epsilon$ -scalars Fig. 3.3. In the case of the first diagram at the left in Fig. 3.3, the algebra (and, by the consequence, the result) will be the same as CDR. By the contrary, in the diagram in the right one uses the following following Dirac's algebra results:

$$\begin{aligned}\tilde{\gamma}^\beta \not{p} \tilde{\gamma}_\beta &= -N_\epsilon \not{p} = -2\epsilon \not{p}, \\ \tilde{\gamma}^\xi \tilde{\gamma}_\xi &= N_\epsilon \mathbb{1} = 2\epsilon \mathbb{1}.\end{aligned}\tag{3.47}$$

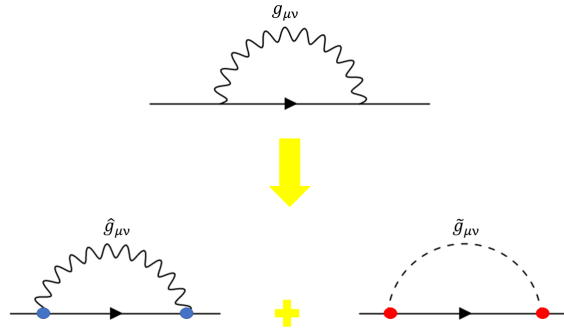


Figure 3.3: Electron self-energy corrections withing DRED. The electron self-energy receives a correction due to a fermion- $\epsilon$ -scalar loop (30).

The last interesting aspect is that the finite parts of the amplitude with IREG are identical to DRED to 1-loop level

$$\tilde{\Sigma}(p, m)^{IREG} = \tilde{\Sigma}(p, m)^{DRED}, \quad (3.48)$$

if the coupling constant  $e^2 = e_\epsilon^2$ , where  $e_\epsilon$  is the coupling constant associated with the introduction of the  $\epsilon$ -scalars.

### 3.3 $I_{log}$ in CDR: correspondence at 1-loop.

In this section, we analyze the equivalence of final results when evaluating the amplitudes of the diagrams by DS once the result in IREG is known at 1-loop. In IREG, the UV log-divergent content of a Feynman amplitude is expressed by the BDI's  $I_{log}(\lambda^2)$ , while in DS they appear as poles in  $\epsilon \rightarrow 0$ . Therefore, given a 1-loop amplitude, one may wonder if extracting the residues of  $\epsilon$  by evaluating  $I_{log}(\lambda^2)$  in  $4 - 2\epsilon$  dimensions is sufficient to map the IREG result on the one obtained in CDR or DRED. Considering the next log-divergent integral composed of the product of two massless propagators:

$$I = \int_k \frac{1}{k^2(k-p)^2} \stackrel{\text{IREG}}{=} I_{log}(\lambda^2) - b \ln \left[ -\frac{p^2}{\lambda^2} \right] + 2b. \quad (3.49)$$

By evaluating  $I_{log}(\lambda^2)$  in  $d = 4 - 2\epsilon$  dimensions and expanding around  $\epsilon = 0$  (4)

$$\begin{aligned} I_{log}(\lambda^2) &\equiv \int_k \frac{1}{(k^2 - \lambda^2)^2} = \mu_{DR}^{4-d} \int \frac{d^d k}{(2\pi)^d} \frac{1}{(k^2 - \lambda^2)^2} \\ &= \mu_{DR}^{4-d} \frac{i(-1)^2 (4\pi)^{-d/2}}{\Gamma(2)(\lambda^2)^{2-d/2}} \Gamma(2 - d/2) \\ &= \frac{i(4\pi)^\epsilon}{(4\pi)^2} \left( \frac{\mu^\epsilon}{\lambda^\epsilon} \right) \Gamma(\epsilon), \end{aligned} \quad (3.50)$$

where we used from Ref. (31)

$$\int \frac{d^d k}{(2\pi)^d} \frac{1}{[k^2 - m^2]^A} = \frac{i(-1)^A (4\pi)^{-d/2}}{\Gamma(A)(m^2)^{A-d/2}} \Gamma(A - d/2). \quad (3.51)$$

It is important in this section not to confuse the  $\mu_{DR}$  for the DS with the  $\mu$  we used in previous sections as a fictitious mass.

Finally using  $\Gamma(\epsilon) \equiv \frac{1}{\epsilon} - \gamma_E + \mathcal{O}(\epsilon)$  and  $a^\epsilon = \exp^{\epsilon \ln a} + \mathcal{O}(\epsilon)$ :

$$I_{log}^d(\lambda^2) = b \left[ \frac{1}{\epsilon} - \gamma_E + \ln(4\pi) + \ln \left( \frac{\mu_{DR}^2}{\lambda^2} \right) \right], \quad (3.52)$$

---

which means:

$$I\Big|_d = b \left[ \frac{1}{\epsilon} - \gamma_E + \ln(4\pi) - \ln \left[ -\frac{p^2}{\mu_{DR}^2} \right] + 2 \right]. \quad (3.53)$$

Notice that the  $\lambda^2$  dependence is automatically traded by  $\mu_{DR}^2$ . This result coincides with the result of DS.

### 3.3.1 About correspondence to higher orders

We began our section by discussing the equivalence between IREG and DS at 1-loop. However, one may wonder if this approach can be extended to higher orders. In this subsection, we discuss some subtleties involved. We proceed to study in analogy to Eq. (3.49) at 1-loop, the n-loop product of massless bubble diagrams proportional to the integrals:

$$J = \int_{k_1} \frac{1}{k_1^2(k_1 - p)^2} \cdots \int_{k_n} \frac{1}{k_n^2(k_n - p)^2}. \quad (3.54)$$

Using the rules of IREG, each integral in  $k_i$  can be independently performed to give:

$$J^{\text{IREG}} = \left[ I_{\log}(\lambda^2) - b \ln \left[ -\frac{p^2}{\lambda^2} \right] + 2b \right]^n. \quad (3.55)$$

To establish a correspondence with DS at n-loop order, the use of Eq. (3.53) is inappropriate, since terms  $\mathcal{O}(\epsilon)$  are needed. Therefore, one should consider  $I_{\log}(\lambda^2)$  before expanding around  $\epsilon = 0$ ,

$$I_{\log}^d(\lambda^2) = (\mu_{DR})^{4-d} \int \frac{d^d k}{(2\pi)^d} \frac{1}{(k^2 - \lambda^2)^2} = \frac{b}{(4\pi)^{-\epsilon}} \left( \frac{\mu_{DR}^2}{\lambda^2} \right)^\epsilon \Gamma(\epsilon), \quad (3.56)$$

and let us rewrite  $\ln(-p^2/\lambda^2)$  so that the scale  $\mu_{DR}^2$  emerges:

$$\ln \left( -\frac{p^2}{\lambda^2} \right) = \lim_{\epsilon \rightarrow 0} \frac{\Gamma(\epsilon)}{(4\pi)^{-\epsilon}} \left[ \left( \frac{\mu_{DR}^2}{\lambda^2} \right)^\epsilon - \left( -\frac{\mu_{DR}^2}{p^2} \right)^\epsilon \right], \quad (3.57)$$

where we have used that  $\ln(x) = \lim_{\epsilon \rightarrow 0} [(x^\epsilon - 1)/\epsilon + \alpha(\epsilon)]$ ,  $\alpha(\epsilon \rightarrow 0) = 0$ . Thus,

$$\mathcal{J}^{\text{IREG}}\Big|_d = b^n \left[ \frac{1}{(4\pi)^{-\epsilon}} \left( -\frac{\mu_{DR}^2}{p^2} \right)^\epsilon \Gamma(\epsilon) + 2 \right]^n, \quad (3.58)$$



which, by construction, is independent of  $\lambda$ . On the other hand, by performing the computation in DS from the start one obtains

$$\mathcal{J}_d = b^n \left[ \frac{1}{(4\pi)^{-\epsilon}} \left( -\frac{\mu_{DR}^2}{p^2} \right)^\epsilon \frac{\Gamma(\epsilon)\Gamma^2(1-\epsilon)}{\Gamma(2-2\epsilon)} \right]^n. \quad (3.59)$$

Expanding Eq. (3.58) and Eq. (3.59) we see that they only agree in the  $\epsilon^{-n}$  and  $\epsilon^{-n+1}$  coefficients.



---

**Part 2:**

Methodology and results

---



## CHAPTER 4

# PRACTICAL APPROACHES TO 2-LOOP CALCULATIONS

In the chapter, we will discuss details related to Lorentz algebra contractions/symmetric integrations inside divergent integrals in 2-loop order. We also discuss the renormalization of the gauge-fixing parameter using the Background Field Method. Finally, we present the  $\beta$ -function at 2-loop within DS and IREG, as well as details of the algorithm used to compute it. In Chapter 5, we will use this procedure to calculate the  $\beta$ -function at 2-loop for pure Yang-Mills, QED, and QCD.

## 4.1 Methodology

As we saw in Chapter 1, the calculation of amplitudes at higher order is essential in QFT. In this direction, it is practical to develop routines for automated calculations. Thus, we developed a code in Mathematica to find the  $\beta$ -function coefficients of gauge couplings, the anomalous dimension  $\gamma$ , and the anomalous mass dimension  $\gamma_m$ .

### 4.1.1 Algorithm: $\beta$ -function

The source code works at 2-loop level based on a bare algorithm developed in Ref. (18). Beginning with stage 1 of the algorithm, we use the Feynman diagram generator FeynArts, which emerged in the 90s by Hagen Eck, Sepp Kueblbeck, and Thomas Hahn (32). This package allows controlling the production of the necessary topologies of interest. Yet, it not only generates the topologies it can also create the Feynman amplitudes of the processes under study. At this stage, we used it for various gauge theories: QED, pure Yang-Mills, and QCD. We present, in this thesis, the results obtained and perspectives for Abelian and non-Abelian gauge theories.

After the amplitudes are constructed using the Feynman rules that the program provides

(or we defined), they are adapted to be used in FormCalc 6 (33). In FormCalc the respective index contractions are performed using Dirac and Lorentz algebra in  $d$ -dimensions. For IREG and DRED we made  $d = 4$  while for CDR  $d = 4 - 2\epsilon$ . For the theories we study in this thesis, the topologies we are going to deal with appear in Fig. 4.1:

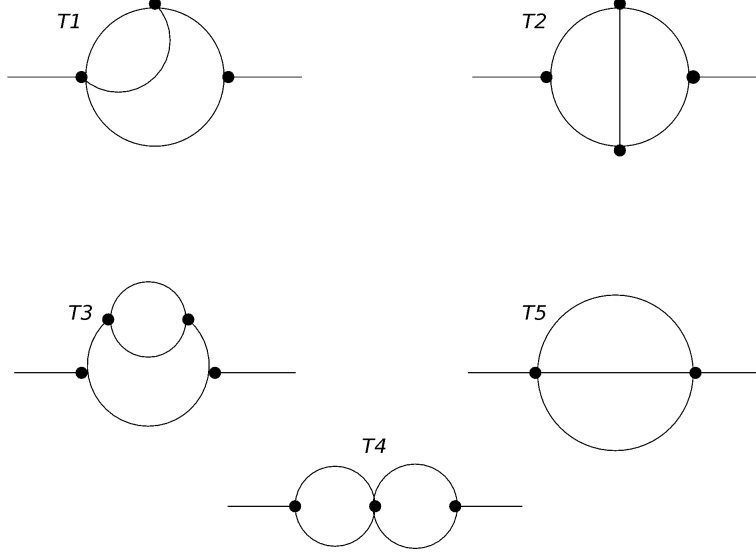


Figure 4.1: Typical topologies generated at 2-loop for 2-point function.

From Fig. 4.1 each topology is given schematically by<sup>1</sup>

$$\begin{aligned}
\mathcal{A}_{T1} &\propto \int_{k,l} \frac{\mathcal{F}_{T1}^{\alpha\beta}(l, k, p)}{k^2(k-p)^2 l^2(l-k)^2}, \\
\mathcal{A}_{T2} &\propto \int_{k,l} \frac{\mathcal{F}_{T2}^{\alpha\beta}(l, k, p)}{k^2(k-p)^2(k-l)^2 l^2(l-p)^2}, \\
\mathcal{A}_{T3} &\propto \int_{k,l} \frac{\mathcal{F}_{T3}^{\alpha\beta}(l, k, p)}{k^4(k-p)^2 l^2(l-k)^2}, \\
\mathcal{A}_{T4} &\propto \int_{k,l} \frac{\mathcal{F}_{T4}^{\alpha\beta}(l, k, p)}{k^2(k-p)^2 l^2(l-p)^2}, \\
\mathcal{A}_{T5} &\propto \int_{k,l} \frac{\mathcal{F}_{T5}^{\alpha\beta}(l, k, p)}{k^2 l^2(l-k+p)^2}.
\end{aligned} \tag{4.1}$$

If possible, we perform the contractions in 4 dimensions and simplify the numerator against the denominator. This simplification is particularly relevant for terms such as (22):

<sup>1</sup>Other perturbative correction proportional to the two-loop tadpole diagram are not represented in the Fig. 4.1, since they have a null contribution in IREG.

$$\int_{k,q} \frac{k^2}{k^2 q^2 (k-q)^2} \Big|_{\text{IREG}} = \int_{k,q} \frac{1}{q^2 (k-q)^2} \Big|_{\text{IREG}}. \quad (4.2)$$

Now let us pass to stage 2: we make the necessary simplifications and reductions for the integrals. These simplifications, as we mentioned in Chapter. 3, depend on the regularization scheme used. In our case, we did it for CDR, DRED, and IREG (where we set STs equal to zero). An important point again is to avoid symmetric integration in IREG. For instance,

$$g_{\mu\nu} \int_k k^\mu k^\nu f(k) \Big|_{\text{IREG}} \neq \int_k k^2 f(k) \Big|_{\text{IREG}}. \quad (4.3)$$

Previous observation is crucial to avoid mismatches during intermediary steps in the reduction process. On the other hand, we also drop quadratically integrals, encoded as  $I_{quad}^{(2)}(\mu^2)^2$ . In the final stage 3: we evaluate the integrals according to the regularization method used. Finally, we use the definition of the  $\beta$ -function to compute it at this stage. For a summary and outline of all these stages, see Fig. 4.2.

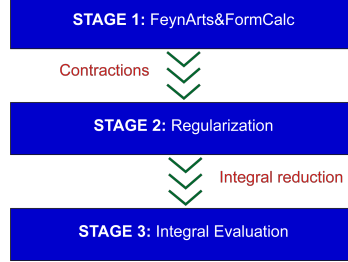


Figure 4.2: Algorithm used in our automatic calculation.

### 4.1.2 Algorithm: anomalous dimensions

We also developed a code in Mathematica to find the  $\gamma$ -function, and  $\gamma_m$ -function coefficients of gauge couplings Fig. 4.3. For this algorithm, first, we use again FeynArts (32) which already has the QED and QCD implemented. We adopted the Feynman gauge equal to 1. Regarding the anomalous dimension, we consider massless fermions, and for the anomalous dimension of the mass: massive fermions. This code is different from the previous one presented in the section because we use FeynCalc instead of FormCalc to work with Dirac's algebra. On the other hand, FeynCalc allows a transparent visualization of the amplitude generated by FeynArts.

<sup>2</sup>These integrals come from diagrams with the tadpole diagram as a subgraph. They are null in IREG. For more references, see Ref. (11)

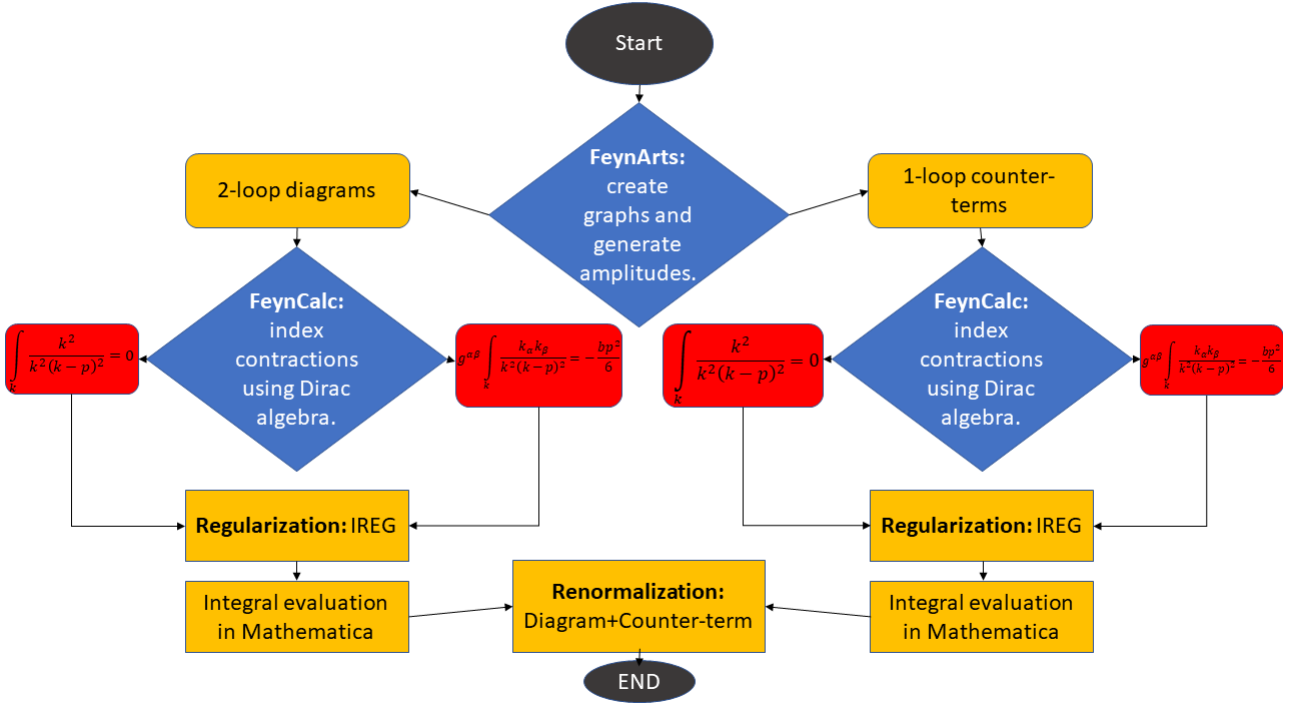


Figure 4.3: Algorithm used for the automatic calculation.

Contrary to Ref. (11), however, in the framework of IREG at 2-loop order, we do not evaluate the sub-diagram first and join the obtained result in the full diagram. As mentioned in Ref. (18), local terms may be generated. These terms could violate gauge invariance.

After carefully treating the quadratic terms in IREG, we continue with the next step of the algorithm in Fig. 4.3. As we are using IREG to evaluate the integrals, we must proceed according to the IREG rules presented in Chapter. 3. After we have the result of all the integrals, we plug the values into Mathematica. By doing this, we will have the appearance of non-local terms which are going to be eliminated when doing the renormalization with the counterterms.

## 4.2 Quadratically divergent terms

In this section, we will explain why the contraction of Lorentz indices in a tensorial integral does not commute with Implicit Regularization (22). IREG satisfies invariance under the shift of the integration momenta. This, as mentioned in Chapter. 3 guarantees the independence of momentum routing. The shift invariance can be related to the vanishing of total derivatives regarding integration momenta:

$$0 = \left[ \int d^n k (f(k+p) - f(k)) \right]^R = p_\nu \left[ \int d^n k \frac{\partial}{\partial k_\nu} f(k) \right]^R + \mathcal{O}(p^2), \quad (4.4)$$



where R indicates that the expression inside the brackets is renormalized. Moreover, the operation is linear, which means:

$$[aF + bG]^R = a[F]^R + b[G]^R, \quad (4.5)$$

being a, and b numbers or external objects.

Let us consider:

$$\begin{aligned} f_{\mu\nu} &= \int d^4k \frac{\partial}{\partial k_\mu} \frac{k_\nu}{(k^2 - m^2)} \\ &= \int d^4k \left( \frac{g_{\mu\nu}}{k^2 - m^2} - 2 \frac{k_\mu k_\nu}{(k^2 - m^2)^2} \right). \end{aligned} \quad (4.6)$$

According to Eq. (4.4),  $[f_{\mu\nu}]^R = 0$ . If we call:

$$I_{\mu\nu} = \int d^4k \frac{k_\mu k_\nu}{(k^2 - m^2)^2}, \quad (4.7)$$

therefore:

$$\begin{aligned} [I_{\mu\nu}]^R &= \frac{1}{2} g_{\mu\nu} \left[ \int d^4k \frac{1}{k^2 - m^2} \right]^R \\ &= \frac{1}{2} g_{\mu\nu} \left( \left[ \int d^4k \frac{k^2}{(k^2 - m^2)^2} \right]^R - \left[ \int d^4k \frac{m^2}{(k^2 - m^2)^2} \right]^R \right) \\ &= \frac{1}{2} g_{\mu\nu} \left( [I_{\alpha\alpha}]^R - \left[ \int d^4k \frac{m^2}{(k^2 - m^2)^2} \right]^R \right). \end{aligned} \quad (4.8)$$

We can rewrite previous Eq. (4.8) as

$$g_{\mu\nu} [I_{\mu\nu}]^R = [g_{\mu\nu} I_{\mu\nu}]^R - \left[ \int d^4k \frac{m^2}{(k^2 - m^2)^2} \right]^R. \quad (4.9)$$

Therefore, we can see that renormalization does not commute with Lorentz index contraction within IREG, as the last preserves shifts of integration momenta. This attribute is what causes that:

$$\int_k \frac{k^2}{k^2(k-p)^2} = \lim_{\mu^2 \rightarrow 0} I_{\text{quad}}(\mu^2) = 0, \quad (4.10)$$

and

---


$$g^{\alpha\beta} \int_k \frac{k_\alpha k_\beta}{k^2(k-p)^2} = -\frac{bp^2}{6}. \quad (4.11)$$

are different.

### 4.3 Gauge theories with IREG at 2-loop: examples

In Section. 3.1.2, we gave a 1-loop example displaying how to use IREG for QED. In the same order of ideas, now we provide two examples of how to proceed in the 2-loop calculation for gauge theories with IREG. Each of these examples employs the algorithms explained in previous sections. The objective is to show the reader the panorama of subtleties to take into account to 2-loop with the scheme. We will see the level of technicality that these computations at 2-loop involve depending on whether the sub-diagram contains gluon lines or fermion lines.

#### 4.3.1 Example 1: 2-loop approach in pure Yang-Mills

Concerning 2-loop diagrams, to contrast the complexities that arise at this level, we consider the diagram of Fig. 4.4 in pure Yang-Mills. We emphasize the fact that the sub-diagram has a gluonic loop:

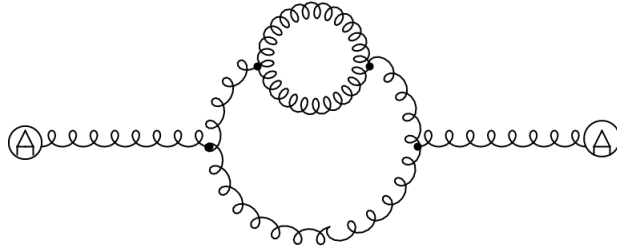


Figure 4.4: In this image, we can observe a particular process at 2-loop in pure Yang-Mills. Field A on the external lines represents the Background Field (BF). The presence of this field provides particular Feynman rules. It is important to mention that we can divide this diagram into two parts, the main diagram and a sub-diagram which is the gluon self-energy.

We will develop this example following the algorithm from the previous sections, see Fig. 4.2. In stage 1, we first apply the Feynman rules to the sub-diagram: the gluon self-energy. This sub-diagram has an internal momentum  $l$ . Notice that at this stage, no regularization scheme has been chosen. We apply the Background Field Method (BFM) Feynman's rules in Fig 4.5:

Our result is:

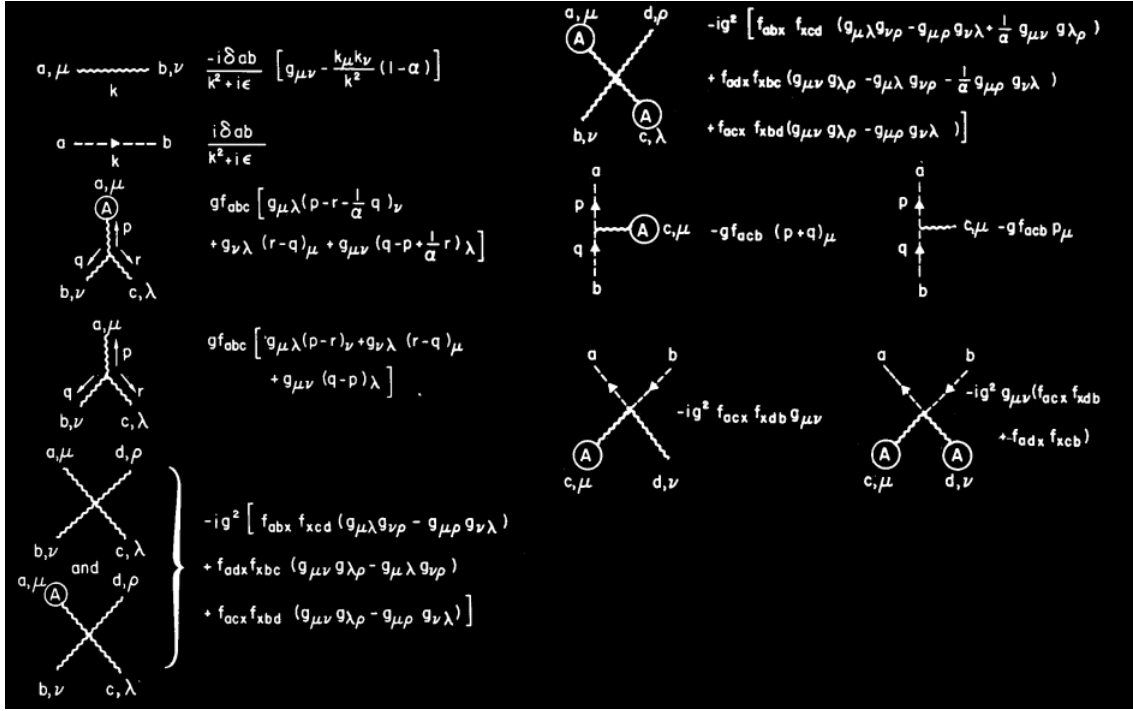


Figure 4.5: Feynman rules for the BFM from Ref. (15).

$$\begin{aligned}
 & \text{Diagram: A loop with momentum } l \text{ and } l-k. \text{ External lines are labeled } a; \alpha, m; \mu, c; \gamma, n; \nu, b; \beta, d; \delta. \text{ The diagram is equal to } \pi_{\mu\nu}^{mn}(l). \\
 & = -g^2 C_A \delta^{mn} \frac{1}{2} \int_l \frac{1}{l^2 (l-k)^2} [2k_\nu k_\mu + 5k_\mu l_\nu + k_\nu l_\mu - 10l_\nu l_\mu - g^{\nu\mu} (5k^2 + 2l^2 - 2k \cdot l)].
 \end{aligned} \tag{4.12}$$

At this point, we have not yet constructed our final amplitude for the 2-loop diagram. We do not evaluate these integrals in the sub-diagram, Eq. (4.12). As the main diagram may contain terms with the metric  $g_{\mu\nu}$ , we want the integral in Eq. (4.12) to commute with them to generate  $l^2$  terms. If we do not do this, we could deal first with the  $l_\mu l_\nu$  integrals, which differ in local terms with the  $l^2$  integral, as explained in Section. 4.2. Therefore, the resulting amplitude (in the Feynman gauge) is given by:

---


$$\begin{aligned}
\Pi_{ls}^{\lambda\sigma} &= \int_k g f^{sra} [g_{\sigma\varrho} 2p_\rho + g_{\rho\varrho} 2k_\sigma - g_{\rho\varrho} p_\sigma - g_{\sigma\rho} 2p_\varrho] \\
&\times \frac{(-1)\delta_{ao}}{(k-p)^2} g^{\omega\varrho} \\
&\times g f^{lot} [-g_{\lambda\tau} 2p_\omega + g_{\omega\tau} 2k_\lambda - g_{\omega\tau} p_\lambda + g_{\lambda\omega} 2p_\tau] \\
&\times \frac{(-i)\delta_{tm}}{k^2} g^{\tau\mu} \\
&\times \pi_{\mu\nu}^{mn}(l) \\
&\times \frac{(-i)\delta_{nr}}{k^2} g^{\nu\rho}.
\end{aligned} \tag{4.13}$$

where  $k$  is the internal momentum of the complete diagram, and  $p$  is the external momentum. Finally:

$$\begin{aligned}
\Pi_{ls}^{\lambda\sigma} &= +ig^4 C_A^2 \delta^{sl} \int_k \frac{1}{k^4 (k-p)^2} \times \xi_{\mu\nu\lambda\sigma} \times \\
&\left[ \frac{1}{2} \int_l \frac{1}{l^2 (l-k)^2} (2k_\nu k_\mu + 5k_\mu l_\nu + k_\nu l_\mu - 10l_\nu l_\mu - g^{\nu\mu} (5k^2 + 2l^2 - 2k \cdot l)) \right]
\end{aligned} \tag{4.14}$$

where:

$$\begin{aligned}
\xi_{\mu\nu\lambda\sigma} &= g^{\nu\rho} [g_{\sigma\varrho} 2p_\rho + g_{\rho\varrho} 2k_\sigma - g_{\rho\varrho} p_\sigma - g_{\sigma\rho} 2p_\varrho] g^{\omega\varrho} \\
&[-g_{\lambda\tau} 2p_\omega + g_{\omega\tau} 2k_\lambda - g_{\omega\tau} p_\lambda + g_{\lambda\omega} 2p_\tau] g^{\tau\mu}.
\end{aligned} \tag{4.15}$$

At this moment, we can perform contractions such as the ones presented in Eq. (4.2). From the many possibilities encoded in the previous amplitude Eq. (4.14), one is simply  $l^\mu l^\nu$  which, after contraction with  $g_{\mu\nu} k_\lambda k_\sigma$ , generates a contribution as:

$$\int_k \frac{k_\lambda k_\sigma}{k^4 (k-p)^2} \int_l \frac{l^2}{l^2 (l-k)^2} \propto \int_k \frac{k_\lambda k_\sigma}{k^4 (k-p)^2} \int_l \frac{1}{(l-k)^2}. \tag{4.16}$$

Notice that the left side of Eq. (4.16) was obtained by applying Feynman rules to the whole multi-loop diagram. By performing contractions and simplifications, we got the right side. After this step, we can enter stage 2 in our algorithm and choose a regularization scheme. For example, if we implement IREG to evaluate the integrals, we must proceed according to the rules sketched in Section. 3.1.1. Moreover, according to Eq. (4.10) we can perceive that a null result will be obtained within the integral in 1.

If we had evaluated the sub-diagram first, we would have obtained:

$$\int_l \frac{l^\alpha l^\beta}{l^2(l-k)^2} \Big|_{\text{IREG}} = k^\alpha k^\beta \mathcal{T}_1 + g^\alpha k^2 \mathcal{T}_2, \quad (4.17)$$

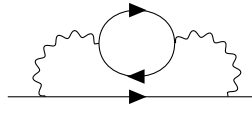
where  $\mathcal{T}_1$  and  $\mathcal{T}_2$  are scalar functions. By contraction with  $g_{\alpha\beta} k_\mu k_\nu$  we get:

$$\int_k \left[ \frac{k_\mu k_\nu k^2}{k^4(k-p)^2} (\mathcal{T}_1 + 4\mathcal{T}_2) \right] = \int_k \left[ \frac{k_\mu k_\nu k^2}{k^4(k-p)^2} \left( -\frac{b}{6} \right) \right] \quad (4.18)$$

which is different from zero. This difference could indicate that if we substitute the sub-diagram first in the case of gluonic loops, inconsistencies terms may be generated, which could violate gauge invariance.

### 4.3.2 Example 2: Quadratic terms in 2-loop QED

In this example, we study one of the electron propagator corrections to 2-loops. Specifically, the one that has a fermionic loop as a sub-diagram. We will call it the electron-bubble diagram. As mentioned in the example from the previous section, we have to apply Feynman's rules to the entire diagram:



$$= \int_l \int_k \frac{ie^2 \gamma^\beta \cdot (l + \not{p}) \cdot \gamma^\nu \text{tr} \left( e^2 \left( -(-\not{k}) \cdot \gamma^\nu \cdot (l - \not{k}) \cdot \gamma^\beta \right) \right)}{(l+p)^2 k^2 l^4 (l-k)^2}. \quad (4.19)$$

If we use the FeynCalc package to solve the trace and then regularize with IREG, it is crucial to be cautious and pay attention to the quadratic terms. If we solve the trace with FeynCalc:

$$\begin{aligned} & \text{tr} \left[ e^2 \left( -(-(\gamma \cdot k)) \cdot \gamma^\nu \cdot (\gamma \cdot (l-k)) \cdot \gamma^\beta \right) \right] \\ &= 4e^2 k^2 g^{\beta\nu} - 4e^2 g^{\beta\nu} (k \cdot l) - 8e^2 k^\beta k^\nu + 4e^2 k^\beta l^\nu + 4e^2 k^\nu l^\beta, \end{aligned} \quad (4.20)$$

and let FeynCalc do the whole product in the numerator:

---


$$\begin{aligned}
& e^2 \gamma^\beta \cdot (\gamma \cdot (l + p)) \cdot \gamma^\nu \left[ 4e^2 k^2 g^{\beta\nu} - 4e^2 g^{\beta\nu} (k \cdot l) - 8e^2 k^\beta k^\nu + 4e^2 k^\beta l^\nu + 4e^2 k^\nu l^\beta \right] \\
& = -e^4 8\gamma^\beta (\gamma \cdot l) \gamma^\nu k_\beta k_\nu + 4e^4 \gamma^\beta (\gamma \cdot l) \gamma^\nu k^2 g_{\beta\nu} + 4e^4 \gamma^\beta (\gamma \cdot l) \gamma^\nu k_\nu l_\beta \\
& + 4e^4 \gamma^\beta (\gamma \cdot l) \gamma^\nu k_\beta l_\nu - 4e^4 \gamma^\beta (\gamma \cdot l) \gamma^\nu (k \cdot l) g_{\beta\nu} - 8e^4 \gamma^\beta (\gamma \cdot p) \gamma^\nu k_\beta k_\nu \\
& + 4e^4 \gamma^\beta (\gamma \cdot p) \gamma^\nu k^2 g_{\beta\nu} + 4e^4 \gamma^\beta (\gamma \cdot p) \gamma^\nu k_\nu l_\beta + 4e^4 \gamma^\beta (\gamma \cdot p) \gamma^\nu k_\beta l_\nu \\
& - 4e^4 \gamma^\beta (\gamma \cdot p) \gamma^\nu (k \cdot l) g_{\beta\nu}.
\end{aligned} \tag{4.21}$$

Still, at this point, we can continue to simplify the Dirac algebra. This point is critical. We must be careful when using FeynCalc before IREG. Contractions as the one in Eq. (4.2) are possible. Nevertheless, FeynCalc will perform other simplifications as the following:

$$\begin{aligned}
-8e^4 \gamma^\beta (\gamma \cdot l) \gamma^\nu k_\beta k_\nu & = -8e^4 \gamma^\beta \gamma^\alpha l_\alpha k_\beta \gamma^\nu k_\nu \\
& = -8e^4 (2g^{\alpha\beta} - \gamma^\alpha \gamma^\beta) l_\alpha k_\beta \gamma^\nu k_\nu \\
& = -16e^4 (l \cdot k) (\gamma \cdot k) + 8e^4 \gamma^\alpha l_\alpha \gamma^\beta k_\beta \gamma^\nu k_\nu \\
& = -16e^4 (l \cdot k) (\gamma \cdot k) + 8e^4 (\gamma \cdot l) \frac{1}{2} (\gamma^\beta \gamma^\nu + \gamma^\nu \gamma^\beta) k_\nu k_\beta \\
& = -16e^4 (l \cdot k) (\gamma \cdot k) + 8e^4 (\gamma \cdot l) g^{\beta\nu} k_\beta k_\nu \\
& = -16e^4 (l \cdot k) (\gamma \cdot k) + 8e^4 (\gamma \cdot l) k^2.
\end{aligned} \tag{4.22}$$

In the last two lines of Eq. (4.22), the package performs simplifications such as Eq. (4.3). Once more, symmetric integration simplifications are prohibited in IREG, as we saw in Section 4.2. We remark then that contractions of  $k^2$  as the one in Eq. (4.2) need to be done before applying IREG.

If we make the Eq. (4.10) and Eq. (4.11) substitutions before applying IREG, what we are doing is not letting the gamma matrices of the trace contract with the gamma matrices outside of it. This procedure is the equivalent of solving the integrals of the sub-diagram first and then contracting with the outer fermionic line. In contrast to the previous example 4.3.1 in this work, this idea possibly indicates that when we have a fermion line in the sub-diagram, we must apply IREG first on it. Otherwise, the anomalous dimension would not give a finite result as expected for the functions of the renormalization group.

## 4.4 The $\beta$ -function in IREG and DS

Until this point, no distinction between regularization in IREG and DS was done for the definition of the  $\beta$ -function in Eq. (2.20). As we mentioned in Sub-section. 2.3.1, physical

predictions cannot depend on the arbitrary mass scales as  $\mu_{DR}$  (in the case of DS schemes) or  $\lambda^2$  (in the case of IREG). If we adopt the framework of DS techniques, the (renormalized) coupling is replaced by:

$$g_R = \mu^{\frac{4-d}{2}} \tilde{g}_R \quad \Rightarrow \quad \beta = \mu \frac{\partial}{\partial \mu} g_R = \frac{4-d}{2} g_R + \mu^{\frac{6-d}{2}} \frac{\partial}{\partial \mu} \tilde{g}_R, \quad (4.23)$$

where  $\tilde{g}_R$  is an adimensional (renormalized) coupling.

We now expand the renormalization constants in terms of the renormalized gauge coupling. Since in the BFM  $Z_g$  and  $Z_A$  are related, we can consider only  $Z_A$ . The constant go at 2-loop as:

$$Z_A = 1 + A_1 \tilde{g}_R^2 + A_2 \tilde{g}_R^4, \quad (4.24)$$

where  $A_1$  and  $A_2$  are the 1-loop and 2-loop coefficients, respectively.

With this Eq. (2.20) transforms into:

$$\beta = \frac{g_R}{2} \lambda \frac{\partial}{\partial \lambda} \left[ A_1 \tilde{g}_R^2 + \left( A_2 - \frac{A_1^2}{2} \tilde{g}_R^4 \right) \right], \quad (4.25)$$

which works for either IREG or DS. In the case of IREG,  $\tilde{g}_R = g$ . To proceed further, we choose a subtraction scheme, which will be the MS-subtraction scheme. Therefore, for DS (where we have to change  $\lambda$  by  $\mu$ ) at 2-loop:

$$\begin{aligned} \beta &= \frac{g_R}{2} \left[ A_1 \mu \frac{\partial}{\partial \mu} (\tilde{g}_R^2) + \left( A_2 - \frac{A_1^2}{2} \right) \mu \frac{\partial}{\partial \mu} (\tilde{g}_R^4) \right], \\ &= \frac{d-4}{2} g_R \left[ A_1 \tilde{g}_R^2 + 2 A_2 \tilde{g}_R^4 \right]. \end{aligned} \quad (4.26)$$

Regarding implicit regularization, IREG's divergent part will depend on the renormalization scale  $\lambda$ , while in DS, this does not occur. By defining the MS-subtraction scheme in IREG as the removal of only basic divergent integrals, the IREG version of Eq. (4.26) will be:

$$\begin{aligned} \beta &= \frac{g_R}{2} \left[ g_R^2 \lambda \frac{\partial}{\partial \lambda} (A_1) + A_1 \lambda \frac{\partial}{\partial \lambda} (g_R^2) + g_R^4 \lambda \frac{\partial}{\partial \lambda} \left( A_2 - \frac{A_1^2}{2} \right) + \left( A_2 - \frac{A_1^2}{2} \right) \lambda \frac{\partial}{\partial \lambda} (g_R^4) \right] \\ &= -g_R \left[ -\frac{g_R^2}{2} \lambda \frac{\partial}{\partial \lambda} A_1 - \frac{g_R^4}{2} \lambda \frac{\partial}{\partial \lambda} A_2 \right]. \end{aligned} \quad (4.27)$$

Therefore, to compute the  $\beta$ -function at 2-loop, we only need to know the 1-loop and

---

2-loop coefficients of  $Z_A$ . In the next chapter, we will see how to get these coefficients for DS and IREG in non-abelian theories.

## 4.5 The anomalous dimensions in gauge theories

As we mentioned in Sub-section. 2.3.2, the anomalous dimensions tell us about the deviation from the classical scaling behavior. The deviation of operators is considered as a function of the running scales:  $\mu$  for DS or  $\lambda^2$  for IREG. Regarding the mass anomalous dimension, this quantity depends on the renormalization scheme adopted at two or higher order (19). Working in a modified minimal subtraction scheme (where our renormalization constants will absorb only the divergences of our amplitudes), we can introduce  $\gamma_m$  in DS and IREG. For DS:

$$\gamma_m^{\overline{DS}}(\mu) = \frac{\mu}{m^{\overline{DS}}} \frac{\partial m^{\overline{DS}}}{\partial \mu} = -\beta^{\overline{DS}}(\mu) \frac{\partial \ln Z_m^{\overline{DS}}}{\partial g^{\overline{DS}}}, \quad (4.28)$$

and for IREG using  $\overline{IREG}$ :

$$\gamma_m^{\overline{IREG}}(\lambda^2) = 2 \frac{\lambda^2}{m^{\overline{IREG}}} \frac{\partial m^{\overline{IREG}}}{\partial \lambda^2} = -\beta^{\overline{IREG}}(\lambda^2) \frac{\partial \ln Z_m^{\overline{IREG}}}{\partial g^{\overline{IREG}}}. \quad (4.29)$$

Notice that in previous Eq. (4.28) and Eq. (4.29) we did the variable change  $m_0 = Z_m m_R$ . Thus, we need to evaluate the renormalization constant  $Z_m$  in a defined renormalization scheme to compute the  $\gamma_m$  of a certain theory. For example, in the case of the quark anomalous mass dimension at 1-loop order within IREG (12):

$$\gamma_m^{\overline{IREG}} = \frac{6g_s^2}{(4\pi)^2} C_2(R), \quad (4.30)$$

where  $C_2(R)\mathbf{1} = t_r^{a\alpha} t_r^{a\alpha}$  is the quadratic Casimir operator and  $g_s$  the strong coupling constant. This result agrees with the minimal subtraction (MS) scheme in CDR, and DRED.

Regarding the anomalous dimension definition in Eq. 2.21, for gauge theories (as QED) at two and higher loops, it depends on the gauge parameter since Green's functions of individual  $\Psi$  and  $\bar{\Psi}$  fields are not gauge invariant. In Chapter. 6, we will return to this point.

## 4.6 The gauge-fixing parameter in IREG

For non-Abelian theories at the end of Section. 2.4, we discussed the gauge-fixing parameter using the Background Field Method (BFM), without specifying the renormalization scheme adopted. We will use the modified minimal subtraction ( $\overline{MS}$ ) scheme. In DS, when we use  $\overline{MS}$  the counterterms are chosen to remove the divergent part of the loops with some terms such as  $\gamma_E$  and  $\ln(4\pi)$ . In IREG at 1-loop, we remove only the  $I_{log}(\lambda^2)$ . Therefore, in IREG



our result for the gluon propagator is:

$$\Pi_{\mu\nu}^{ab}|_{\text{div}} = -i5g^2 C_A I_{\log}(\lambda^2) (g_{\mu\nu} p^2 - p_\mu p_\nu) \delta^{ab}. \quad (4.31)$$

Since, given we are in Feynman gauge, we should obtain the relation:

$$\Pi_{\mu\nu}^{ab}|_{\text{div}} + \delta_\alpha p_\mu p_\nu \delta^{ab} \propto g_{\mu\nu} \delta^{ab}. \quad (4.32)$$

The final result in IREG is:

$$\delta_\alpha = -i5g^2 C_A I_{\log}(\lambda^2), \quad (4.33)$$

which agrees with the DS result in Ref. (17) after inspecting the correspondence among IREG and DS discussed in Secion. (3.3).



## CHAPTER 5

THE TWO-LOOP GAUGE  $\beta$ -FUNCTION FOR ABELIAN AND  
NON-ABELIAN THEORIES

In this chapter, as an explicit application of our 2-loop approach, we apply the procedure discussed in Chapter 4 to pure Yang-Mills, QED, and QCD. Using IREG and the BFM, we compute the first two coefficients of the gauge coupling  $\beta$ -function for non-Abelian theories. These computations provide a consistent test of our method. The results for the DS (CDR and DRED) are also shown.

## 5.1 Pure Yang-Mills

As we discussed in Section 2.4 by using the BFM, the  $\beta$ -function can be determined by calculating the renormalization constant  $Z_A$  which only requires knowledge of the BF 2-point function. No vertex function needs to be considered. The Feynman rules employed in the present calculation can be found in Fig 4.5.

The diagrams needed to compute  $Z_A$  at the 1-loop level are given in Fig C.1.



Figure 5.1: Diagrams for the calculation of the pure YM  $\beta$ -function at 1-loop. The **black** dot will stand for the BF  $A$  in the diagrams. Greek letters indicate Lorentz indices while Latin letters (without arrows) indicate color indices.

The divergent amplitudes after applying the Feynman rules are

$$\text{Diagram: a wavy line connected to a dashed circle, which is then connected to another wavy line.} = +g^2 C_A \delta_{mn} \times [(\frac{1}{3}k^2 g_{\mu\nu} I_{\log}(\lambda^2)) - (\frac{1}{3}k_\mu k_\nu I_{\log}(\lambda^2))] \quad (5.1)$$

and

$$\bullet \text{---} \text{loop} \text{---} \bullet = +g^2 C_A \delta_{mn} \times [(\frac{10}{3} k^2 g_{\mu\nu} I_{log}(\lambda^2)) - (\frac{10}{3} k_\mu k_\nu I_{log}(\lambda^2))], \quad (5.2)$$

where the  $g$  with the color blue (and without indices) is the coupling constant (not to be confused with the metric). Adding these together, we can determine  $Z_A$  which in IREG:

$$Z_A = 1 + g^2 C_A \frac{11}{3} I_{\log}(\lambda^2). \quad (5.3)$$

Hence using the  $\beta$ -function definition in Eq. (2.20) and, the BF relation  $Z_g = Z_A^{-1/2}$  from Chapter 4, we determine the well-known 1-loop YM  $\beta$ -function as

$$\beta = -\frac{11C_A}{3} \frac{g^3}{(4\pi)^2}. \quad (5.4)$$

Now we will work with the 2-loop graphs to compute  $Z_A$  using the diagrams in Fig. 5.2.

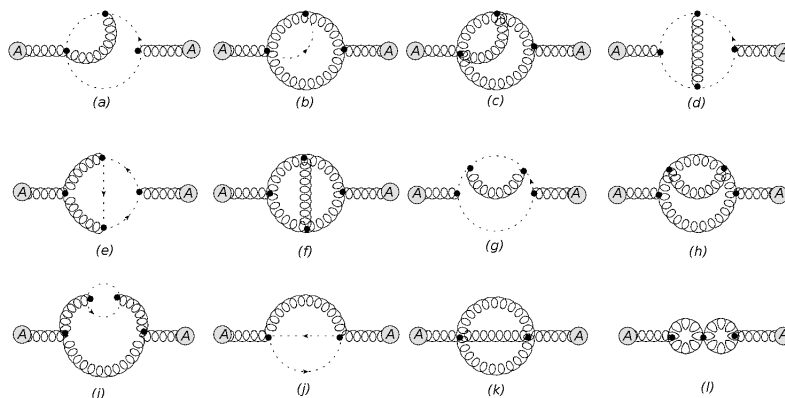


Figure 5.2: 2-loop correction to the 2-point function of the BF A for pure Yang-Mills.

All the topologies from Fig. 4.1 appear, which later will show us the presence of not only terms with  $I_{log}(\lambda^2)$  in our 2-loop amplitudes, but also  $I_{log}^{(2)}(\lambda^2)$ , and  $I_{log}^2(\lambda^2)$ . As well, the 1-loop correction to the gluon self-energy appears as a sub-diagram in diagrams (h) and (i). Therefore, we will need to consider counterterms related to the gauge fixed-renormalization as discussed in Chapter 4.

To present our results, we define the 2-loop correction to the BF in the amplitude to be of the form:

$$\frac{ig_s^4 C_A^2 \delta^{ab}}{(4\pi)^4} [Ag_{\mu\nu} p^2 - Bp_\mu p_\nu], \quad (5.5)$$

where  $p$  is the external momenta carried by the BF. Our results, for IREG, are presented in Table 5.1.

Diagram	A				B			
	$I_{log}^{(2)}(\lambda^2)$	$I_{log}^2(\lambda^2)$	$\rho_{IREG}$	$I_{log}(\lambda^2)$	$I_{log}^{(2)}(\lambda^2)$	$I_{log}^2(\lambda^2)$	$\rho_{IREG}$	$I_{log}(\lambda^2)$
$a$	$\frac{1}{3b}$	$-\frac{1}{3b^2}$	$\frac{1}{3b}$	$-\frac{29}{18b}$	$\frac{1}{3b}$	$-\frac{1}{3b^2}$	$\frac{1}{3b}$	$-\frac{17}{18b}$
$b$	$\frac{5}{12b}$	$-\frac{5}{12b^2}$	$\frac{5}{12b}$	$-\frac{97}{72b}$	$\frac{5}{12b}$	$-\frac{5}{12b^2}$	$\frac{5}{12b}$	$-\frac{109}{72b}$
$c$	$\frac{9}{4b}$	$-\frac{9}{4b^2}$	$\frac{9}{4b}$	$-\frac{39}{8b}$	$\frac{9}{4b}$	$-\frac{9}{4b^2}$	$\frac{9}{4b}$	$-\frac{75}{8b}$
$d$	$-\frac{1}{12b}$	$\frac{1}{12b^2}$	$-\frac{1}{12b}$	$\frac{47}{72b}$	$-\frac{1}{12b}$	$\frac{1}{12b^2}$	$-\frac{1}{12b}$	$\frac{35}{72b}$
$e$	$\frac{1}{2b}$	$-\frac{1}{2b^2}$	$\frac{1}{2b}$	$-\frac{7}{4b}$	$\frac{1}{2b}$	$-\frac{1}{2b^2}$	$\frac{1}{2b}$	$-\frac{7}{4b}$
$f$	$-\frac{27}{4b}$	$\frac{27}{4b^2}$	$-\frac{27}{4b}$	$\frac{195}{8b}$	$-\frac{27}{4b}$	$\frac{27}{4b^2}$	$-\frac{27}{4b}$	$\frac{207}{8b}$
$g$	$-\frac{1}{3b}$	$\frac{1}{3b^2}$	$-\frac{1}{3b}$	$\frac{29}{18b}$	$-\frac{1}{3b}$	$\frac{1}{3b^2}$	$-\frac{1}{3b}$	$\frac{13}{9b}$
$h + i$	$-\frac{25}{3b}$	$\frac{25}{3b^2}$	$-\frac{25}{3b}$	$\frac{521}{18b}$	$-\frac{25}{3b}$	$\frac{25}{3b^2}$	$-\frac{25}{3b}$	$\frac{268}{9b}$
$j$	0	0	0	$\frac{1}{4b}$	0	0	0	0
$k$	0	0	0	$-\frac{9}{4b}$	0	0	0	0
$l$	0	$-\frac{6}{b^2}$	$\frac{12}{b}$	$-\frac{24}{b}$	0	$-\frac{6}{b^2}$	$\frac{12}{b}$	$-\frac{24}{b}$
Sum	$-\frac{12}{b}$	$\frac{6}{b^2}$	0	$\frac{20}{b}$	$-\frac{12}{b}$	$\frac{6}{b^2}$	0	$\frac{20}{b}$

Table 5.1: Results for pure Yang-Mills using IREG where  $\rho_{IREG} = I_{log}(\lambda^2) \ln \left[ -\frac{p^2}{\lambda^2} \right]$ .

Let us remember that as the calculation was performed in the Feynman gauge  $\alpha = 1$ , the gauge fixed-renormalization insertion diagrams will also be included as we mentioned in Chapter 4. For the counterterms corresponding to Fig. 5.3 our results are shown in Table 5.2.

Notice in the IREG results that, apart from minus signs and/or global factors encoded in the parameter  $b = i/(4\pi)^2$ , diagrams (a) to (i) have the same coefficients for  $I_{log}^{(2)}(\lambda^2)$ ,  $I_{log}^2(\lambda^2)$ , and  $\rho_{IREG} = I_{log}(\lambda^2) \ln(-p^2/\lambda^2)$ . We can understand this fact in the following way: considering the amplitude of one of those diagrams is given by

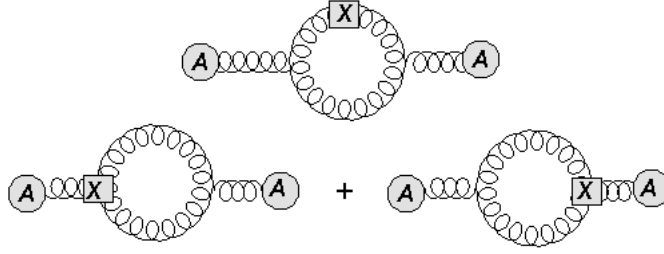


Figure 5.3: Counterterms diagrams.

Counterterm	A				B			
	$I_{log}^{(2)}(\lambda^2)$	$I_{log}^2(\lambda^2)$	$\rho_{IREG}$	$I_{log}(\lambda^2)$	$I_{log}^{(2)}(\lambda^2)$	$I_{log}^2(\lambda^2)$	$\rho_{IREG}$	$I_{log}(\lambda^2)$
$AA\hat{A}$ Coupling	0	$-\frac{25}{9b}$	$\frac{25}{9b}$	$-\frac{140}{27b}$	0	$-\frac{25}{9b}$	$\frac{25}{9b}$	$-\frac{140}{27b}$
Gluon self-energy	0	$\frac{25}{9b}$	$-\frac{25}{9b}$	$\frac{230}{27b}$	0	$\frac{25}{9b}$	$-\frac{25}{9b}$	$\frac{230}{27b}$
Sum	0	0	0	$\frac{10}{3b}$	0	0	0	$\frac{10}{3b}$

Table 5.2: Counterterms results for pure Yang-Mills using IREG where  $\rho_{IREG} = I_{log}(\lambda^2) \ln \left[ -\frac{p^2}{\lambda^2} \right]$ .

$$\mathcal{A} = \int_{k,l} \mathcal{F}(l, k, p). \quad (5.6)$$

We will separate the amplitude  $\mathcal{F}(l, k, p)$  into different pieces based on the order of integration of the internal momenta (34):

$$\mathcal{A} \supset \int_k G(k, p, \mu^2) \int_l F(l, k, p, \mu^2). \quad (5.7)$$

Solving the integral in l first, we identify the BDIs and, using the scale relation Eq. (3.30) we get:

$$\mathcal{A} \supset \int_k G(k, p, \mu^2) [a_1 I_{log}(\mu^2) + a_2] = \int_k G(k, p, \mu^2) \left[ a_1 I_{log}(\lambda^2) - a_1 b \ln \left[ -\frac{k^2}{\lambda^2} \right] + \bar{a}_2 \right],$$

where the actual form of  $a_2$  and  $\bar{a}_2$  are not relevant here. Then we will solve the integral in momentum k. We will again identify the BDIs:

$$\begin{aligned}
 \mathcal{A} &\supset a_1 I_{\log}(\lambda^2) \int_k G(k, p, \mu^2) - a_1 b \int_k G(k, p, \mu^2) \ln \left[ -\frac{k^2}{\lambda^2} \right] \\
 &= a_1 I_{\log}(\lambda^2) \left[ A_1 I_{\log}(\mu^2) + \dots \right] - a_1 b \left[ A_1 I_{\log}^{(2)}(\mu^2) + \dots \right] \\
 &= a_1 A_1 \left[ I_{\log}^2(\lambda^2) - b I_{\log}(\lambda^2) \ln \left[ -\frac{p^2}{\lambda^2} \right] - b I_{\log}^{(2)}(\lambda^2) + \dots \right], \tag{5.8}
 \end{aligned}$$

where we made use of the relation (18):

$$\int_k G(k, p, \mu^2) \ln^n \left[ -\frac{k^2}{\lambda^2} \right] = A_1 I_{\log}^{(n+1)}(\mu^2) + \dots \tag{5.9}$$

What we observed in Eq. (5.8) is that the factors are correlated. There is a minus sign and  $b$  factor difference among  $I_{\log}^{(2)}(\lambda^2)$ ,  $\rho_{IREG}$ , and  $I_{\log}^2(\lambda^2)$ , which reproduces the pattern we found for diagrams (a) to (i) in Table 5.1.

On the other hand, our results for the DS are presented in Table 5.3. Notice also for the DS that the  $\rho$  terms (non-local terms) vanish after summing all the diagrams, the same as in the IREG case. Since there is a correlation among  $\epsilon^{-2}$  and the  $\rho$  coefficient for all topologies, no term is proportional to  $\epsilon^{-2}$  can survive. We also notice that there are some differences between CDR and DRED in diagrams (c), (f), and (h), although their sum vanishes. The reason can be traced to the contractions of the metric, as  $g_{ab}g^{ab} = d$ . For the counterterms in the DS, our results for the gauge-coupling renormalization diagrams are in Table. 5.4.

Finally, we notice that our results in Tables 5.1 5.2 5.3 5.4 are gauge invariant (in the amplitude), local (since non-local terms, as  $\rho$  or  $\rho_{IREG}$  vanish), and transverse. With these results, we can determine the coefficients of the  $\beta$ -function for pure Yang-Mills.

### 5.1.1 Summary of results for pure YM

Using our results collected in Tables 5.1 5.2 for IREG and Tables 5.3 5.4 for DS, in this section we compute  $Z_A$  and then, finally, the  $\beta$ -function for pure Yang-Mills.

From Chapter 4, Eq. (4.24), we can define the renormalisation function of the background gauge boson as:

$$Z_A = 1 + \frac{g^2}{(4\pi)^2} \delta_A^{(1)} + \frac{g^4}{(4\pi)^4} \delta_A^{(2)}. \tag{5.10}$$

In DS, considering the diagrams in Fig. C.1, the divergent contributions in the amplitudes at 1-loop order have the form

Diagram	$A_{\text{CDR}}$	$A_{\text{DRED}} - A_{\text{CDR}}$	$B_{\text{CDR}}$	$B_{\text{DRED}} - B_{\text{CDR}}$
$a$	$-\frac{1}{6\epsilon^2} + \frac{-13+4\rho}{12\epsilon}$	0	$-\frac{1}{6\epsilon^2} + \frac{-9+4\rho}{12\epsilon}$	0
$b$	$-\frac{5}{24\epsilon^2} + \frac{-41+20\rho}{12\epsilon}$	0	$-\frac{5}{24\epsilon^2} + \frac{5(-9+4\rho)}{48\epsilon}$	0
$c$	$-\frac{9}{8\epsilon^2} + \frac{-57+36\rho}{16\epsilon}$	$\frac{3}{4\epsilon}$	$-\frac{9}{8\epsilon^2} + \frac{-93+36\rho}{16\epsilon}$	$\frac{3}{4\epsilon}$
$d$	$\frac{1}{24\epsilon^2} + \frac{19-4\rho}{48\epsilon}$	0	$\frac{1}{24\epsilon^2} + \frac{15-4\rho}{48\epsilon}$	0
$e$	$-\frac{1}{4\epsilon^2} + \frac{-9+4\rho}{8\epsilon}$	0	$-\frac{1}{4\epsilon^2} + \frac{-9+4\rho}{8\epsilon}$	0
$f$	$\frac{27}{8\epsilon^2} + \frac{233-108\rho}{16\epsilon}$	$\frac{3}{4\epsilon}$	$\frac{27}{8\epsilon^2} + \frac{245-108\rho}{16\epsilon}$	$\frac{3}{4\epsilon}$
$g$	$\frac{1}{6\epsilon^2} + \frac{13-4\rho}{12\epsilon}$	0	$\frac{1}{6\epsilon^2} + \frac{3-\rho}{3\epsilon}$	0
$h+i$	$\frac{25}{6\epsilon^2} + \frac{215-100\rho}{12\epsilon}$	$-\frac{3}{2\epsilon}$	$\frac{25}{6\epsilon^2} + \frac{110-50\rho}{6\epsilon}$	$-\frac{3}{2\epsilon}$
$j$	$\frac{1}{8\epsilon}$	0	0	0
$k$	$-\frac{9}{8\epsilon}$	0	0	0
$l$	$-\frac{6}{\epsilon^2} + \frac{12(-2+\rho)}{\epsilon}$	0	$-\frac{6}{\epsilon^2} + \frac{12(-2+\rho)}{\epsilon}$	0
Sum	$\frac{7}{3\epsilon}$	0	$\frac{7}{3\epsilon}$	0

Table 5.3: Results for pure Yang-Mills using CDR and DRED, where  $\rho = \gamma_E - \ln 4\pi + \ln(p^2/\mu_{DR}^2)$ .

Counterterm	$A_{\text{CDR}}$	$A_{\text{DRED}} - A_{\text{CDR}}$	$B_{\text{CDR}}$	$B_{\text{DRED}} - B_{\text{CDR}}$
$AAA\hat{\text{Coupling}}$	$-\frac{25}{9\epsilon^2} + \frac{5(-28+15\rho)}{27\epsilon}$	0	$-\frac{25}{9\epsilon^2} + \frac{5(-28+15\rho)}{27\epsilon}$	0
Gluon self-energy	$\frac{25}{9\epsilon^2} + \frac{5(46-15\rho)}{27\epsilon}$	0	$\frac{25}{9\epsilon^2} + \frac{5(46-15\rho)}{27\epsilon}$	0
Sum	$\frac{10}{3\epsilon}$	0	$\frac{10}{3\epsilon}$	0

Table 5.4: Counterterms results for pure Yang-Mills using CDR and DRED, where  $\rho = \gamma_E - \ln 4\pi + \ln(p^2/\mu_{DR}^2)$ .

$$\frac{ig_s^2 C_A \delta^{ab}}{(4\pi)^2} \left( \frac{11}{3\epsilon} \right) [g_{\mu\nu} p^2 - p_\mu p_\nu]. \quad (5.11)$$

At 2-loop, considering all the diagrams in Fig. 5.2 and Fig.2.7, whose results are collected in Tables 5.3 and 5.4, the divergent contributions in the amplitudes have the form:



$$\frac{ig_s^4 C_A^2 \delta^{ab}}{(4\pi)^4} \left( \frac{17}{3\epsilon} \right) [g_{\mu\nu} p^2 - p_\mu p_\nu]. \quad (5.12)$$

Therefore, we found for pure Yang-Mills in DS:

$$\delta_A^{(1)}|_{\text{DS}} = \frac{11C_A}{3\epsilon}, \quad \delta_A^{(2)}|_{\text{DS}} = \frac{17C_A^2}{3\epsilon}. \quad (5.13)$$

With the value of the renormalization constant for the BF, we can compute the  $\beta$ -function. As standard, one can also define the expansion of the  $\beta$ -function in the adimensional coupling constant as (18; 17):

$$\beta = -g_R \left[ \beta_0 \left( \frac{\tilde{g}_R}{4\pi} \right)^2 + \beta_1 \left( \frac{\tilde{g}_R}{4\pi} \right)^4 \right]; \quad (5.14)$$

which for DS, after comparison with Eq. (4.26) gives us:

$$\beta_0 \propto \epsilon A_1, \quad \beta_1 \propto 2\epsilon A_2. \quad (5.15)$$

Now if we compare the previous result with Eq. (4.24) and Eq. (5.10), we get:

$$\beta_0 = \epsilon \delta_A^{(1)}, \quad \beta_1 = 2\epsilon \delta_A^{(2)}, \quad (5.16)$$

since  $d = 4 - 2\epsilon$ . Thus our final result for DS using Eq. (5.13) will be:

$$\beta|_{\text{DS}} = -g_R \left[ \frac{11}{3} C_A \left( \frac{\tilde{g}_R}{4\pi} \right)^2 + \frac{34}{3} C_A^2 \left( \frac{\tilde{g}_R}{4\pi} \right)^4 \right]. \quad (5.17)$$

Let us see now what happens for our method in the physical dimension. For IREG, the divergent contributions at 2-loop order have the form:

$$\frac{ig_s^4 C_A^2 \delta^{ab}}{(4\pi)^4} \left( -\frac{12}{b} I_{\log}^{(2)}(\lambda^2) + \frac{6}{b^2} I_{\log}^2(\lambda^2) + \frac{70}{3b} I_{\log}(\lambda^2) \right) [g_{\mu\nu} p^2 - p_\mu p_\nu]. \quad (5.18)$$

We found for pure Yang-Mills in IREG:

$$\delta_A^{(1)}|_{\text{IREG}} = \frac{11}{3b} C_A I_{\log}(\lambda^2), \quad \delta_A^{(2)}|_{\text{IREG}} = \left( -\frac{12}{b} I_{\log}^{(2)}(\lambda^2) + \frac{6}{b^2} I_{\log}^2(\lambda^2) + \frac{70}{3b} I_{\log}(\lambda^2) \right) C_A^2. \quad (5.19)$$

For IREG, after comparison with Eq. (5.14), Eq. (4.27), Eq. (4.24) and Eq. (5.10), implies:

$$\beta_0 = -\frac{1}{2} \lambda \frac{\partial}{\partial \lambda} \delta_A^{(1)}, \quad \beta_1 = -\frac{1}{2} \lambda \frac{\partial}{\partial \lambda} \delta_A^{(2)}. \quad (5.20)$$

---

Using:

$$\lambda \frac{\partial}{\partial \lambda} I_{\log}(\lambda^2) = -2b; \quad \lambda \frac{\partial}{\partial \lambda} I_{\log}^{(2)}(\lambda^2) = -2b - 2I_{\log}(\lambda^2); \quad (5.21)$$

which enables us to perform the calculations without explicitly evaluating the BDI's, we get:

$$\beta_0 = \frac{11C_A}{3}, \quad \beta_1 = \frac{34C_A^2}{3}. \quad (5.22)$$

Our final result for IREG will be:

$$\beta|_{\text{IREG}} = -g_R \left[ \frac{11}{3} C_A \left( \frac{\tilde{g}_R}{4\pi} \right)^2 + \frac{34}{3} C_A^2 \left( \frac{\tilde{g}_R}{4\pi} \right)^4 \right]. \quad (5.23)$$

It is evident that Eq. (5.17) and Eq. (5.23) are equal. Up to 2-loops,  $\beta$ -function does not depend on the regularization scheme used. Notice also that the  $\beta$ -function is finite and there are no terms that contain the divergences, such as  $\epsilon \rightarrow 0$  poles or the BDIs.

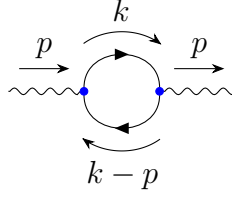
## 5.2 QED

For quantum electrodynamics (QED), we expect that even fewer diagrams will contribute. As we mentioned in Section 2.2, photons do not interact with themselves. This means, that only topologies T2 and T3 from Fig 4.1, need to be considered. Regarding the counterterms, they can also be omitted. First, the gauge-fixing parameter renormalization in Fig. 5.3 can only affect diagrams that contain a gauge propagator correction as a sub-diagram, which is not the case here. Second, the counterterms related to the renormalization of the QED vertex and the fermion self-energy must cancel, since our result will not contain any non-local terms before the inclusion of the counterterms. For completeness, we computed them and checked that they cancel.

Again, the only point that one should be careful about in gauge theories is how the Dirac algebra is performed, as we explained in Chapter 4. In the case of dimensional regularization schemes (DS), spurious terms  $\mathcal{O}(\epsilon)$  will appear, implying that the results in CDR and DRED, are not identical diagram by diagram, although the final result should be. This is indeed the case. In the framework of IREG, some care should also be exercised, to perform tensor identification consistently. As we argued in Section 4.1.1, we perform Dirac and Lorentz algebra on the whole diagram.

The diagram needed to compute  $Z_A$  at the 1-loop level in QED is given in Fig. 5.4. We do the detailed 1-loop calculation within IREG in Appendix B.

For the 1-loop calculation:

Figure 5.4: Diagrams for the calculation of QED's  $\beta$ -function at one-loop.

$$Z_A = 1 - e^2 \frac{4}{3b} I_{\log}(\lambda^2) \quad (5.24)$$

and therefore, the  $\beta$ -function for QED at 1-loop within IREG is:

$$\beta = + \frac{e^3}{12\pi^2}. \quad (5.25)$$

For the 2-loop calculation, as we did for YM, we will define the two-loop correction to the photon field in QED adopting a conversion similar to the one in Eq. (5.5). The form will be:

$$\mathcal{A}_{\mu\nu} = \frac{ig_e^4}{(4\pi)^4} [Ag_{\mu\nu}p^2 - Bp_\mu p_\nu], \quad (5.26)$$

where  $p$  is the momentum carried by the external photon. With this definition, the explicit results for each topology can be read in the next tables for each regularization scheme:

Topology	A				B			
	$I_{\log}^{(2)}(\lambda^2)$	$I_{\log}^2(\lambda^2)$	$\rho_{IREG}$	$I_{\log}(\lambda^2)$	$I_{\log}^{(2)}(\lambda^2)$	$I_{\log}^2(\lambda^2)$	$\rho_{IREG}$	$I_{\log}(\lambda^2)$
$T2$	$\frac{8}{3b}$	$-\frac{8}{3b^2}$	$\frac{8}{3b}$	$-\frac{52}{3b}$	$\frac{8}{3b}$	$-\frac{8}{3b^2}$	$\frac{8}{3b}$	$-\frac{16}{b}$
$T3$	$-\frac{8}{3b}$	$\frac{8}{3b^2}$	$-\frac{8}{3b}$	$\frac{40}{3b}$	$-\frac{8}{3b}$	$\frac{8}{3b^2}$	$-\frac{8}{3b}$	$\frac{12}{b}$
Sum	0	0	0	$-\frac{4}{b}$	0	0	0	$-\frac{4}{b}$

Table 5.5: Results for QED using IREG where  $\rho_{IREG} = I_{\log}(\lambda^2) \ln \left[ -\frac{p^2}{\lambda^2} \right]$ 

Diagram	$A_{CDR}$	$A_{DRED} - A_{CDR}$	$B_{CDR}$	$B_{DRED} - B_{CDR}$
$T2$	$\frac{4}{3\epsilon^2} + \frac{8(2-\rho)}{3\epsilon}$	$\frac{4}{3\epsilon}$	$\frac{4}{3\epsilon^2} + \frac{2(7-4\rho)}{3\epsilon}$	$\frac{4}{3\epsilon}$
$T3$	$-\frac{4}{3\epsilon^2} - \frac{2(11-4\rho)}{3\epsilon}$	$-\frac{4}{3\epsilon}$	$-\frac{4}{3\epsilon^2} - \frac{4(5-2\rho)}{3\epsilon}$	$-\frac{4}{3\epsilon}$
Sum	$-\frac{2}{\epsilon}$	0	$-\frac{2}{\epsilon}$	0

Table 5.6: Results QED using CDR and DRED, where  $\rho = \gamma_E - \ln 4\pi + \ln(p^2/\mu_{DR}^2)$

Counterterm	A				B			
	$I_{log}^{(2)}(\lambda^2)$	$I_{log}^2(\lambda^2)$	$\rho_{IREG}$	$I_{log}(\lambda^2)$	$I_{log}^{(2)}(\lambda^2)$	$I_{log}^2(\lambda^2)$	$\rho_{IREG}$	$I_{log}(\lambda^2)$
Coupling	0	$\frac{8}{3b^2}$	$-\frac{8}{3b}$	$\frac{56}{9b}$	0	$\frac{8}{3b^2}$	$-\frac{8}{3b}$	$\frac{56}{9b}$
Fermion self-energy	0	$-\frac{8}{3b^2}$	$\frac{8}{3b}$	$-\frac{56}{9b}$	0	$-\frac{8}{3b^2}$	$\frac{8}{3b}$	$-\frac{56}{9b}$
Sum	0	0	0	0	0	0	0	0

Table 5.7: Counterterm results for QED using IREG where  $\rho_{IREG} = I_{log}(\lambda^2) \ln \left[ -\frac{p^2}{\lambda^2} \right]$

Counterterm	$A_{CDR}$	$A_{DRED} - A_{CDR}$	$B_{CDR}$	$B_{DRED} - B_{CDR}$
Coupling	$\frac{8}{3\epsilon^2} + \frac{8(7-3\rho)}{9\epsilon}$	0	$\frac{8}{3\epsilon^2} + \frac{8(7-3\rho)}{9\epsilon}$	0
Fermion self-energy	$-\frac{8}{3\epsilon^2} - \frac{8(7-3\rho)}{9\epsilon}$	0	$-\frac{8}{3\epsilon^2} - \frac{8(7-3\rho)}{9\epsilon}$	0
Sum	0	0	0	0

Table 5.8: Counterterm results for QED using CDR and DRED, where  $\rho = \gamma_E - \ln 4\pi + \ln(p^2/\mu_{DR}^2)$

Notice in previous tables that for QED, the final result after doing the sum depends only on  $I_{log}(\lambda^2)$ .

## 5.2.1 Summary of results for QED

Here, we collect the results we found, aiming to compute the renormalization function of the photon for QED. We will use the same definition for  $Z_A$  in Eq. (5.10) for the external gauge boson in QED (the photon). We obtained:

$$\delta_A^{(1)}|_{IREG} = -\frac{4}{3b}I_{log}(\lambda^2), \quad \delta_A^{(1)}|_{CDR} = -\frac{4}{3\epsilon}, \quad (5.27)$$

$$\delta_A^{(2)}|_{IREG} = -\frac{4}{b}I_{log}(\lambda^2), \quad \delta_A^{(2)}|_{CDR} = -\frac{2}{\epsilon}, \quad (5.28)$$

$$(5.29)$$

and then, the  $\beta$ -function according to Eq. (5.14) for DS will be:

$$\beta|_{DS} = -e \left[ -\frac{4}{3} \left( \frac{e}{4\pi} \right)^2 - 4 \left( \frac{e}{4\pi} \right)^4 \right], \quad (5.30)$$

and for IREG, using the Eq. (5.20), and Eq. (5.21):

$$\beta|_{IREG} = -e \left[ -\frac{4}{3} \left( \frac{e}{4\pi} \right)^2 - 4 \left( \frac{e}{4\pi} \right)^4 \right]. \quad (5.31)$$

As expected, the  $\beta$ -function for QED is the same at 2-loop order (regardless of the regularization scheme used). In the next section, we will see the same for QCD.

## 5.3 QCD

Since quantum chromodynamics (QCD) is a specific case of a Yang-Mills theory, as we discussed in Section 2.2, we can evaluate the results we obtained for the general Yang-Mills, and include the corrections due to fermions, which are depicted in Fig. 5.5. For QCD, we consider also the counterterms from the gauge-fixing parameter mentioned in Section 2.4. In the case of the analysis with DS, the same patterns presented in QED appear here also, namely, in all diagrams, there is a mismatch between CDR and DRED, although the sum is the same in both methods.

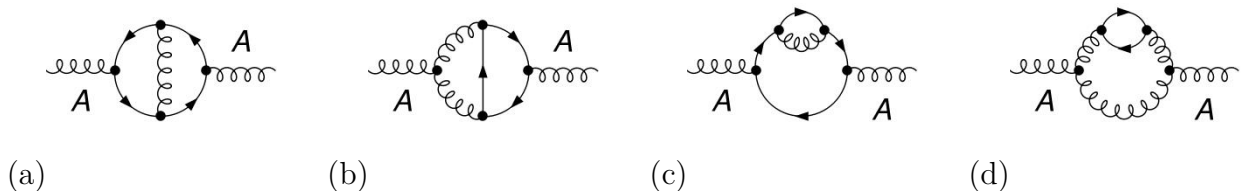


Figure 5.5: Two-loop correction to the two-point function of the background field - fermionic contribution of QCD

In the case of the 1-loop calculation within IREG for the  $\beta$ -function and diagrams, we refer the reader to Ref. (12). For the 2-loop computation, we adopted a similar convention of Eq. (5.5),

$$\frac{ig_s^4 n_f}{(4\pi)^4} [Ag_{\mu\nu}p^2 - Bp_\mu p_\nu], \quad (5.32)$$

where  $n_f$  is the number of fermions. We can express our results in tables 5.9 and 5.10. We see that for QCD, only terms proportional to  $I_{\log}(\lambda^2)$  survive in the result, as we already noticed in the QED case.

One may notice that, in all diagrams, there is a mismatch between CDR and DRED, although the sum is the same in both methods, as in all other examples we considered here. Finally, as in the case of YM, the result is gauge invariant and local, although we still need to add counterterms. The results of the counterterms follow a similar pattern to the one seen in the Yang-Mills theory, and they can be read from tables 5.11, and 5.12.

### 5.3.1 Summary of results for QCD

Using Eq. 5.10, we obtain for QCD:

Diagram	A				B			
	$I_{log}^{(2)}(\lambda^2)$	$I_{log}^2(\lambda^2)$	$\rho_{IREG}$	$I_{log}(\lambda^2)$	$I_{log}^{(2)}(\lambda^2)$	$I_{log}^2(\lambda^2)$	$\rho_{IREG}$	$I_{log}(\lambda^2)$
$a$	$-\frac{2}{9b}$	$\frac{2}{9b^2}$	$-\frac{2}{9b}$	$\frac{35}{27b}$	$-\frac{2}{9b}$	$\frac{2}{9b^2}$	$-\frac{2}{9b}$	$\frac{32}{27b}$
$b$	$-\frac{8}{b}$	$\frac{8}{b^2}$	$-\frac{8}{b}$	$\frac{44}{3b}$	$-\frac{8}{b}$	$\frac{8}{b^2}$	$-\frac{8}{b}$	$\frac{50}{3b}$
$c$	$-\frac{16}{9b}$	$\frac{16}{9b^2}$	$-\frac{16}{9b}$	$\frac{208}{27b}$	$-\frac{16}{9b}$	$\frac{16}{9b^2}$	$-\frac{16}{9b}$	$\frac{184}{27b}$
$d$	$\frac{10}{b}$	$-\frac{10}{b^2}$	$\frac{10}{b}$	$-\frac{97}{3b}$	$\frac{10}{b}$	$-\frac{10}{b^2}$	$\frac{10}{b}$	$-\frac{100}{3b}$
Sum	0	0	0	$\frac{70}{27b}$	0	0	0	$-\frac{70}{27b}$

Table 5.9: Results for fermionic part of QCD using IREG where  $\rho_{IREG} = I_{log}(\lambda^2) \ln \left[ -\frac{p^2}{\lambda^2} \right]$ .

Diagram	$A_{CDR}$	$A_{DRED} - A_{CDR}$	$B_{CDR}$	$B_{DRED} - B_{CDR}$
$a$	$\frac{1}{9\epsilon^2} + \frac{11-4\rho}{18\epsilon}$	$\frac{1}{9\epsilon}$	$\frac{1}{9\epsilon^2} + \frac{5-2\rho}{9\epsilon}$	$\frac{1}{9\epsilon}$
$b$	$\frac{4}{\epsilon^2} + \frac{13-8\rho}{\epsilon}$	$-\frac{2}{\epsilon}$	$\frac{4}{\epsilon^2} + \frac{2(7-4\rho)}{\epsilon}$	$-\frac{2}{\epsilon}$
$c$	$\frac{8}{9\epsilon^2} + \frac{16(2-\rho)}{9\epsilon}$	$\frac{8}{9\epsilon}$	$\frac{8}{9\epsilon^2} + \frac{4(7-4\rho)}{9\epsilon}$	$\frac{8}{9\epsilon}$
$d$	$-\frac{5}{\epsilon^2} - \frac{39-20\rho}{\epsilon}$	$\frac{1}{\epsilon}$	$-\frac{5}{\epsilon^2} - \frac{10(2-\rho)}{\epsilon}$	$\frac{1}{\epsilon}$
Sum	$-\frac{7}{3\epsilon}$	0	$-\frac{7}{3\epsilon}$	0

Table 5.10: Results for fermionic part of QCD using CDR and DRED.

Counterterm	A				B			
	$I_{log}^{(2)}(\lambda^2)$	$I_{log}^2(\lambda^2)$	$\rho_{IREG}$	$I_{log}(\lambda^2)$	$I_{log}^{(2)}(\lambda^2)$	$I_{log}^2(\lambda^2)$	$\rho_{IREG}$	$I_{log}(\lambda^2)$
$AA\hat{A}$ Coupling	0	$\frac{10}{3b^2}$	$-\frac{10}{3b}$	$\frac{56}{9b}$	0	$\frac{10}{3b^2}$	$-\frac{10}{3b}$	$\frac{56}{9b}$
Gluon self-energy	0	$-\frac{10}{3b^2}$	$\frac{10}{3b}$	$-\frac{92}{9b}$	0	$-\frac{10}{3b^2}$	$\frac{10}{3b}$	$-\frac{92}{9b}$
Sum	0	0	0	$-\frac{4}{b}$	0	0	0	$-\frac{4}{b}$

Table 5.11: Results for fermionic part of QCD using IREG where  $\rho_{IREG} = I_{log}(\lambda^2) \ln \left[ -\frac{p^2}{\lambda^2} \right]$ .

$$\delta_A^{(1)}|_{IREG} = \left( \frac{11}{b} - \frac{2}{3b}n_f \right) I_{log}(\lambda^2), \quad \delta_A^{(1)}|_{CDR} = \frac{11}{\epsilon} - \frac{2}{3\epsilon}n_f, \quad (5.33)$$

$$\delta_A^{(2)}|_{IREG} = \frac{54}{b^2} \left[ I_{log}^2(\lambda^2) - 2bI_{log}^{(2)}(\lambda^2) \right] + \left( \frac{210}{b} - \frac{38}{3b}n_f \right) I_{log}(\lambda^2), \quad (5.34)$$

$$\delta_A^{(2)}|_{CDR} = \frac{51}{\epsilon} - \frac{19}{3\epsilon}n_f. \quad (5.35)$$

Notice that in the one-loop contribution,  $I_{log}(\lambda^2)/b$  and  $\epsilon^{-1}$  share the same coefficient as explained in Section 3.3.

Finally, by applying our results collected in Eq. (5.33) to Eq. (5.35), we obtain the well-known one and two-loop contributions for the gauge  $\beta$  coupling in QCD:

Counterterm	$A_{\text{CDR}}$	$A_{\text{DRED}} - A_{\text{CDR}}$	$B_{\text{CDR}}$	$B_{\text{DRED}} - B_{\text{CDR}}$
$AA\hat{A}$ Coupling	$\frac{10}{3\epsilon^2} + \frac{2(28-15)\rho}{9\epsilon}$	0	$\frac{10}{3\epsilon^2} + \frac{2(28-15\rho)}{9\epsilon}$	0
Gluon self-energy	$-\frac{10}{3\epsilon^2} - \frac{2(46-15\rho)}{9\epsilon}$	0	$-\frac{10}{3\epsilon^2} - \frac{2(46-15\rho)}{9\epsilon}$	0
Sum	$-\frac{4}{\epsilon}$	0	$-\frac{4}{\epsilon}$	0

Table 5.12: Results for fermionic part of QCD using CDR and DRED.

$$\beta_0|_{\text{IREG}} = 11 - \frac{2}{3}n_f; \quad \beta_0|_{\text{CDR}} = 11 - \frac{2}{3}n_f; \quad (5.36)$$

$$\beta_1|_{\text{IREG}} = 102 - \frac{38}{3}n_f; \quad \beta_1|_{\text{CDR}} = 102 - \frac{38}{3}n_f. \quad (5.37)$$

Finally, as in the pure Yang-Mills case, we reproduce previous results in the literature Ref. (35).







---

where  $S_0(p)$  is the tree-level electron propagator<sup>1</sup>,  $(-i)\Sigma(p)$  is the electron self-energy sum of all 1PI<sup>2</sup>. We can write the recursive series in Eq. (6.1) as:

$$S(p) = S_0(p) + S_0(p)\Sigma(p)S(p), \quad (6.2)$$

therefore:

$$S(p) = \frac{1}{S_0^{-1}(p) - \Sigma(p)}. \quad (6.3)$$

In QED, if we assume the electron has no mass, any diagram for  $\Sigma(p)$  contains an odd number of  $\gamma$  matrices, hence:

$$\Sigma(p) = \not{p}\Sigma_v(p^2) \quad (6.4)$$

Finally, if we substitute Eq. (6.4) in Eq. (6.3):

$$S(p) = \frac{1}{1 - \Sigma_v(p^2)} \frac{1}{\not{p}}. \quad (6.5)$$

The bare electron propagator  $S(p)$  in Eq. (6.5) should be equal to  $Z_\Psi S_r(p)$  when we renormalize, where  $Z_\Psi$  is the renormalization constant of the field, and  $S_r(p)$  is the renormalized electron propagator. As we mention in Section. 2.2.1, the renormalization constants will absorb the divergences of the theory order by order.

By renormalizing with  $\Psi_0 = Z_\Psi^{1/2}\Psi_r$ , the kinetic term of QED also changes. It passed to be:

$$\bar{\Psi}\not{D}\Psi \rightarrow \bar{\Psi}_r\not{D}\Psi_r + (Z_\Psi - 1)\bar{\Psi}_r\not{D}\Psi_r, \quad (6.6)$$

where the second term is treated perturbatively, giving origin to the counterterm for the fermion propagator in QED:

$$\Sigma_{c.t} = \delta_\Psi = (Z_\Psi - 1), \quad (6.7)$$

these counterterms must be added to the electron self-energy in each order to absorb the divergences.

Therefore,  $Z_\Psi$  will be:

---

<sup>1</sup> $S_0(p) = \frac{1}{\not{p} - m}$

<sup>2</sup>Again, 1PI means one-particle irreducible diagrams. The 1PI cannot be separate into two disconnect pieces by cutting a single line.



---


$$\begin{array}{c} \text{---} \text{---} \text{---} \end{array} = \int_l \int_k \frac{ie^4 \bar{\gamma}^\nu \cdot (\not{p} - \not{k}) \cdot \bar{\gamma}^\beta \cdot (\not{l} - \not{k}) \cdot \bar{\gamma}^\nu \cdot (\not{l}) \cdot \bar{\gamma}^\beta}{l^2 k^2 (k-l)^2 (k-p)^2 (l-p)^2} \quad (6.12)$$

and,

$$\begin{array}{c} \text{---} \text{---} \text{---} \end{array} = \int_l \int_k \frac{ie^2 \bar{\gamma}^\beta \cdot (\not{l} + \not{p}) \cdot \bar{\gamma}^\nu \text{tr} \left( e^2 \left( -(-\not{k}) \cdot \bar{\gamma}^\nu \cdot (\not{l} - \not{k}) \cdot \bar{\gamma}^\beta \right) \right)}{(l+p)^2 k^2 l^4 (l-k)^2}. \quad (6.13)$$

Contrary to (11), however, in the framework of IREG, we do not evaluate the sub-diagram first and join the obtained result in the whole diagram. As mentioned in (18), local terms may be generated. These terms could violate gauge invariance. We gave an example of this in Sub-section. 4.3.1.

## 6.3 Non-local terms and counterterms

### 6.3.1 $Z_\Psi$ at 1-loop order

From Eq. (6.9), the only relevant diagram to compute the correction of the electron propagator at 1-loop is the electron self-energy. For the massless case:

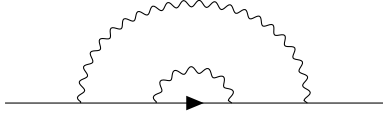
$$\begin{array}{c} \text{---} \text{---} \text{---} \end{array} = S(p) = \Sigma_v(p^2) \Big|_{div} \not{p} + (Z_\Psi - 1) \not{p} + finite. \quad (6.14)$$

As we did in previous sections, we will choose a renormalization scheme called  $IREG$ , a minimal subtraction scheme for IREG. In this scheme, the counterterms absorb only the divergences (in the case of IREG, the basic divergent integrals). Therefore, we do not have to consider the finite terms in Eq. (6.14). In this way, we can write the field renormalization constant of QED as:

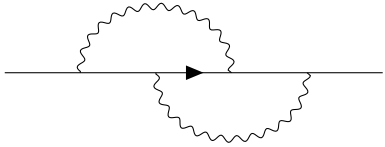
$$Z_\Psi = 1 + \delta_\Psi^{(1)} = 1 + ie^2 I_{log}(\lambda^2). \quad (6.15)$$

### 6.3.2 $Z_\Psi$ at 2-loop order

After carefully treating the quadratic terms in IREG as mentioned in Section. 4.2 and Subsection. 4.3.2, we continue with the next step of the algorithm in Fig. 4.3. As we are using IREG to evaluate the integrals, we must proceed according to the IREG rules sketched in (18). After we have the result of all the integrals, we plug the values into Mathematica. The regularized amplitudes are:

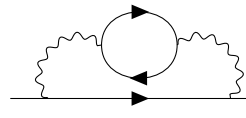


$$= -\frac{1}{2}ie^4 \left( 2bI_{\log}^{(2)}(\lambda^2) + 2bI_{\log}(\lambda^2) \log \left( -\frac{p^2}{\lambda^2} \right) - 7bI_{\log}(\lambda^2) - 2I_{\log}^2(\lambda^2) \right) \not{p} + finite, \quad (6.16)$$



$$= ie^4 \left( 2bI_{\log}^{(2)}(\lambda^2) + 2bI_{\log}(\lambda^2) \log \left( -\frac{p^2}{\lambda^2} \right) - 7bI_{\log}(\lambda^2) - 2I_{\log}^2(\lambda^2) \right) \not{p} + finite \quad (6.17)$$

and,



$$= 2ibe^4 I_{\log}(\lambda^2) \not{p} + finite. \quad (6.18)$$

Subsequently, we notice we have non-local terms in Eq. (6.16), (6.17) and, (6.18); such as  $I_{\log}^2(\lambda^2 \ln(-p^2/\lambda^2))$ . These terms will be eliminated when doing the renormalization with the counterterms. For the 2-loop fermionic correction in QED, the necessary counterterms are:

---


$$\begin{aligned}
& \text{Diagram: a horizontal line with a wavy loop on top, connected to a circle with an 'X' inside.} \\
& = e^4 \delta_\psi^{(1)} \left( b \log \left( -\frac{p^2}{\lambda^2} \right) - 2b - I_{\log}(\lambda^2) \right) \not{p},
\end{aligned} \tag{6.19}$$

$$\begin{aligned}
& \text{Diagram: a horizontal line with a wavy loop on top, connected to a circle with an 'X' inside, and an arrow pointing right.} \\
& + \text{Diagram: a horizontal line with a wavy loop on top, connected to a circle with an 'X' inside, and an arrow pointing left.} \\
& = 2e^4 \delta_\psi^{(1)} \left( b \log \left( -\frac{p^2}{\lambda^2} \right) - 2b - I_{\log}(\lambda^2) \right) \not{p}
\end{aligned} \tag{6.20}$$

and,

$$\begin{aligned}
& \text{Diagram: a horizontal line with a wavy loop on top, connected to a circle with an 'X' inside, and an arrow pointing right.} \\
& = -e^4 b \delta_A^{(1)} \not{p}.
\end{aligned} \tag{6.21}$$

From Eq. (6.38), we have the value of  $\delta_\psi^{(1)}$ . In the case of  $\delta_A^{(1)}$ , we can get its value from Eq. (5.27) in Chapter. 5. Again, we only need the divergent part of the total amplitude to compute the anomalous dimension. If we add all the diagrams with their respective counterterms, we get the final total amplitude at 2-loop:

$$\Sigma^{(2)}(p) \Big|_{div} = -e^4 b \not{p} I_{\log}^{(2)}(\lambda^2) + \frac{5}{6} e^4 b \not{p} I_{\log}(\lambda^2), \tag{6.22}$$

where the non-local terms were removed as they should.

## 6.4 The renormalization constant of the electron field

The renormalization constant of the fermionic field from Eq. (6.22) will be:

$$Z_\Psi \Big|_{IREG} = 1 + ie^2 I_{\log}(\lambda^2) + e^4 b \left[ -I_{\log}^{(2)}(\lambda^2) + \frac{5}{6} I_{\log}(\lambda^2) \right]. \tag{6.23}$$

As was discussed in (18) and in Sub-section. 3.3.1, to obtain a correspondence with DS of Eq. (6.23), we could consider to replace the  $I_{\log}^{(2)}(\lambda^2)$  in the renormalization constant by:

$$\begin{aligned}
 I_{\log}^{(2)}(\lambda^2) &= \int \frac{d^4 k}{(2\pi)^4} \frac{1}{(k^2 - \lambda^2)^2} \ln \left[ -\frac{k^2}{\lambda^2} \right], \\
 I_{\log}^{(2)}(\lambda^2) \Big|_d &= (\mu_{DR}^2)^\epsilon \int \frac{d^d k}{(2\pi)^d} \frac{1}{(k^2 - \lambda^2)^2} \frac{1}{(4\pi)^{-\epsilon}} \left[ \left( \frac{\mu_{DR}^2}{\lambda^2} \right)^\epsilon - \left( -\frac{\mu_{DR}^2}{k^2} \right)^\epsilon \right] \Gamma(\epsilon) \\
 &= \frac{b}{(4\pi)^{-2\epsilon}} \left( \frac{\mu_{DR}^2}{\lambda^2} \right)^{2\epsilon} \Gamma(\epsilon) \left[ \Gamma(\epsilon) - \frac{\Gamma(2-4\epsilon)\Gamma(2\epsilon)}{\Gamma(2-3\epsilon)} \right].
 \end{aligned} \tag{6.24}$$

In principle, the factor that goes with the  $\epsilon^{-2}$  must match the one from DS.

If the calculation is done in CDR from the start as in (10), one gets the renormalization constant:

$$Z_\Psi \Big|_{CDR} = 1 - a \frac{\alpha}{4\pi\epsilon} + \left[ \frac{a^2}{2} + \left( n_f + \frac{3}{4} \right) \epsilon \right] \left( \frac{\alpha}{4\pi\epsilon} \right)^2 + \dots \tag{6.25}$$

where  $a$  is a dimensionless constant. In both, IREG and DS, the factor that goes with  $\epsilon^{-2}$  for  $Z_\Psi$  is  $+b/2$ . Therefore, the terms in  $\epsilon^{-2}$  can be reproduced. This observation allows us to check our result in Eq. (6.23) as we did in (18) diagram-by-diagram.

## 6.5 The anomalous dimension at 2-loop

In this section, let us first see the definition of the anomalous dimension for the free theory. The core idea behind renormalization in QFT is that observables are finite and in-principle calculable functions of other observables (9). For the divergences, there should be a free parameter to absorb it. For the free theory  $\phi^3$  (19), from Section. 2.3 we get the anomalous dimension definition in Eq. (2.21).

If  $A$  can be expanded in Eq. (2.18) as  $A = A_1 g^2 + A_2 g^4 + O(g^6)$  in the coupling constant  $g$ , then

$$\ln Z_\psi = A_1 g^2 + \left( A_2 - \frac{A_1^2}{2} g^4 \right) O(g^6). \tag{6.26}$$

And, if  $\gamma = \gamma_1 g^2 + \gamma_2 g^4 + O(g^6)$ , therefore:

$$\gamma_1 g^2 + \gamma_2 g^4 = \frac{\lambda}{2} \frac{\partial}{\partial \lambda} \left( A_1 g^2 + \left( A_2 - \frac{A_1^2}{2} g^4 \right) \right). \tag{6.27}$$

We can also expand the  $\beta$ -function as:

$$\beta = \beta_1 g^3 + \beta_2 g^5 + O(g^6). \tag{6.28}$$

Using Eq. (6.28) in Eq. (6.27), we get the next relations:

$$\begin{aligned}\gamma_1 &= \frac{\lambda}{2} \frac{\partial}{\partial \lambda} A_1, \\ \gamma_2 &= \beta_1 A_1 + \frac{\lambda}{2} \frac{\partial}{\partial \lambda} \left( A_2 - \frac{A_1^2}{2} \right).\end{aligned}\tag{6.29}$$

Nevertheless, if we use the definitions in Eq. (6.29) with our  $Z_\Psi$  result from Eq. (6.23), we end up with a final result that still preserves the divergent terms. The error of using the free theory definition from (19) comes from not considering the gauge parameter as we are working with gauge theories. As mentioned in (31),  $\gamma$  for QED depends on the gauge parameter because Green's functions of individual  $\Psi$  and  $\bar{\Psi}$  are not gauge-invariant. On the contrary, the  $\beta$ -function is gauge-invariant. We will explore this in the next section. We will deduce the correct definition of the anomalous dimension for gauge theories within IREG.

## 6.6 The gauge parameter dependence for $\gamma$ -function

Let us suppose our renormalization constant of the field  $\Psi$  is of the form:

$$Z_\Psi = 1 + aA_1g^2 + A_2g^4, \quad (6.30)$$

where we consider the gauge dependence at 1-loop order encoded in the parameter  $a$ . We do not have to consider the gauge parameter dependence in the second order because those terms will enter  $O(g^6)$  in the anomalous dimension definition. If we consider the gauge dependence at 1-loop order, the amplitude will be:

$$\text{---}\overbrace{\hspace{0.8cm}}^{\text{wavy loop}}\text{---} = \Sigma(p) = e^2 a_0 I_{\log}(\lambda^2) \not{p}, \quad (6.31)$$

where  $a_0$  is the bare gauge parameter in Eq. (2.12).

If we do again the series expansion of the logarithm as we did in Eq. (6.26), then we have:

$$\ln(Z_\Psi) = aA_1g^2 + \left(A_2 - \frac{A_1^2}{2}\right)g^4 + O(g^6). \quad (6.32)$$

Using the previous equation in our anomalous dimension definition in Eq. (2.21) we get the coefficients:



$$\begin{aligned}\gamma_1 &= \frac{\lambda}{2} a \frac{\partial}{\partial \lambda} A_1, \\ \gamma_2 &= a \beta_1 A_1 + \frac{\lambda}{2} \frac{\partial}{\partial \lambda} \left( A_2 - \frac{a^2 A_1^2}{2} \right) + \frac{1}{2} \gamma_A^{(1)} A_1,\end{aligned}\tag{6.33}$$

where  $\gamma_A^{(1)}$  is the first coefficient of the renormalization function of the photon. These are the correct coefficients for the 2-loop anomalous dimension for gauge theories within IREG. Notice in the previous equation we must be careful applying the chain rule for the term that depends on the gauge parameter.

## 6.7 Results of $\gamma$ -function for the massless case

Using the previous Eq. (6.33) we get the correct anomalous dimension for QED at 2-loop within IREG. Remark that there is no BDI appearing now:

$$\begin{aligned}\gamma_1 e^2 &= \frac{e^2}{16\pi^2}, \\ \gamma_2 e^4 &= -\frac{1}{3} \frac{e^4}{2(4\pi)^4}.\end{aligned}\tag{6.34}$$

The first coefficient, as expected, corresponds to the first-order universal result. While the second depends on the renormalization method used. In general, if we compare it with the CDR result in (10):

$$\gamma_2 e^4 \Big|_{CDR} = -7 \frac{e^4}{2(4\pi)^4}\tag{6.35}$$

Our result matches in sign with a difference of one factor. It would be interesting to compare this result with the one from DRED.

## 6.8 Perspectives and discussion: the anomalous mass dimension for QED and non-Abelian theories

We showed how to compute the  $\beta$ -function for gauge theories on Chapter. 5 to 2-loop accuracy within IREG and DS. We also showed how we calculate the  $\gamma$ -function in Section. 6.6 with IREG. Therefore, to pursue the IREG program to apply it to precision calculations, we need to evaluate the anomalous dimensions for massive gauge theories. This procedure will be a new consistent test of our method. It will allow us to have all the renormalization group functions at 2-loop for gauge theories. According to Eq. (2.19), the renormalization constant

of the mass allows us to determine the anomalous mass dimension. The relevant Feynman diagrams for this computation are the same we present in Fig. 2.3 for QED and in Fig. 2.5 for QCD. In this section of the text, we do not intend to show a final result since this topic is still under research. Nevertheless, we do comment on the advances we have made in terms of calculation to obtain the  $\gamma_m^{IREG}$ .

### 6.8.1 The renormalization constant of the mass in QED

By renormalizing at 1-loop order with  $m_0 = Z_m m_R$  the massive theory, our propagator structure changes to:

$$\begin{aligned}
 \text{---}\!\!\!\!\!\rightarrow \text{---}\!\!\!\!\!\rightarrow \text{---}\!\!\!\!\!\rightarrow &= \text{---}\!\!\!\!\!\rightarrow \text{---}\!\!\!\!\!\rightarrow \text{---}\!\!\!\!\!\rightarrow + \text{---}\!\!\!\!\!\rightarrow \otimes \text{---}\!\!\!\!\!\rightarrow \\
 &= \Sigma^{(1)}(p, m) + \delta_\Psi^{(1)} \not{p} - (\delta_m^{(1)} + \delta_\Psi^{(1)})m,
 \end{aligned} \tag{6.36}$$

where, as we saw in Eq. (3.41):

$$\text{---}\!\!\!\!\!\rightarrow \text{---}\!\!\!\!\!\rightarrow = \Sigma^{(1)}(p, m) = \Sigma_v(p^2) \Big|_{div} \not{p} + \Sigma_s(p^2) \Big|_{div} m + finite. \tag{6.37}$$

Notice we wrote the amplitude of the electron-self energy as a combination of a “scalar” and a “vector” part. We will say the scalar is the part multiplied by the mass. The vector is the part multiplied by the momentum.

Thus, in QED, the fermion mass and field renormalization can be written as:

$$\begin{aligned}
 Z_\Psi &= 1 + \Sigma_v \Big|_{div}, \\
 Z_m &= 1 - \Sigma_v \Big|_{div} - \Sigma_s \Big|_{div}.
 \end{aligned} \tag{6.38}$$

We remark from Eq. (6.38) that the renormalization constant of the field will be the same as in the massless case of the theory. This observation is interesting. In principle, if we work with the massive QED, we should be able to reproduce the same  $Z_\Psi$  results as when we worked with the massless theory.

Finally, in 1-loop for massive QED:

$$Z_m = 1 + i3e^2 I_{log}(\lambda^2), \tag{6.39}$$

and by consequence using Eq. (4.30):

$$\gamma_m^{IREG} = \frac{6e^2}{(4\pi)^2}. \quad (6.40)$$

This result corresponds with  $\bar{MS}$  for CDR. Moreover, it is the same result as in Eq. (4.30) for QCD. The only difference is the color factor for non-Abelian theories.

### 6.8.2 Mass insertion and helicity flip

In contrast to the techniques developed at 1-loop during Chapter. 3 and in Appendix. B; we can observe the increase in the level of complexity and technicality when we go to 2-loop order. Currently, many of the well defined calculations in the community of theoretical precision at  $N^2LO$  are carried out on a case-by-case basis.

For the case of our project, although the electron mass anomalous dimension can be found in a similar way to the  $\gamma$ -function (and even more straightforward because  $Z_m$  does not depend on the gauge parameter), analytical simplifications are welcome. For the massive theory, we have used up to this point a technique that we will call “mass insertion”.

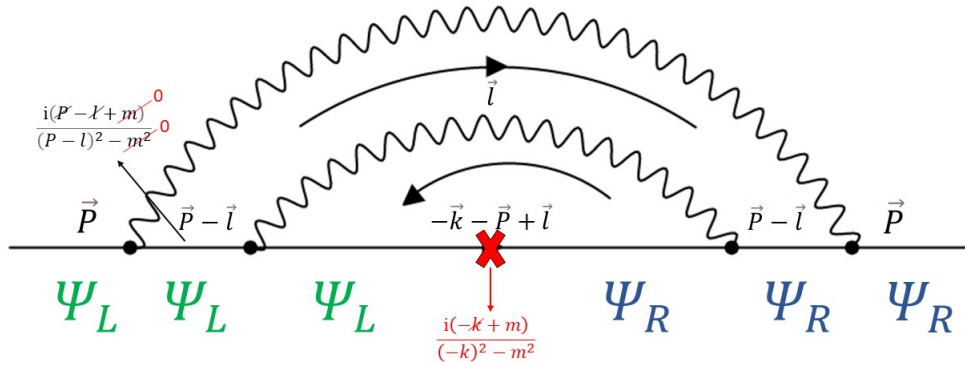


Figure 6.1: If we took the rainbow diagram as an example, we have to leave the mass in one of the propagators. In this case, we leave the mass of the propagator that has the X, and we make  $m_0 \rightarrow 0$  in the others.

As we can see schematically in Fig. 6.1 for one of the diagrams in Fig. 2.3, we need to insert the mass in one of the propagators to guarantee the helicity flip of the external electron. The “mass insertion” helps us have fewer mass-dependent integrals to solve within IREG and considerably simplifies the number of 2-loop integrals to do.

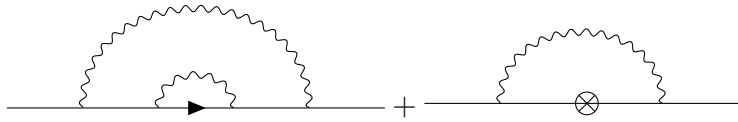
The coupling with the photon in QED will preserve helicity. On the other hand, when

we insert a mass in a fermion propagator we change helicity from left to right and vice-versa. According to Ref. (10):

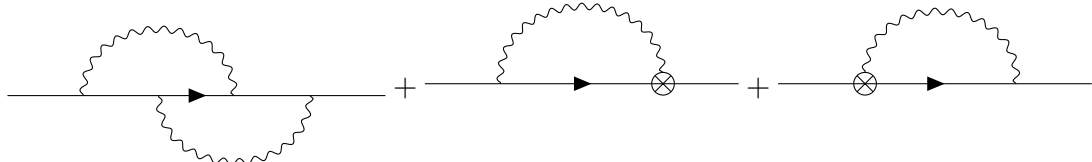
“We are able to calculate  $\Sigma_s$  at 2-loop by holding  $m_0$  within the numerator of a single electron propagator in Fig. 2.3 and setting  $m_0 \rightarrow 0$  in all the other places. This single  $m_0$  must be someplace along the electron line, which goes through all the graphs. We require one helicity flip of the external electron. One helicity flip in a loop yields zero contribution.”

### 6.8.3 Amplitudes and counterterms for massive QED

For the 2-loop fermionic correction in massive QED, the diagrams we have so far are:

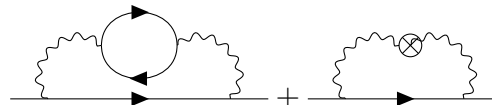


$$= -\frac{1}{2}ibe^4 \left( (2I_{log}^{(2)}(\lambda^2) - 3I_{log}(\lambda^2))\not{p} + 32m_e(I_{log}^{(2)}(\lambda^2) - 2I_{log}(\lambda^2)) + finite \right), \quad (6.41)$$



$$= ibe^4 \left( (2I_{log}^{(2)}(\lambda^2) - 3I_{log}(\lambda^2))\not{p} - 4I_{log}(\lambda^2)m_e + finite \right), \quad (6.42)$$

and:



$$= \frac{2}{3}ibe^4 \left( I_{log}(\lambda^2)\not{p} + 2m_e(3I_{log}^{(2)}(\lambda^2) - 5I_{log}(\lambda^2)) + finite \right). \quad (6.43)$$

If we add all the diagrams with their respective counterterms, we got the total amplitude at 2-loop:

$$\Sigma^{(2)}(p, m) \Big|_{div} = -be^4 b \left( I_{\log}^{(2)}(\lambda^2) - \frac{5}{6} I_{\log}(\lambda^2) \right) \not{p} - ibe^4 \left( -12 I_{\log}^{(2)}(\lambda^2) + \frac{64}{3} I_{\log}(\lambda^2) \right) m. \quad (6.44)$$

We reproduce with this the massless result in Eq. (6.22) and by consequence,  $Z_\Psi$ . Moreover, if we analyze the equivalence of  $I_{\log}^{(2)}$  to CDR, the factors that go with the  $\epsilon^{-2}$  match the 2-loop results in Ref. (36). Nevertheless, we still need to define the structure of  $Z_m$  at 2-loop within IREG to compute  $\gamma_m$ . We are currently working on this.

#### 6.8.4 Quark mass anomalous dimension in QCD

For QCD, the precise evaluation of the quark mass anomalous dimension has been performed up to 5-loop order in CDR (37). It also was calculated at the 3-loop level in Ref. (38) with DRED. Likewise, we intend to follow these steps and independently evaluate this quantity in 2-loops order with IREG (a regularization scheme that does not depend on analytical continuations of the dimension). This 2-loop calculation within IREG is new.

For the technical tools in this new project, we will keep developing and improving the algorithm that automated the computations using Mathematica at 2-loops with IREG. Part of the setup will still be the public FeynArts code. Furthermore, it will be interesting to study the  $\gamma_m$ -function in the DS and compare it to IREG. Specifically, we want to compare with quasi-dimensional methods such as DRED. One of the main drawbacks of the former is that some modifications at the Lagrangian level become necessary, which may translate in additional terms to the  $\gamma_m$ -function.

Turning now to the 2-loop correction, in Fig 2.5 we can see the relevant diagrams to compute the anomalous mass dimension. However, each diagram in Fig. 2.5 generates 2-loop integrals to solve. For example, let us see the third diagram in Fig. 2.5. We will call it the “quark bubble” After performing the necessary Dirac algebra in the amplitude, we obtain in Eq. 6.45 at least seven unique integrals to solve:

---


$$\begin{aligned}
& \int_l \int_k \frac{1}{(l - m_u^2) \cdot (k - m_u^2) \cdot (l - p)^2 \cdot ((-k + l - p)^2 - m_u^2)}, \\
& \int_l \int_k \frac{(\not{k}) \cdot (\not{l})}{(l - m_u^2) \cdot (k - m_u^2) \cdot (l - p)^2 \cdot ((-k + l - p)^2 - m_u^2)}, \\
& \int_l \int_k \frac{k^2}{(l - m_u^2) \cdot (k - m_u^2) \cdot (l - p)^2 \cdot ((-k + l - p)^2 - m_u^2)}, \\
& \int_l \int_k \frac{k \cdot l}{(l - m_u^2) \cdot (k - m_u^2) \cdot (l - p)^2 \cdot ((-k + l - p)^2 - m_u^2)}, \\
& \int_l \int_k \frac{\not{k} (k \cdot l)}{(l - m_u^2) \cdot (k - m_u^2) \cdot (l - p)^2 \cdot ((-k + l - p)^2 - m_u^2)}, \\
& \int_l \int_k \frac{(k \cdot l) \not{l}}{(l - m_u^2) \cdot (k - m_u^2) \cdot (l - p)^2 \cdot ((-k + l - p)^2 - m_u^2)}, \\
& \int_l \int_k \frac{l^2 \not{k}}{(l - m_u^2) \cdot (k - m_u^2) \cdot (l - p)^2 \cdot ((-k + l - p)^2 - m_u^2)}.
\end{aligned} \tag{6.45}$$

Since there is no IREG package (yet) to calculate Feynman loop integrals, this is a very time-consuming task. In principle, the rainbow diagram, the quark bubble, and the overlapped diagram for QCD should match our results for QED, with the only difference being the color factor. Still, we have three more original diagrams to solve in QCD. Thus, being able to use the mass insertion technique is an effective way to reduce the level of complexity of the calculation. Nevertheless, a practical and effective way to solve this problem is to do the calculations in the massless case first as we did for QED. Since the renormalization constant of the field is the same for the theory with mass and without mass, to have more control in this study, we can work with the massless case first and get  $Z_\Psi$  for QCD. With this result (which can be verified for the theory with mass later), we can calculate the anomalous dimension  $\gamma$  of the quark too.

In the future, we plan to develop a Mathematica package within IREG with all the integrals in Appendix. E. With this, the whole process of the algorithm in Section. 4.1.2 will be completely automated and ready to be used for other gauge theories.



## CHAPTER 7

## CONCLUSIONS

The high energy regime in collider physics demands that new theoretical challenges are faced. To extract any deviation between theory and experimental data in the SM, precision observables demand at least  $N^2LO$  and  $N^3LO$  approximations. When we work at these orders, for the management of divergent integrals, we must renormalize and regularize. At 2-loops and beyond, it is a laborious process to tackle. The choice of the regularization scheme to separate  $UV-div$  that enters into the computer code is important. For these reasons, regularization frameworks that work in the physical dimension are desirable.

In this work, the approach we used to handle the  $UV-div$  is through the set of rules of IREG. With this, we first calculate  $\beta$ -function to 2-loop order for Abelian and non-Abelian theories. Thus in this thesis, we discussed how the technique works at 2-loop order and we applied it to pure Yang-Mills, QED, and QCD. In order to raise a non-dimensional scheme such as IREG to the level of more conventional methods, a series of rules had to be followed as we showed in Chapter. 3. We have obtained the renormalization constants by conducting the subtraction of subdivergences within IREG and compared with CDR and DRED. As we have verified, evaluating the BDI's of IREG in  $4 - 2\epsilon$  dimensions at the end of the calculation does not yield the same residues for the DS poles of arbitrary orders. Also the finite pieces are different. Still, as we have shown in Tables 5.3 5.4, a systematic summation among different contributions from Feynman graphs and counterterms renders an identical result for CDR and DRED. Finally, we have computed the universal two-loop  $\beta$ -functions with IREG for pure Yang-Mills, QED, and QCD in a quadridimensional framework ( $d = 4$ ) by defining the renormalization constants as BDI's.

One of the products of this thesis was a first algorithm developed with FeynArts and FormCalc which simplified and automated our computations. We use it for the automated



calculation of the  $\beta$ -function at 2-loops. This algorithm was evaluated as a consistency test for IREG in different gauge theories.

On the other hand, we proceeded to compute the rest of the functions of the renormalization group. We calculate the  $\gamma$ -function to 2-loop order for QED. For this objective, we developed a new algorithm to automatate the computation of the divergent amplitudes in Mathematica, this time using FeynCalc to do the algebra. We study the subtlety of the calculation in the presence of fermionic loops at 2-loop order where it was crucial to evaluate the integrals of the sub-diagram first. We obtained the renormalization constant of the field,  $Z_\Psi$ , working in  $\overline{IREG}$ , a minimal subtraction renormalization scheme for IREG. For the renormalization constant  $Z_\Psi$  in IREG, we study its correspondence with DS at 2-loop. The factor that goes with  $\epsilon^{-2}$  for  $Z_\Psi$  was the same. Therefore, the terms in  $\epsilon^{-2}$  were reproduced. In the end, we present the results of the anomalous dimension coefficients at 2-loop for QED within IREG in Chapter. 6. These coefficients, as expected, were finite. In the case of the anomalous mass dimension, we are in the last steps to finish this computation. We already have all the diagrams for QED and we are currently defining the structure of the electron propagator at 2-loop to get the renormalization constants.

All the computations at 2-loop in this thesis consider only the divergent term of the diagram, without taking into account the finite pieces. In future works, we intend to complete and consider these integrals with the perspective of possible calculations of precision observable within 2-loop gauge theories. For example, the boson  $W$  mass, since the electroweak observables are sensitive to the effects of loop corrections. Therefore, with the result from divergent and finite parts, we plan to develop a Mathematica package within IREG with all the integrals as mentioned at the end of Chapter. 6. A related example of applying IREG would be the calculation of the two-loop contribution for the EulerHeisenberg effective Lagrangian. This Lagrangian describes the nonlinear dynamics of the electromagnetic field in a vacuum. The Lagrangian effect was tested through measurements of the change in the polarization of light as it passed through a magnetic field. Another relevant project to apply IREG could be the calculation of the effective potential. Lastly, the evaluation of the anomalous mass dimension also has important applications. For example, the Higgs boson decay rate into the charm and bottom quarks is proportional to the square of respective quark mass (37) which depends on  $\beta$  and  $\gamma_m$ . Thus, it is interesting to independently evaluate  $\gamma_m$  within IREG.



# Appendices

## APPENDIX A

APPENDIX A: NOTATIONS, FEYNMAN RULES, AND LIST  
OF ACRONYMS**Feynman rules:**

For QED, and QCD, we refer to (9) for the Feynman rules and conventions. As for Yang-Mills and QCD with a background field  $A$ , we follow the conventions of (17) to yield the rules in Fig. 4.5.

**Notations:**

$$\int_{-\infty}^{+\infty} \frac{d^4 k}{(2\pi)^4} = \int_k. \quad (\text{A.1})$$

$$b \equiv \frac{i}{(4\pi)^2}. \quad (\text{A.2})$$

$$\not{p} = \gamma^\mu p_\mu. \quad (\text{A.3})$$

**List of acronyms:**

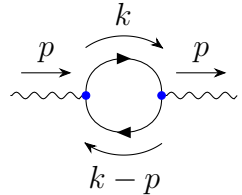
- **IREG:** Implicit Regularization.
- **CDR:** Dimensional Regularization.
- **DRED:** Dimensional reduction.
- **YM:** Yang-Mills.
- **QCD:** Quantum Chromodynamics.

- **QED:** Quantum Electrodynamics.
- **QFT:** Quantum Field Theory.
- **SM:** Standard Model.
- **BSM:** Beyond the Standard Model.
- **DS:** Dimensional schemes.
- **BFM:** Background Field Method.
- **BF:** Background Field.
- **1PI diagrams:** one particle irreducible diagrams.
- $N^2LO$ : Next-to-next-to leading order.
- $N^3LO$ : Next-to-next-to-next-to leading order.

## APPENDIX B

APPENDIX B: ANOTHER APPLICATION EXAMPLE OF  
IREG AT 1-LOOP

We will develop in this appendix another example with the basic concepts of IREG (4). We will explicitly evaluate two of the integrals that appear in the vacuum polarization tensor in massless QED. After applying the Feynman rules:



$$\Pi_{\tau\nu}(k) = (-) \text{Tr} \left[ \int_k (-ie\gamma_\nu) \frac{i}{\not{k}} (-ie\gamma_\tau) \frac{i}{\not{k} - \not{p}} \right], \quad (\text{B.1})$$

where again  $\int_k = \int_{-\infty}^{+\infty} \frac{d^4k}{(2\pi)^4}$ . The next step is to use Dirac algebra in 4 dimensions. Thus, we get:

$$\Pi_{\tau\nu}(k) = -4e^2 \left[ \underbrace{2 \int_k \frac{k_\tau k_\nu}{D}}_{\Delta=2} - p_\tau \underbrace{\int_k \frac{k_\nu}{D}}_{\Delta=1} - p_\nu \underbrace{\int_k \frac{k_\tau}{D}}_{\Delta=1} - g_{\tau\nu} \underbrace{\int_k \frac{k^2}{D}}_{\Delta=2} + g_{\tau\nu} p^\sigma \underbrace{\int_k \frac{k_\sigma}{D}}_{\Delta=1} + g_{\tau\nu} \underbrace{\int_k \frac{1}{D}}_{\Delta=0} \right] \quad (\text{B.2})$$

where  $D = (k^2)(k-p)^2$ . Let us study the superficial degree of divergence in Eq. (B.2). In the first integral, we have in the numerator 4+2 powers of k. In the denominator of the first integral, we have 4 powers of k, therefore  $\Delta = 6 - 2 = 2$  which indicates the presence of a quadratic divergence. For the other integrals, when  $\Delta = 1$ , we have a linear divergence, and

finally, when  $\Delta = 0$  the divergence is logarithmic. Considering the linear divergence integral:

$$I_\tau = \int_k \frac{k_\tau}{D} = \int_k \frac{k_\tau}{(k^2)(k-p)^2}. \quad (\text{B.3})$$

The next step in IREG (for massless theories also) is to introduce a fictitious mass  $\mu$  in the propagators which will allow us to control spurious **IR-div** introduced in the course of the computation. Thus, the integral can be rewritten as:

$$I_\tau = \lim_{\mu^2 \rightarrow 0} \int_k \frac{k_\tau}{(k^2 - \mu^2)[(k-p)^2 - \mu^2]}. \quad (\text{B.4})$$

In the next step, the following algebraic identity need to be used recursively as many times as necessary to isolate the physical parameters (the external momenta) in the finite part (20):

$$\frac{1}{(k-p)^2 - \mu^2} = \frac{1}{k^2 - \mu^2} - \frac{p^2 - 2p \cdot k}{(k^2 - \mu^2)[(k-p)^2 - \mu^2]}. \quad (\text{B.5})$$

For the linear integral in our example, we end up with the following divergent expression:

$$I_\tau \Big|_{div} = \lim_{\mu^2 \rightarrow 0} \left[ 2p^\alpha \int_k \frac{k_\tau k_\alpha}{(k^2 - \mu^2)^3} + \int_k \frac{k_\tau}{(k^2 - \mu^2)^2} \right]. \quad (\text{B.6})$$

When using Eq. (B.5) to get Eq. (B.6), we obtain two terms, one with a logarithmic divergence plus one with a linear divergence. In our example, the logarithmic term is a particular case of the general expressions:

$$\begin{aligned} I_{log}(\mu^2) &\equiv \int_k \frac{1}{(k^2 - \mu^2)^2}, & I_{log}^{\nu_1 \nu_2}(\mu^2) &\equiv \int_k \frac{k_{\nu_1} k_{\nu_2}}{(k^2 - \mu^2)^3}, \\ I_{quad}(\mu^2) &\equiv \int_k \frac{1}{(k^2 - \mu^2)}. \end{aligned} \quad (\text{B.7})$$

On the other hand the finite terms in our linear example Eq. (B.4) after using Eq. (B.5) are:

$$I_\tau \Big|_{finite} = -p^2 \lim_{\mu^2 \rightarrow 0} \int_k \frac{k_\tau}{(k^2 - \mu^2)^3} + \lim_{\mu^2 \rightarrow 0} \int_k k_\tau \frac{p^2 - 2pk}{(k^2 - \mu^2)^3[(k-p)^2 - \mu^2]}. \quad (\text{B.8})$$

Let us look now at another example. If we take the logarithmic integral of Eq. (B.2):

$$I = \int_k \frac{1}{D} = \int_k \frac{1}{(k^2)(k-p)^2} = \lim_{\mu^2 \rightarrow 0} \int_k \frac{1}{(k^2 - \mu^2)[(k-p)^2 - \mu^2]}, \quad (\text{B.9})$$

and apply Eq. (B.5), we get:

---


$$I = I\Big|_{div} + I\Big|_{finite} = I_{log}(\mu^2) - \lim_{\mu^2 \rightarrow 0} \int_k \frac{(p^2 - 2pk)}{(k^2 - \mu^2)^2 [(k-p)^2 - \mu^2]}. \quad (\text{B.10})$$

Again, the objective of IREG will be to use Eq. (B.5) as many times as necessary to write the **UV-div** in terms of the BDI in Eq. (B.7) (19), composed of scalar and tensorial integrals with Lorentz indices. The last ones may be expressed as a linear combination of the scalar integrals  $I_{log}(\mu^2)$  or  $I_{quad}(\mu^2)$ , according to the superficial degree of divergence of the original integral plus well-defined surface terms (ST's). In our linear example:

$$\Upsilon_0^{(1)\mu\nu} = \int_k \frac{\partial}{\partial k_\mu} \frac{k^\nu}{(k^2 - \mu^2)^2} = 4 \left[ \frac{g_{\mu\nu}}{4} I_{log}(\mu^2) - I_{log}^{\mu\nu}(\mu^2) \right]. \quad (\text{B.11})$$

The surface term is arbitrary in principle.

We need to take the limit  $\mu^2 \rightarrow 0$  in the end. In the case of our  $I_\tau$  example, although  $I_{log}(\mu^2)$  parametrizes the **UV-div**, both  $I_{log}(\mu^2)$  and the finite terms, develop an **IR-div** which is spurious since our original integral Eq. (B.4) was **IR** safe. Therefore, as mentioned in Ref. (21), we define a mass-independent scheme in IREG by replacing  $\mu^2$  with an arbitrary mass parameter  $\lambda^2 \neq 0$ . For instance:

$$I_{log}(\mu^2) = I_{log}(\lambda^2) - \frac{i}{(4\pi)^2} \ln \frac{\lambda^2}{\mu^2} \quad (\text{B.12})$$

which enables us to write a basic divergent integral (BDI) as a function of  $\lambda^2$  plus logarithmic functions of  $\mu^2/\lambda^2$ .

In this calculation of the vacuum polarization tensor, we have omitted the quadratic integrals from the discussion because they are more laborious to demonstrate. However, we can finally write the vacuum polarization tensor in IREG by only taking the divergent part from our results and making the surface terms equal to zero:

$$\Pi_{\tau\nu}(k)|_{div} = -\frac{4e^2}{3} (g_{\mu\nu} p^2 - p_\mu p_\nu) I_{log}(\mu^2), \quad (\text{B.13})$$

which is transverse as required by gauge invariance.



## APPENDIX C

APPENDIX C: THE BACKGROUND FIELD METHOD FOR  
YANG-MILLS AT 1-LOOP ORDER

We notice in Section. 2.4 that for the infinities in the effective action to take the gauge invariant form of divergent constant times the gauge field strength tensor, we need  $Z_g = Z_A^{-1/2}$ . This previous relation makes that the knowledge of 2-point functions is the only one necessary to compute the  $\beta$ -function for YM, as in QED. The Greens functions will also respect Ward's identities like the ones in QED. Furthermore, notice that different from the traditional pure YM theory, we do not need to compute the gauge Q propagator, the ghost propagator, or the gauge Q-ghost-ghost vertex. Therefore the BFM simplifies the calculations (of course, with the disadvantage that we will have more Feynman rules.

To compute the  $\beta$ -function using the BFM and IREG for 1-loop YM, we will need the 2 point graphs for the gluon-bubble and the ghost-bubble:



Figure C.1: Diagrams for the calculation of the pure YM  $\beta$ -function at one-loop. The orange dot will stand for the BF  $A$  in the diagram. Greek letters indicate Lorentz indices while Latin letters (without arrows) indicate color indices.

For the ghost-bubble after applying the Feynman rules:

---


$$\begin{aligned}
\sum_{\epsilon\xi}^{ef} \overbrace{(k)}^{\text{external momentum}} &= \overbrace{(-1)}^{\text{ghost anticommuting}} \int_l (-g) f^{hfgj} (2l_\xi - k_\xi) \frac{i\delta_{ji}}{(l-k)^2} (-g) \\
&\times f^{ieg} (2l_\epsilon - k_\epsilon) \frac{i\delta_{gh}}{l^2} \\
&= -g^2 C_A \delta_{ef} \left[ 4 \int_l \frac{l_\xi l_\epsilon}{l^2(l-l)^2} - 2k_\epsilon \int_l \frac{l_\xi}{l^2(l-l)^2} - 2k_\xi \int_l \frac{l_\epsilon}{l^2(l-l)^2} \right. \\
&\quad \left. + k_\xi k_\epsilon \int_l \frac{1}{l^2(l-l)^2} \right]. \tag{C.1}
\end{aligned}$$

And for the gluon bubble after applying the Feynman rules:

$$\begin{aligned}
\prod_{\mu\nu}^{mn}(k) &= \overbrace{\frac{1}{2}}^{\text{symmetry factor}} \int_l g f^{nbd} [g_{\nu\delta} 2k_\beta + g_{\beta\delta} (2l_\nu - k_\nu) - g_{\nu\beta} 2k_\delta] \frac{(-i)\delta_{dc}}{(l-k)^2} g_{\delta\gamma} \\
&\times g f^{mca} [-g_{\mu\alpha} 2k_\gamma + g_{\gamma\alpha} (2l_\mu - k_\mu) + g_{\mu\gamma} 2k_\alpha] \frac{(-i)\delta_{ab}}{l^2} g_{\alpha\beta} \\
&= \frac{1}{2} g^2 C_A \delta_{nm} \left[ 8 \int_l \frac{k \cdot k g_{\mu\nu}}{l^2(l-k)^2} - 4 \int_l \frac{k_\mu k_\nu}{l^2(l-k)^2} - 8 \int_l \frac{k_\mu l_\nu}{l^2(l-k)^2} + 16 \int_l \frac{l_\mu l_\nu}{l^2(l-k)^2} \right. \\
&\quad \left. - 8 \int_l \frac{k_\nu l_\mu}{l^2(l-k)^2} \right]. \tag{C.2}
\end{aligned}$$

In both Eq. (C.1) and Eq. (C.2) we use the *Casimir operator*<sup>1</sup> relation in the adjoint representation  $f^{acd} f^{bcd} = C_A \delta_{ab}$ .

We are going to solve using IREG one of the diagrams to illustrate the process. In this case, we are going to solve the ghost-bubble diagram. First we need to deal with the **IR-div** part when  $l \rightarrow 0$ . We add a virtual mass  $\mu^2$  that appears as a divergent in the limit  $\mu^2 \rightarrow 0$  in the propagator. Thus:

$$\begin{aligned}
\sum_{\epsilon\xi}^{ef}(k) &= -g^2 C_A \delta_{ef} \left[ \lim_{\mu^2 \rightarrow 0} 4 \int_l \frac{l_\xi l_\epsilon}{(l^2 - \mu^2)[(l-l)^2 - \mu^2]} - 2k_\epsilon \int_l \frac{l_\xi}{(l^2 - \mu^2)[(l-l)^2 - \mu^2]} \right. \\
&\quad \left. - 2k_\xi \int_l \frac{l_\epsilon}{(l^2 - \mu^2)[(l-l)^2 - \mu^2]} + k_\xi k_\epsilon \int_l \frac{1}{(l^2 - \mu^2)[(l-l)^2 - \mu^2]} \right] \tag{C.3}
\end{aligned}$$

From this point, we are going to rename the denominator  $(l^2 - \mu^2)[(l-l)^2 - \mu^2] = D$ .

---

<sup>1</sup>Casimir operators are extremely useful for having a basis-independent way to characterize representations in non-Abelian theories Ref. (9). They are the elements of the group that commute with any other element. In the fundamental representation  $(T^a T^a)_{ij} = C_F \delta_{ij}$ .

Then the amplitude from the ghost-bubble can be displayed in terms of typical basic IREG integrals:

$$\sum_{\epsilon\xi}^{ef}(k) = -g^2 C_A \delta_{ef} \left[ \lim_{\mu^2 \rightarrow 0} \left( 4 \underbrace{I_{\xi\epsilon}}_{\text{Quadratic}} - 2k_\epsilon \underbrace{I_\xi}_{\text{Linear}} - 2k_\xi \underbrace{I_\epsilon}_{\text{Lineal}} + k_\xi k_\epsilon \underbrace{I}_{\text{Logarithm}} \right) \right] \quad (\text{C.4})$$

where:

$$(I, I_\xi, I_{\xi\epsilon}) = \int_l \frac{(1, l_\xi, l_\xi l_\epsilon)}{D}. \quad (\text{C.5})$$

The explicit calculation using IREG of each of these integrals is in the other Appendices. E. As we saw in Sub-section. 2.3.1 we will only need the divergent part of the integrals to calculate the  $\beta$ -function. Surface terms will be null at the end to respect momentum routing invariance Ref. (4). If we put all these results together:

$$\begin{aligned} \sum_{\epsilon\xi}^{ef}(k) = & -g^2 C_A \delta_{ef} \times \left[ \lim_{\mu^2 \rightarrow 0} \left( 4 \left( \frac{g_{\xi\epsilon}}{2} \right) I_{quad}(\mu^2) - g_{\xi\epsilon} k^2 \frac{1}{12} I_{log}(\mu^2) + \frac{1}{3} k_\xi k_\epsilon I_{log}(\mu^2) \right) \right. \\ & \left. - 2k_\epsilon \left( \frac{k_\xi}{2} I_{log}(\mu^2) \right) - 2k_\xi \left( \frac{k_\epsilon}{2} I_{log}(\mu^2) \right) + k_\xi k_\epsilon (I_{log}(\mu^2)) \right] \end{aligned} \quad (\text{C.6})$$

which finally is:

$$\begin{aligned} \sum_{\epsilon\xi}^{ef}(k) = & + g^2 C_A \delta_{ef} \times \left[ \lim_{\mu^2 \rightarrow 0} \left( -2g_{\xi\epsilon} I_{quad}(\mu^2) \right. \right. \\ & + \frac{1}{3} k^2 g_{\xi\epsilon} I_{log}(\mu^2) \\ & \left. \left. - \frac{1}{3} k_\epsilon k_\xi I_{log}(\mu^2) \right) \right]. \end{aligned} \quad (\text{C.7})$$

For the integrals in Eq. (C.2) regardless of the bubble diagram, we do the same previous procedure. We insert again a mass  $\mu^2$  in the limit  $\mu^2 \rightarrow 0$  to deal with the **IR-div** and for the **UV-div** we use IREG and the integrals from Appendices. E. We get that our result with the divergent parts is:

---


$$\begin{aligned}
\prod_{\mu\nu}^{mn}(k) = & +g^2 C_A \delta_{mn} \times (-2) \times \left( \lim_{\mu^2 \rightarrow 0} \times [-2k^2 g_{\mu\nu} (I_{\log}(\mu^2)) \right. \\
& - 4 \left( \frac{g_{\mu\nu}}{2} I_{quad}(\mu^2) - g_{\mu\nu} k^2 \frac{1}{12} I_{\log}(\mu^2) + \frac{1}{3} k_\mu k_\nu I_{\log}(\mu^2) \right) \\
& + 2k_\nu \left( \frac{k_\mu}{2} I_{\log}(\mu^2) \right) + 2k_\mu \left( \frac{k_\nu}{2} I_{\log}(\mu^2) \right) \\
& \left. + k_\mu k_\nu (I_{\log}(\mu^2)) \right] \Big)
\end{aligned} \tag{C.8}$$

which gives:

$$\prod_{\mu\nu}^{mn}(k) = +g^2 C_A \delta_{mn} \times \left( \lim_{\mu^2 \rightarrow 0} [4g_{\mu\nu} I_{quad}(\mu^2) + \frac{10}{3} k^2 I_{\log}(\mu^2) - \frac{10}{3} k_\mu k_\nu I_{\log}(\mu^2)] \right). \tag{C.9}$$

Now, in IREG for the elimination of the  $I_{quad}(\mu^2)$  we need to compute the tadpole graph:



Figure C.2: Tadpole diagrams for the calculation of the pure YM  $\beta$ -function at one-loop.

For the ghost tadpole:

$$\begin{aligned}
\mathcal{M}_{ef}^{\epsilon\xi} = & (-1) \int_l (-i) g^2 g_{\epsilon\xi} (f^{gex} f^{x fh} + f^{gfx} f^{x eh}) \frac{i\delta_{gh}}{l^2} \\
= & +2g^2 C_A \delta_{ef} g_{\epsilon\xi} \lim_{\mu^2 \rightarrow 0} \int_l \frac{1}{l^2 - \mu^2} \\
= & +2g^2 C_A \delta_{ef} g_{\epsilon\xi} \lim_{\mu^2 \rightarrow 0} I_{quad}(\mu^2).
\end{aligned} \tag{C.10}$$

For the gluon tadpole:

$$\begin{aligned}
 \mathcal{M}_{\mu\nu}^{mn} &= \frac{1}{2} \int_l (-i) g^2 [f^{ma} f^{xb} (g_{\mu\nu} g_{\alpha\beta} - g_{\mu\beta} g_{\alpha\nu} + g_{\mu\alpha} g_{\nu\beta}) \\
 &\quad + f^{mb} f^{xa} (g_{\mu\alpha} g_{\nu\beta} - g_{\mu\nu} g_{\alpha\beta} - g_{\mu\beta} g_{\alpha\nu}) \\
 &\quad + f^{mnx} f^{xab} (g_{\mu\alpha} g_{\nu\beta} - g_{\mu\beta} g_{\alpha\nu})] \\
 &\quad \times (-i) \frac{\delta^{ab}}{l^2} g^{\alpha\beta} \\
 &= -g^2 4C_A \delta_{mn} g_{\mu\nu} \lim_{\mu^2 \rightarrow 0} \int_l \frac{1}{l^2 - \mu^2} \\
 &= -g^2 4C_A \delta_{mn} g_{\mu\nu} \lim_{\mu^2 \rightarrow 0} I_{quad}(\mu^2).
 \end{aligned} \tag{C.11}$$

As we mentioned, we can compute the  $\beta$ -function by calculating the graph in Fig. C.1 and Fig. C.2. Specifically, we need the information of the 2-point functions to calculate the  $Z_A$  (in the  $IREG$ ):

$$\text{[Gluon self-energy loop]} + \text{[Ghost loop]} + \text{[Ghost self-energy loop]} + \text{[Gluon self-energy loop]} \tag{C.12}$$

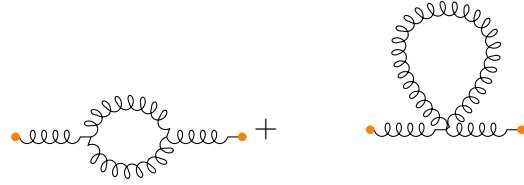
For the ghost graphs where our divergences will be in the  $I_{log}(\mu^2)$ :

$$\text{[Ghost loop]} + \text{[Gluon loop]} \tag{C.13}$$

$$= +g^2 C_A \delta_{ef} \times \left[ \lim_{\mu^2 \rightarrow 0} \left( +\frac{1}{3} k^2 g_{\xi\epsilon} I_{log}(\mu^2) - \frac{1}{3} k_\epsilon k_\xi I_{log}(\mu^2) \right) \right]$$

while the gluon one:

---



$$(C.14)$$

$$= +g^2 C_A \delta_{mn} \times \left( \lim_{\mu^2 \rightarrow 0} \left[ \frac{10}{3} k^2 I_{log}(\mu^2) - \frac{10}{3} k_\mu k_\nu I_{log}(\mu^2) \right] \right).$$

Adding boht Eq. (C.13) and Eq. (C.14)<sup>2</sup>:

$$\sum_{\epsilon\xi}^{ef}(k) + \prod_{\mu\nu}^{mn}(k) + \mathcal{M}_{ef}^{\epsilon\xi} + \mathcal{M}_{\mu\nu}^{mn} = g^2 C_A \delta_{mn} \frac{11}{3} \lim_{\mu^2 \rightarrow 0} [g_{\mu\nu} k^2 - k_\mu k_\nu] I_{log}(\mu^2). \quad (C.15)$$

With this result, we can write the renormalization constants  $Z_A$  as a sum in the  $I_{log}(\mu^2)$ :

$$Z_A = 1 + g^2 C_A \frac{11}{3} I_{log}(\mu^2). \quad (C.16)$$

Finally, using our equation Eq.(2.20) and the main BFM result Eq.(2.34):

$$\beta = \frac{-11C_A}{3} \frac{g^3}{(4\pi)^2}. \quad (C.17)$$

This Eq. (C.17) matches the  $\beta$ -function in Ref. (15) which was calculated using CDR. This result at 1-loop also coincides with the result of the dimensional method using the algorithm that we developed in Chapter. 4.

---

<sup>2</sup>And changing the index  $\xi\epsilon \rightarrow \mu\nu$  and e;f for m;n in the ghost result.

## APPENDIX D

# APPENDIX D: ELECTRON PROPAGATOR OF QED AT 1-LOOP WITH CDR AND DRED

As explained in Ref. (4), we can obtain consistent results after regularizing and summing all the divergent parts of the expressions in our QFT computations. After the renormalization process, a finite, physical, and regularization-scheme independent result is obtained.

The choice of the regularization scheme matters in different conceptual and practical aspects:

- **Mathematical consistency:** The calculations must be consistent so that the final results do not contradict each other.
- **Unitarity and causality:** We need the different regularization schemes to preserve the unitarity and causality of the finite results that come from n-loops Feynman's graphs computations.
- **Symmetries:** Symmetries should be preserved to the largest extent.
- **Quantum action principle:** From this, basic properties such as Ward/Slavnov-Taylor identities, follow all orders. Therefore, we want the regularization scheme to follow this principle for the study of symmetry properties to be simplified.
- **Computational efficiency:** The regularization scheme should allow for efficient computational techniques.

We develop in this appendix the same example as in Sub-section. 3.1.2 with the basic procedure of CDR and DRED. The initial no regularize expression using QED's Feynman Rules is the same as in Eq. 3.13.

## D.1 Electron-propagator in CDR at 1-loop

Dimensional schemes, such as CDR, are based on analytical continuations of the space from 4 to d-dimensions. Thus to regularize the divergent integrals, they change the dimensionality of the space of momenta. As we can see:<sup>1</sup>:

$$\int_{-\infty}^{+\infty} \frac{d^4 k_{[4]}}{(2\pi)^4} \rightarrow \underbrace{\mu^{4-d}}_{\text{scale}} \int_{-\infty}^{+\infty} \frac{d^d k_{[d]}}{(2\pi)^d}, \quad (\text{D.1})$$

where  $d \equiv 4 - 2\epsilon$ . Then the **IR-div** and **UV-div** manifest as poles of the form  $1/\epsilon^n$ .

According to Ref. (31), the techniques from CDR to all loop calculations:

- Draw the diagram(s) and write down the amplitude.
- Introduce Feynman parameters to combine the denominators of the propagators.
- Complete the square in the new denominator by shifting them to a new loop momentum variable,  $l$ .
- Write the denominator in terms of this new loop momentum variable  $l$ . Drop odd powers of  $l$ , and rewrite even powers using symmetry integration identities.
- Perform the integrals: one option will be to perform the momentum integral employing a Wick rotation and 4-dimensional spherical coordinates. Another option will be to use a table of d-dimensional integrals in Minkowski space.

On the second step, we need to use the Feynman parameters technique in all the integrals of Eq. 3.13 to combine propagator denominators. In the case of only two denominators factors, we need to use:

$$\frac{1}{AB} = \int_0^1 dx \frac{1}{[xA + (1-x)B]^2}. \quad (\text{D.2})$$

So:

$$\frac{1}{l^2[(p+l)^2 - m^2]} = \frac{1}{[x[(p+l)^2 - m^2] + (1-x)l^2]^2} = \frac{1}{[(l+px)^2 + [p^2(1-x) - m^2]x]^2}, \quad (\text{D.3})$$

where we complete the squares in the denominator.

---

<sup>1</sup>When we carry out the dimensional analysis in d dimensions, our coupling constant in the Lagrangian density will carry out a dimension. Therefore, we introduce the arbitrary mass scale  $\mu$  to keep our integral in four dimensions, and as consequence, the coupling constant is dimensionless.





---

### D.1.1 Finite terms with CDR

We have two finite terms in Eq. (D.8) that we can simplify more. They are:

$$\begin{aligned} & \int_0^1 dx \ln \left( \frac{4\pi\mu}{x[m^2 - p^2(1-x)]} \right), \\ & \int_0^1 dx (1-x) \ln \left( \frac{4\pi\mu}{x[m^2 - p^2(1-x)]} \right). \end{aligned} \quad (\text{D.9})$$

As mentioned in Ref. (39), at low or high energies, we can expand the logarithm as a Taylor series. With the low energy assumption  $p^2 \ll m^2$ , we find:

$$\begin{aligned} \int_0^1 dx \ln \left( \frac{4\pi\mu}{x[m^2 - p^2(1-x)]} \right) &= 2 - 4\gamma_E - 2\frac{p^2}{m^2} + 4 \ln \left( \frac{4\pi\mu}{m^2} \right), \\ \int_0^1 dx (1-x) \ln \left( \frac{4\pi\mu}{x[m^2 - p^2(1-x)]} \right) &= \frac{5}{2} + \gamma_E - \frac{1}{3}\frac{p^2}{m^2} - \ln \left( \frac{4\pi\mu}{m^2} \right). \end{aligned} \quad (\text{D.10})$$

## D.2 Electron-propagator in DRED at 1-loop

In Sub-section. 3.2.1, we mentioned that DRED modifies the Lagrangian. As a consequence of it, we have the extra diagram with the evanescent coupling in Fig. 3.3. For both diagrams, we follow the techniques of CDR from Ref. (31). The non-evanescent part will be identical to the CDR computation we just developed. In the case of the evanescent part, the only difference will be the Dirac algebra of Eq. (3.47). Using this algebra:

$$\begin{aligned} \Sigma^{(1)}(p, m) \Big|_{DRED} &= +\mu^{2\epsilon} i e_\epsilon^2 N_\epsilon \not{p} \int \frac{d^d l}{(2\pi)^d} \int_0^1 \frac{dx(1-x)}{(l^2 - \Delta)^2} \\ &\quad - \mu^{2\epsilon} i e_\epsilon^2 N_\epsilon m \int \frac{d^d l}{(2\pi)^d} \int_0^1 \frac{dx}{(l^2 - \Delta)^2}. \end{aligned} \quad (\text{D.11})$$

From this point we can use the same table of integrals in d-dimensions from Ref. (31) as we did for CDR. With this, the evanescent amplitude will be:

$$\begin{aligned}
 \Sigma^{(1)}(p, m) \Big|_{DRED} &= -\frac{e_\epsilon^2}{(4\pi)^2} \left( -\not{p} \left[ \frac{1}{2} N_\epsilon \frac{1}{\epsilon} + \frac{1}{2} N_\epsilon \ln \left( \frac{4\pi\mu^2}{m^2} \right) - \frac{1}{2} N_\epsilon \gamma_E \right. \right. \\
 &\quad \left. \left. - \int_0^1 (1-x) N_\epsilon dx \ln \left( \frac{1}{x + (\frac{xp}{m})^2} \right) \right] \right. \\
 &\quad \left. m \left[ N_\epsilon \frac{1}{\epsilon} + N_\epsilon \ln \left( \frac{4\pi\mu^2}{m^2} \right) - N_\epsilon \gamma_E + \int_0^1 N_\epsilon dx \ln \left( \frac{1}{x + (\frac{xp}{m})^2} \right) \right] \right). \tag{D.12}
 \end{aligned}$$

Previous Eq. (D.12) is all finite at 1-loop since  $1/\epsilon N_\epsilon = 2$ . Also, when we do  $\epsilon \rightarrow 0$  the other terms disappear. Our final amplitude for the electron-propagator at 1-loop DRED will consider both the non-evanescent part in Eq. (D.8) and the evanescent part with the coupling  $e_\epsilon$  in Eq. (D.12).

As we mentioned at the end of the Sub-section. 3.2.1, if we make the evanescent coupling equal to the non-evanescent,  $e_\epsilon = e$  the finite terms of  $CDR + DRED$  will be the same as the finite terms of IREG for the electron-propagator at 1-loop.

## APPENDIX E

## APPENDIX E: EXPLICIT RESULTS OF INTEGRALS

Here we present explicit results for the integrals used in this work. They were obtained combining the IREG procedure in Section. 3.1.1 with 1-loop evaluation of some integrals performed with *Package X* (26).

### E.1 General IREG integrals

Where  $k$  is the internal momentum in the loop.

#### E.1.1 1-loop: two point functions

$$\int_k \frac{1}{k^2(k+p)^2} = I_{log}(\lambda^2) - b \ln \left( -\frac{p^2}{\lambda^2} \right) + 2b, \quad (\text{E.1})$$

$$\int_k \frac{k_\mu}{k^2(k+p)^2} = -\frac{p_\mu}{2} \left[ I_{log}(\lambda^2) - b \ln \left( -\frac{p^2}{\lambda^2} \right) + 2b \right], \quad (\text{E.2})$$

$$\begin{aligned} \int_k \frac{k_\mu k_\nu}{k^2(k+p)^2} = & -\frac{g_{\mu\nu} p^2}{12} \left[ I_{log}(\lambda^2) - b \ln \left( -\frac{p^2}{\lambda^2} \right) + \frac{8b}{3} \right] \\ & + \frac{p_\mu p_\nu}{3} \left[ I_{log}(\lambda^2) - b \ln \left( -\frac{p^2}{\lambda^2} \right) + \frac{13b}{6} \right] \end{aligned} \quad (\text{E.3})$$

#### E.1.2 1-loop: three point functions

$$\int_k \frac{k_\mu k_\nu}{k^4(k+p)^2} = \frac{g_{\mu\nu}}{4} \left[ I_{log}(\lambda^2) - b \ln \left( -\frac{p^2}{\lambda^2} \right) + 2b \right] + \frac{p_\mu p_\nu}{p^2} \frac{b}{2} \quad (\text{E.4})$$

### E.1.3 2-loop: explicit results involving logarithms

The general structure is:

$$I^{\nu_1 \dots \nu_m} = \int_{k_l} \frac{A^{\nu_1 \dots \nu_m}(k_l, q_i)}{\prod_i [(k_l - q_i)^2 - \mu^2]} \ln^{l-1} \left( -\frac{k_l^2 - \mu^2}{\lambda^2} \right), \quad (\text{E.5})$$

Considering the 2-loop case ( $l = 2$ ) and relabeling  $k_2 = k$ , it simplifies to:

$$I^{\nu_1 \dots \nu_m} = \int_k \frac{A^{\nu_1 \dots \nu_m}(k, q_i)}{\prod_i [(k - q_i)^2 - \mu^2]} \ln \left( -\frac{k^2 - \mu^2}{\lambda^2} \right), \quad (\text{E.6})$$

#### E.1.3.1 One point functions

$$\int_k \frac{1}{(k+p)^2} \ln \left( -\frac{k^2}{\lambda^2} \right) = \frac{p^2}{2} I_{\log}(\lambda^2) + \text{finite}, \quad (\text{E.7})$$

#### E.1.3.2 Two point functions

$$\int_k \frac{1}{k^2(k+p)^2} \ln \left( -\frac{k^2}{\lambda^2} \right) = I_{\log}^{(2)}(\lambda^2) + \text{finite}, \quad (\text{E.8})$$

$$\int_k \frac{k_\mu}{k^2(k+p)^2} \ln \left( -\frac{k^2}{\lambda^2} \right) = -\frac{p_\mu}{2} \left[ I_{\log}^{(2)}(\lambda^2) + \frac{I_{\log}(\lambda^2)}{2} + \text{finite} \right], \quad (\text{E.9})$$

#### E.1.3.3 Three point functions

$$\int_k \frac{k_\mu k_\nu}{k^4(k+p)^2} \ln \left( -\frac{k^2}{\lambda^2} \right) = \frac{g_{\mu\nu}}{4} \left[ I_{\log}^{(2)}(\lambda^2) + \frac{I_{\log}(\lambda^2)}{2} + \text{finite} \right] + \frac{p_\mu p_\nu}{p^2} \text{finite}, \quad (\text{E.10})$$

### E.1.4 2-loop: overlapped integrals

We will have the general structure:

$$I[f(k, q)] = \int_k \int_q \frac{f(k, q)}{k^2(k-p)^2(k-q)^2 q^2(q-p)^2} \quad (\text{E.11})$$

---


$$I[k_\mu q_\nu] = \frac{g_{\mu\nu}}{4} [I_{\log}(\lambda^2) + \text{finite}] + \frac{p_\mu p_\nu}{p^2} \text{finite} \quad (\text{E.12})$$

$$I[k_\mu k_\nu] = \frac{g_{\mu\nu}}{4} \left\{ I_{\log}^2(\lambda^2) - bI_{\log}^{(2)}(\lambda^2) + bI_{\log}(\lambda^2) \left[ \frac{9}{2} - \ln \left( -\frac{p^2}{\lambda^2} \right) \right] + \text{finite} \right\} \\ + \frac{p_\mu p_\nu}{p^2} \text{finite} \quad (\text{E.13})$$

$$I[k_\mu k \cdot q] = \frac{p_\mu}{8} \left\{ I_{\log}^2(\lambda^2) - bI_{\log}^{(2)}(\lambda^2) + bI_{\log}(\lambda^2) \left[ \frac{19}{2} - \ln \left( -\frac{p^2}{\lambda^2} \right) \right] + \text{finite} \right\}. \quad (\text{E.14})$$

## E.2 Integrals for QED

### E.2.1 Massless case

$$\int_k \int_l \frac{\not{k}(k \cdot p)}{(l+p)^2 k^2 (l^2)^2 (k-l)^2} = \frac{1}{12} bI_{\log}(\lambda^2) \not{p} + \text{finite}, \quad (\text{E.15})$$

$$\int_k \int_l \frac{l^2 \not{k}}{(l+p)^2 k^2 (l^2)^2 (k-l)^2} = \frac{1}{4} bI_{\log}^{(2)}(\lambda^2) \not{p} + \frac{1}{4} bI_{\log}(\lambda^2) \ln \left( -\frac{p^2}{\lambda^2} \right) \not{p} \\ - \frac{7}{8} bI_{\log}(\lambda^2) \not{p} - \frac{1}{4} I_{\log}^2(\lambda^2) \not{p} + \text{finite}, \quad (\text{E.16})$$

$$\int_k \int_l \frac{(k \cdot l) \not{l}}{(l+p)^2 k^2 (l^2)^2 (k-l)^2} = \frac{1}{4} bI_{\log}^{(2)}(\lambda^2) \not{p} + \frac{1}{4} bI_{\log}(\lambda^2) \ln \left( -\frac{p^2}{\lambda^2} \right) \not{p} \\ - \frac{7}{8} bI_{\log}(\lambda^2) \not{p} - \frac{1}{4} I_{\log}^2(\lambda^2) \not{p} + \text{finite}, \quad (\text{E.17})$$

$$\int_k \int_l \frac{\not{k}(k \cdot l)}{(l+p)^2 k^2 (l^2)^2 (k-l)^2} = \frac{1}{8} bI_{\log}^{(2)}(\lambda^2) \not{p} + \frac{1}{8} bI_{\log}(\lambda^2) \ln \left( -\frac{p^2}{\lambda^2} \right) \not{p} \\ - \frac{7}{16} bI_{\log}(\lambda^2) \not{p} - \frac{1}{8} I_{\log}^2(\lambda^2) \not{p} + \text{finite}, \quad (\text{E.18})$$

$$\int_k \int_l \frac{(k \cdot p) \not{l}}{(l+p)^2 k^2 (l^2)^2 (k-l)^2} = -\frac{1}{8} bI_{\log}^{(2)}(\lambda^2) \not{p} - \frac{1}{8} bI_{\log}(\lambda^2) \ln \left( -\frac{p^2}{\lambda^2} \right) \not{p} \\ + \frac{11}{16} bI_{\log}(\lambda^2) \not{p} + \frac{1}{8} I_{\log}^2(\lambda^2) \not{p} + \text{finite}, \quad (\text{E.19})$$

$$\begin{aligned} \int_k \int_l \frac{\not{k}(l \cdot p)}{(l+p)^2 k^2 (l^2)^2 (k-l)^2} &= -\frac{1}{8} b I_{log}^{(2)}(\lambda^2) \not{p} - \frac{1}{8} b I_{log}(\lambda^2) \ln \left( -\frac{p^2}{\lambda^2} \right) \not{p} \\ &+ \frac{11}{16} b I_{log}(\lambda^2) \not{p} + \frac{1}{8} I_{log}^2(\lambda^2) \not{p} + \text{finite}, \end{aligned} \quad (\text{E.20})$$

$$\begin{aligned} \int_k \int_l \frac{(k \cdot l) \not{l}}{(l+p)^2 k^2 (l^2)^2 (k-l)^2} &= \frac{1}{4} b I_{log}^{(2)}(\lambda^2) \not{p} + \frac{1}{4} b I_{log}(\lambda^2) \ln \left( -\frac{p^2}{\lambda^2} \right) \not{p} \\ &- \frac{7}{8} b I_{log}(\lambda^2) \not{p} - \frac{1}{4} I_{log}^2(\lambda^2) \not{p} + \text{finite}, \end{aligned} \quad (\text{E.21})$$

$$\begin{aligned} \int_k \int_l \frac{\not{k}(k \cdot l)}{l^2 k^2 (k-l)^2 (k-p)^2 (l-p)^2} &= -\frac{1}{8} b I_{log}^{(2)}(\lambda^2) \not{p} - \frac{1}{8} b I_{log}(\lambda^2) \ln \left( -\frac{p^2}{\lambda^2} \right) \not{p} \\ &+ \frac{19}{16} b I_{log}(\lambda^2) \not{p} + \frac{1}{8} I_{log}^2(\lambda^2) \not{p} + \text{finite}, \end{aligned} \quad (\text{E.22})$$

$$\begin{aligned} \int_k \int_l \frac{(k \cdot l) \not{l}}{l^2 k^2 (k-l)^2 (k-p)^2 (l-p)^2} &= -\frac{1}{8} b I_{log}^{(2)}(\lambda^2) \not{p} - \frac{1}{8} b I_{log}(\lambda^2) \ln \left( -\frac{p^2}{\lambda^2} \right) \not{p} \\ &+ \frac{19}{16} b I_{log}(\lambda^2) \not{p} + \frac{1}{8} I_{log}^2(\lambda^2) \not{p} + \text{finite}, \end{aligned} \quad (\text{E.23})$$

$$\int_k \int_l \frac{\not{k}(l \cdot p)}{l^2 k^2 (k-l)^2 (k-p)^2 (l-p)^2} = \frac{1}{4} b I_{log}(\lambda^2) \not{p} + \text{finite}, \quad (\text{E.24})$$

$$\begin{aligned} \int_k \int_l \frac{\not{l}(l \cdot p)}{l^2 k^2 (k-l)^2 (k-p)^2 (l-p)^2} &= -\frac{1}{4} b I_{log}^{(2)}(\lambda^2) \not{p} - \frac{1}{4} b I_{log}(\lambda^2) \ln \left( -\frac{p^2}{\lambda^2} \right) \not{p} \\ &+ \frac{9}{8} b I_{log}(\lambda^2) \not{p} + \frac{1}{4} I_{log}^2(\lambda^2) \not{p} + \text{finite}. \end{aligned} \quad (\text{E.25})$$

Notice all the integrals are proportional to  $\not{p}$  as expected for the massless case.





## BIBLIOGRAPHY

- [1] R. P. Feynman, *Very high-energy collisions of hadrons* Phys. Rev. Lett. **23**, 1415 (1969).
- [2] ATLAS, *Standard Model Summary Plots June 2021* ATL-PHYS-PUB-2021-032.
- [3] C. Anastasiou, C. Duhr, F. Dulat, E. Furlan, T. Gehrmann, F. Herzog, A. Lazopoulos and B. Mistlberger, *High precision determination of the gluon fusion Higgs boson cross-section at the LHC*, JHEP **05** (2016), 058 doi:10.1007/JHEP05(2016)058 [arXiv:1602.00695 [hep-ph]].
- [4] Gnendiger, C., Signer, A., Stöckinger, D. et al. *To d, or not to d: recent developments and comparisons of regularization schemes*. Eur. Phys. J. C 77, 471 (2017). <https://doi.org/10.1140/epjc/s10052-017-5023-2>
- [5] S. P. Martin, *A Supersymmetry primer*. Adv. Ser. Direct. High Energy Phys. **21** (2010), 1-153 [arXiv:hep-ph/9709356 [hep-ph]].
- [6] D. Stockinger, *Regularization by dimensional reduction: consistency, quantum action principle, and supersymmetry*. JHEP **03** (2005), 076 doi:10.1088/1126-6708/2005/03/076 [arXiv:hep-ph/0503129 [hep-ph]].
- [7] J. G. Korner and M. M. Tung, *Dimensional reduction methods in QCD*. Z. Phys. C **64** (1994), 255-265 doi:10.1007/BF01557396
- [8] T. Lancaster and S. J. Blundell, *Quantum Field Theory for the Gifted Amateur*. Oxford University Press, 2014, ISBN 978-0-19-969933-9
- [9] M. D. Schwartz, *Quantum Field Theory and the Standard Model*. Cambridge University Press, 2014, ISBN 978-1-107-03473-0, 978-1-107-03473-0

- [10] A. Grozin, *Lectures on QED and QCD: Practical calculation and renormalization of one- and multi-loop Feynman diagrams*. World Scientific, 2007, ISBN 978-981-256-914-1, 978-981-256-914-1
- [11] E. W. Dias, A. P. Baeta Scarpelli, L. C. T. Brito, M. Sampaio and M. C. Nemes, *Implicit regularization beyond one loop order: Gauge field theories*, Eur. Phys. J. C **55**, 667-681 (2008) doi:10.1140/epjc/s10052-008-0614-6 [arXiv:0801.2703 [hep-th]].
- [12] M. D. Sampaio, A. P. Baeta Scarpelli, J. E. Ottoni and M. C. Nemes, *Implicit regularization and renormalization of QCD*. Int. J. Theor. Phys. **45**, 436-457 (2006) doi:10.1007/s10773-006-9045-z [arXiv:hep-th/0509102 [hep-th]].
- [13] A. Nyffeler. *Basics of perturbative QCD*. Lectures at Advanced School on Radiative Corrections for the LHC (2011).
- [14] Burdman, G. *4 The Beta Function and Renormalization Group Flow*. Lecture notes. Instituto de Física, USP. Delivered in 2018.
- [15] L. Abbott, *Introduction to the Background Field Method*. Acta Phys. Polon. B **13**, 33 (1982) CERN-TH-3113.
- [16] B. S. DeWitt, *Quantum Theory of Gravity. 2. The Manifestly Covariant Theory*. Phys. Rev. **162** (1967), 1195-1239 doi:10.1103/PhysRev.162.1195
- [17] L. Abbott, *The Background Field Method Beyond One Loop*. Nucl. Phys. B **185** (1981), 189-203 doi:10.1016/0550-3213(81)90371-0
- [18] A. Cherchiglia, D. C. Arias-Perdomo, A. R. Vieira, M. Sampaio and B. Hiller, *Two-loop renormalisation of gauge theories in 4D Implicit Regularisation: transition rules to dimensional methods*. [arXiv:2006.10951 [hep-ph]].
- [19] Cherchiglia, A.L. Master's degree dissertation. *Implementação sistemática da regularização implícita para diagramas de Feynman a muitos laços*. Universidade Federal de Minas Gerais (2011). <http://hdl.handle.net/1843/BUOS-8GBKWY>
- [20] Filho, H. Master's degree dissertation. *Sistematização do Cálculo das Funções do Grupo de Renormalização através da Regularização Implícita* Universidade Federal de Minas Gerais (2008). [http://lilith.fisica.ufmg.br/posgrad/Dissertacoes\\_Mestrado/decada2000/helvecio-filho/DissHelvecio.pdf](http://lilith.fisica.ufmg.br/posgrad/Dissertacoes_Mestrado/decada2000/helvecio-filho/DissHelvecio.pdf)

- 
- [21] Dias, E. PhD thesis. *Generalização do procedimento de Regularização Implícita para ordens superiores em teorias de calibre abelianas*. Universidade Federal de Minas Gerais (2008). <https://www.fisica.ufmg.br/posgraduacao/defesas/doutorado-2008-edson-dias/>
- [22] Bruque, A.M., Cherchiglia, A.L. and Pérez-Victoria, M. *Dimensional regularization vs methods in fixed dimension with and without  $\gamma_5$* . J. High Energ. Phys. 2018, 109 (2018).
- [23] Battistel, O. PhD thesis. *Uma estratégia para manipulações e cálculos envolvendo divergências em TQC*. Universidade Federal de Minas Gerais (1996). [http://lilith.fisica.ufmg.br/posgrad/Teses\\_Doutorado/decada90/orimar-batistel/](http://lilith.fisica.ufmg.br/posgrad/Teses_Doutorado/decada90/orimar-batistel/)
- [24] A. R. Vieira, A. L. Cherchiglia, and Marcos Sampaio, *Momentum Routing Invariance in Extended QED: Assuring Gauge Invariance Beyond Tree Level*, Phys. Rev. D **93** (2016) 025029.
- [25] H. Fargnoli, B. Hiller, A. Scarpelli, Marcos Sampaio, M. C. Nemes, *Regularisation Independent Analysis of the Origin of Two Loop Contributions to  $N = 1$  Super Yang-Mills Beta Function*, Eur. Phys. J. C **71** (2011) 1633.
- [26] H. H. Patel, *Package-X 2.0: A Mathematica package for the analytic calculation of one-loop integrals*, Comput. Phys. Commun. **218**, 66-70 (2017) doi:10.1016/j.cpc.2017.04.015 [arXiv:1612.00009 [hep-ph]].
- [27] W. Siegel, *Supersymmetric Dimensional regularisation via Dimensional Reduction*, Phys. Lett. B **84**(1979) 193; idem, *Inconsistency of Supersymmetric Dimensional regularisation*, Phys. Lett. B **94**(1980) 37.
- [28] A. Signer and D. Stöckinger, *Using dimensional reduction for hadronic collisions*. Nuclear Physics B, Volume 808, Issues 1-2, 2009, Pages 88-120, ISSN 0550-3213. <https://doi.org/10.1016/j.nuclphysb.2008.09.016>.
- [29] Visconti, A. PhD thesis. *Regularization-Scheme Dependence of QCD Amplitudes*. University of Zurich (2016). <https://www.zora.uzh.ch/id/eprint/127072/>
- [30] D. M. Capper, D. R. T. Jones and P. van Nieuwenhuizen, *Regularization by Dimensional Reduction of Supersymmetric and Nonsupersymmetric Gauge Theories*, Nucl. Phys. B **167**, 479-499 (1980) doi:10.1016/0550-3213(80)90244-8
- [31] M.E.Peskin and D.V.Schroeder, *An Introduction to quantum field theory*. Addison-Wesley, 1995, ISBN 978-0-201-50397-5

- [32] T. Hahn, *Generating Feynman diagrams and amplitudes with FeynArts 3*. Comput. Phys. Commun. **140** (2001), 418-431 doi:10.1016/S0010-4655(01)00290-9 [arXiv:hep-ph/0012260 [hep-ph]].
- [33] T. Hahn, S. PaSSehr and C. Schappacher, *FormCalc 9 and Extensions*. PoS **LL2016** (2016), 068 doi:10.1088/1742-6596/762/1/012065 [arXiv:1604.04611 [hep-ph]].
- [34] A. Cherchiglia, Marcos Sampaio, M. C. Nemes, *Systematic Implementation of Implicit regularisation for Multi-Loop Feynman Diagrams*, Int. J. Mod. Phys. A **26** (2011) 1.
- [35] L. F. Abbott, M. T. Grisaru and R. K. Schaefer, *The Background Field Method and the S Matrix*. Nucl. Phys. B **229** (1983), 372-380 doi:10.1016/0550-3213(83)90337-1 203 citations counted in INSPIRE as of 23 Jun 2022
- [36] G. S. Adkins, R. N. Fell and J. Sapirstein, Phys. Rev. D **63**, 125009 (2001) doi:10.1103/PhysRevD.63.125009
- [37] P. A. Baikov, K. G. Chetyrkin and J. H. Kühn, *Towards QCD running in 5 loops: quark mass anomalous dimension*, PoS **RADCOR2013** (2013), 056 doi:10.22323/1.197.0056 [arXiv:1402.6606 [hep-ph]].
- [38] R. Harlander, P. Kant, L. Mihaila and M. Steinhauser, *Dimensional Reduction applied to QCD at three loops*, JHEP **09** (2006), 053 doi:10.1088/1126-6708/2006/09/053 [arXiv:hep-ph/0607240 [hep-ph]].
- [39] R. Ticciati, *Quantum field theory for mathematicians*. Cambridge, UK: Univ. Pr. (1999) 699 p , (Encyclopedia of mathematics and its applications. 72)